NTNU – Trondheim
Norwegian University of
Science and Technology

Auralization using headphones

Ingebjørg Nordstoga Eide

Master of Science in Electronics
Submission date: June 2012
Supervisor: Peter Svensson, IET
Co-supervisor: Tonni Franke Johansen, SINTEF

Norwegian University of Science and Technology
Department of Electronics and Telecommunications

NTNU – Trondheim
Norwegian University of
Science and Technology

Ingebjørg Nordstoga Eide

Auralization using earplugs

Supervisors:
Peter Svensson
Tonni Franke Johansen

TTT 4990 Signal processing and communication
Master's thesis

The Norwegian University of Science and Technology
Faculty of Information Technology, Mathematics and Electrical Engineering
Department of Electronics and Telecommunications

June 20, 2012

1 Problem description

QuietPro is a hearing protection device that allows for radio communication between the users. It has earlier been shown that the system maintains good sound localization performance in quiet environments [28], and it is desirable to achieve localization ability when the radio system is in use under noisy conditions as well.

The task is to investigate various approaches for auralization in the QuietPro system, and test their performance in the horizontal plane. A theoretical and experimental study of auralizations will be carried out, to discover possibilities and limitations of the system.

2 Acknowledgment

I would like to thank the people in the acoustics department at SINTEF research institute for giving me the opportunity to work with this exciting project. My professor and supervisor Peter Svensson and co-supervisor Tonni Franke Johansen from SINTEF deserve special attention, as they gave me valuable input and contributed to interesting discussions during the period. Olav Kvaløy helped in providing necessary equipment and assisted me in some of the measurements, and this was greatly appreciated. I would also like to thank the subjects who participated in the listening tests, and my friends and family for all their support.

3 Abstract

In this report various techniques used to estimate head related impulse responses are compared. The purpose is to investigate the effectiveness of presenting auralization via the QuietPro system's earplugs, and see if sound localization in the horizontal plane is possible. In addition, a theoretical study to relate pinna dimensions to features found in measured head related impulse responses is described.

In the theoretical part, impulse responses for 33 left ears found in the CIPIC database were investigated, as an attempt to relate reflection coefficients and time delays associated with reflections from the pinna to physical dimensions of the ear. Unfortunately, no clear connection was found.

In the listening test, the participants were sitting in the middle of a circle, surrounded by 36 numbered pieces of paper (either standing on top of e.g loudspeakers or attached to microphone stands) that indicated possible sound directions. 14 subjects performed sound localization tests by listening to three consecutive noise bursts of 150 ms duration with 100 ms silence between. Prior to the experiment, measurements of the subject's head were made and used for customization of the models. The task was to determine which of the 36 possible directions the sound was meant to come from. Seven simulation conditions were evaluated, each including 33 stimuli. Four test stimuli were also presented, resulting in a total of 235 noise bursts for each subject.

The results show that the presented methods provide directionality to the stimuli, and that sound localization is possible. However, a significant reduction in localization performance compared to what could be expected for normal hearing conditions is observed. A high number of front/back confusion is reported, and even some instances of left/rigth confusion. Accuracy of the results was not predicted by model complexity, and in some cases it turned out that adding more features significantly degraded the performance.

4 Sammendrag

I denne rapporten blir ulike teknikker som benyttes til å beregne head related impulse responser sammenliknet. Målet er å undersøke hvor gode resultater man kan oppnå når man presenterer auraliseringer gjennom øreproppene som hører til systemet QuietPro, og om lokalisering i horisontalplanet er mulig. I tillegg presenteres en teoretisk studie som har til hensikt å relatere størrelser i det ytre øre til ulike observerte hendelser i målte head related impulse responser.

I den teoretiske delen ble 33 ører fra CIPIC databasen gransket. Man ønsket å relatere refleksjoners tidsforsinkeler (observert i ulike head related impulse responser) til ørets dimensjoner. Refleksjonskoeffesienter ble også undersøkt. I dette tilfellet ble dessverre ingen sammenheng oppdaget.

En praktisk lyttetest ble gjennomført ved at papirark nummerert fra 1 til 36 ble plassert i en ring med 10 graders mellomrom (arkene stod oppå høyttalere eller var festet på mikrofonstativ), og indikerte mulige retninger for lydkilden. 14 personer deltok i testen, som gikk ut på å lytte til tre 150 ms lange støysekvenser med 100 ms mellomrom. Før eksperimentet startet ble ulike størrelser relatert til forsøkspersonens hode målt, og på den måten kunne man tilpasse modellene til hver enkelt deltaker. Sju simuleringsmetoder ble undersøkt ved at forsøkspersonen oppga hvor han eller hun trodde lyden kom fra, og 33 signaler ble testet i hver simuleringsmetode. Det ble også presentert fire test-signaler, så totalt 235 støysekvenser ble avspilt for hver deltaker.

Det viste seg at det gikk an å få lyden til å bli oppfattet fra ulike vinkler, og det var tydelig at deltakerene til en viss grad var i stand til å retningsbestemme den. Auralisering ved bruk av øreproppene i QuietPro systemet er altså mulig. En reduksjon i lokaliseringsevne ble påvist, siden større og flere feil enn hva man kan forvente under normale omstendigheter ble observert. Lyd som skulle vært oppfattet foran ble i flere tilfeller registrert bak, og noen tilfeller av kildereversering mellom høyre og venstre side forekom. Det var ingen sammenheng mellom hvor godt en metode fungerte og grad av kompleksitet. I enkelte tilfeller ble faktisk resultatene dårligere da flere komponenter ble lagt til.

Contents

List of Figures

List of Tables

5 Introduction

Our hearing provides us with important information about the environment, and enables efficient communication with the humans around us. Mechanical pressure waves are translated into electrical impulses the brain can interpret, and makes it possible for us to enjoy music and detect potential danger. Humans are quite skilled in discriminating between different sounds, and pitch, sound level and sound direction are easily detected. This is a natural part of our daily lives, and although the process is highly complex, most people don't even notice it.

In many contexts, the ability to accurately localize sound sources is especially useful, e.g when crossing a road. The time it takes from the sound wave reaches one ear until it arrives at the second, as well as the level difference experienced by the two ears, reveal information about where a sound source is located. The sound specter will provide additional cues, which are crucial for discriminating between sounds from the front and the back, and determining source elevation.

It is utterly important to protect the hearing from exposure to excessive noise, as hearing damage in many cases are permanent. Unfortunately, this is a fact a lot of people become aware of after the damage has occurred. Some ways to avoid the risk of hearing loss include wearing simple foam plugs, and all together avoid situations where high sound levels will occur. A perhaps more sophisticated way is the use of specially developed electronic hearing protectors, like the QuietPro system.

The QuietPro system was primary developed for military purposes, but recently also the oil industry has become interested in the benefits of this hearing protection device. It consists of a digital signal processing (DSP) unit and two earplugs. Sound from the environment is recorded and played back to the person via the earplugs, and the system is designed to let all signals that are not considered harmful pass through. Radio communication between the users is also possible. It has previously been shown [28] that the system maintains directional information in low-noise conditions, i.e when recorded sound is played back. However, during radio communication, no localization cues are provided. This could be beneficial in a number of situations, e.g when interacting with more than one person at a time. The purpose of the study is to explore the possibility of auralization in the QuietPro earplugs, and several simulation methods are compared in listening tests.

In chapter 6 necessary background information is presented. An overview of the ear is given, and mechanisms involved in directional hearing are described. The most important features of the QuietPro system are outlined. The theory behind the calculation methods is given in section 7 and 8. Section 7 also provides details from the investigation of the CIPIC database. In chapter 9, the laboratory set-up is shown and information about the subjects, stimuli and practical aspects regarding the listening test is given. Chapter 10 presents the results from the listening tests and two different statistical analyses. In section 11, possible explanations for the findings presented in chapter 10 are provided. The results are discussed, and suggestions for further studies are given. Chapter 12 sums up the most important results. Matlab code, various plots and all details from the statistical analyses are found in the appendices.

6 Background

In this chapter, an overview of the ear is provided, and mechanisms involved in sound localization are described. Background information about the QuietPro system is given, and applied coordinate system in the listening test is defined. The "optimal" choice of sphere radius for the simulation methods is also presented.

6.1 The ear

Sound consists of pressure waves that are transmitted through an elastic medium, e.g air or water. The ears transform the pressure waves to signals the brain can understand, and consist of the outer, middle and inner ear.

6.1.1 The outer ear

The outer ear is separated from the middle ear by the tympanic membrane (the ear drum), and includes the pinna and the ear canal. Figure 1 shows various parts of the human pinna.

The shape and size of the pinna affect the spectral content of the incoming sound wave, and provide important cues for localization of sound sources. There is great variability in pinna details for different people.

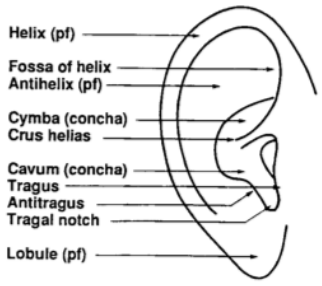

Figure 1: Human pinna. Figure found in [1].

Battau argued that when the wavelength is small compared to the pinna dimensions, sound waves are reflected, and interference between the direct and the reflected path leads to notches in the resulting spectrum [46]. If the time delay for the reflection T is known, the frequencies for the notches are separated by $\frac{1}{T}$. Many researchers have argued that these spectral notches are crucial for determining source elevation [16]-[20]. Attempts have been made to determine the notches from measured responses [14] [15], and from pinna anthropometry [21] [23].

The frequency response of the pinna was studied by Edgard Shaw and his coworkers [1]-[7], and it was found that the concha acts as a resonator. The resonant frequencies and Q factors seem to be independent of incidence angle, but the magnitude of the responses are highly dependent of direction. Different resonant modes in pinna cavities were identified, and five of these are shown in figure 2.

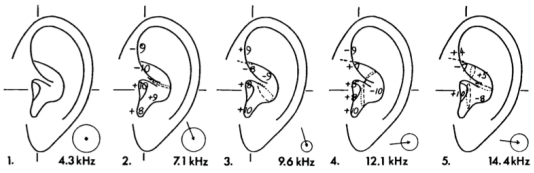

Figure 2: Resonant normal modes in pinna (average of ten subjects). Circles indicate relative degrees of excitation and arrows show directions of maximum response at grazing incidence. Nodal surfaces are shown as broken lines, and relative pressures are given by numerals. Figure found in [1].

The primary resonance of the concha is located at 4.3 kHz. For this mode, there is a uniform pressure distribution which is equally excited from all incidence angles. The other modes display zones with pressure distributions in opposite phase, separated by nodal surfaces. As seen in figure 2, mode 2 and 3 have greatest response at about 75 degrees elevation (grazing incidence), and mode 4 and 5 are strongly excited from the front.

6.1.2 The middle ear

The middle ear is shown in figure 3, and consists of the tympanic membrane, the ossicles and the oval window. Here, the pressure waves are converted into mechanical vibrations, and transmitted to the fluid-filled inner ear.

The ossicles constitute a chain of three movable bones, and are called the malleus, incus, and stapes. It is also common to refer to them as the hammer, the anvil and the stirrup. The malleus is attached to the tympanic membrane, and transmits the vibrations to the stapes via the incus. The stapes is connected to the oval window, which is the opening to the vestibule of the inner ear.

In this process, the pressure is amplified about 25 times, enabling energy transmission from the ear canal to the fluid in the inner ear. The tympanic membrane is about 20 times the size of the the oval window, and rotational motion of the ossicles provide additional amplification. Certain muscles control the movement of the ossicles, and it is believed that they can protect the inner ear from very loud noises by reducing the responses when needed [26] [30].

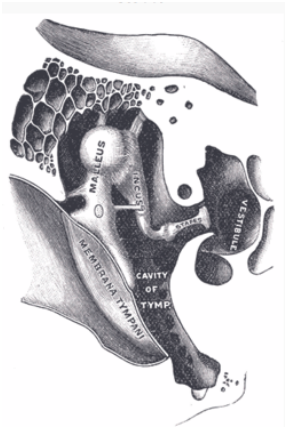

Figure 3: The middle ear. Three small bones transmit vibrations from the ear drum to the oval window. Figure found in [25].

6.1.3 The inner ear

The inner ear includes two main functional parts, the cochlea and the vestibular system. The cochlea coverts the signals received from the middle ear into neural signals that are transmitted to the brain, whereas the vestibular system is involved in the process of controlling balance.

The cochlea is coiled and consists of three parallel chambers filled with liquid, the scala vestibuli, the scala media and the scala tympani (see figure 4). The scala vestibuli and the scala media are separated by a very thin membrane, the Reissner's membrane. The basilar membrane is found between the scala media and the scala tympani, and this is also where the organ of Corti is located. This organ is an important part of the cochlea, and contains between 15 000 and 20 000 auditory sensory cells. The cells are often referred to as "hair cells" , because they have thin "hairs" that are connected to the tectorial membrane. The scala vestibuli starts at the oval window, and the scala tympali terminates at the round window. At the end of the spiral (the apex), the scala vestibuli and the scala tympani are connected. The scala media has a different ion concentration and is separated from the other chambers.

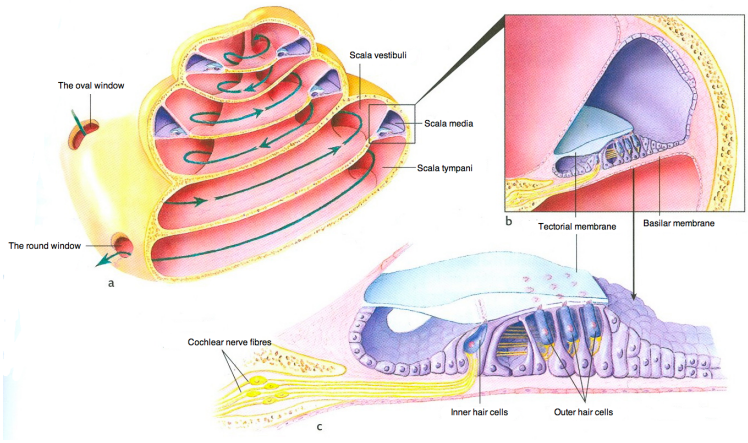

Figure 4: The cochlea is coiled and consists of three parallel chambers filled with liquid. The organ of Corti contains between 15000 and 20000 auditory sensory cells. Figure found in [26].

Figure 5 shows a "folded out" version of the cohclea. When an impulse is received at the oval window, the fluid at the top of the basilar membrane is displaced. The basilar membrane is pushed downwards, and the membrane at the round window bends out. The displacement results in a wave that propagates down the basilar membrane, causing the "hairs" on the hair cells to bend. The basilar membrane becomes wider and softer towards the apex, and resonates close to the base at high frequencies, and near the apex at low frequencies.

When the "hairs" on the inner hair cells are bent, ion gates are opened, and positively charged ions flow into the cell. These ions depolarize the cell, and the resulting receptor potential opens voltage gated calcium channels. Calcium ions enter the cell, and the cell releases neurotransmitters that bind to receptors and trigger transmission of electrical nerve signals. When the basilar membrane is pulled in the opposite direction, the ion gates close, and transmission stops. Up to 1-2 kHz, the nerve impulses track the positive parts of the waveform, and the hearing is phase-locked. Above this area, the envelope, rather than the waveform is followed, so the transients of the signals are detected [10] [33].

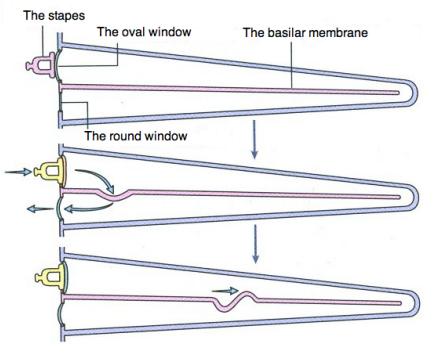

Figure 5: A wave propagates down the basilar membrane. Figure found in [26].

The resonance area on the basilar membrane for a single frequency is narrow, and only a few sensory nerve fibers are affected. This makes humans capable of differentiating between sounds with slightly different pitches. The outer hair-cells narrows the resonance area by attenuating responses on the sides, and amplifying the main signal. The amplification of quiet sounds is greater than the amplification of sounds with high intensity, which is advantageous for perceiving weak sounds.

6.2 Directional hearing

Humans are quite skilled in figuring out where sounds come from. Best localization ability is found in the frontal direction, where displacements as small as one degree can be detected. Towards the sides, the angular resolution decreases to about ten degrees. Because of this, one of the most effective ways to determine the sound direction is turning the head. Other, maybe obvious, important factors are how familiar the sound is and whether the sound source is visible.

Besides from this, there are three main features that are believed to contribute to the process of sound localization. These are interaural level difference (ILD), interaural time difference (ITD) and spectral content. Whereas the two first mechanisms are based on binaural information, spectral information can reveal placement of sound sources from monaural cues. See [32] and [33] for more information.

6.2.1 Interaural level difference

Interaural level difference is the difference between the sound levels at the two ears. For sound incidence from the side, the head causes an acoustical "shadow zone" by blocking the sound path. The effect is hardly noticeable below 500 Hz, but for higher frequencies differences as large as 20 dB can be observed.

6.2.2 Interaural time difference

Interaural time difference is the time it takes from a sound wave reaches the first ear, until it hits the second ear. The largest difference occurs when a sound is presented directly from one side, and corresponds to a ITD of about 700 μs. A certain time delay in the range 1-2 Hz can provide ambigious directional information, and because of this, the localization ability for stationary sounds is limited in this area. Below approximately 100 Hz, the time difference leads to a very small phase difference, which the auditory system is unable to detect.

6.2.3 Spectral cues

Earlier, ITD and ILD were assumed to be the only localization cues humans employed. It was believed that the time difference dominated the process at low frequencies, whereas for high frequencies, the level difference was most significant. This is commonly know as the duplex theory, and was first introduced by Lord Rayleigh [8]. Indeed, ITD and ILD provide useful information for localization of sounds in the horizontal plane (zero degrees elevation). However, the theory cannot explain how discrimination between directions with identical cues take place. These directions are often referred to as "cones of confusion" (see figure 6).

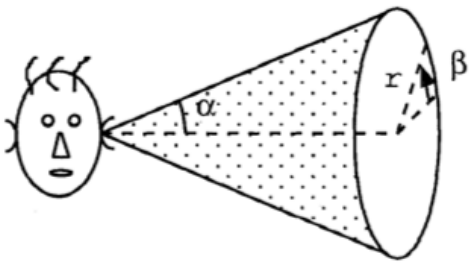

Figure 6: "Cone of confusion" is a term used to denote directions with identical ITD and ILD cues. Figure found in [34].

The third known localization technique is retrieving information from the spectral content. Diffraction around the head, as well as reflections from e.g the shoulders and the pinna will cause modifications in the sound spectrum. As mentioned in section 6.1.1, the pinna is essential for determining source elevation.

Langendijk and Bronkhorst [16] studied the effect of spectral cues on sound localization by removing information from different frequency bands, varying in bandwidth and center frequency. The experiment revealed that the most important cues for discrimination between up and down are likely to be found in the area 5.7-11.3 kHz. Similarly, the frequency band 8-16 kHz seem to provide information about localization in the front and the back. The results also indicated that frequency content below 4 kHz has little effect on localization performance.

6.2.4 Head Related Transfer Functions

The effect of all localization cues can be completely described by head related transfer functions (HRTFs). These are defined in [36] as "a specific individual's left- or right-ear far-field frequency response, as measured from a specific point in the free field to a specific point in the ear canal". Their time-domain counterparts are called head related impulse responses (hrirs), and are obtained by taking the inverse Fourier transform of the HRTFs [37].

Figure 7 illustrates how many of the previously mentioned mechanisms involved in localizing can be seen from HRTFs and hrirs.

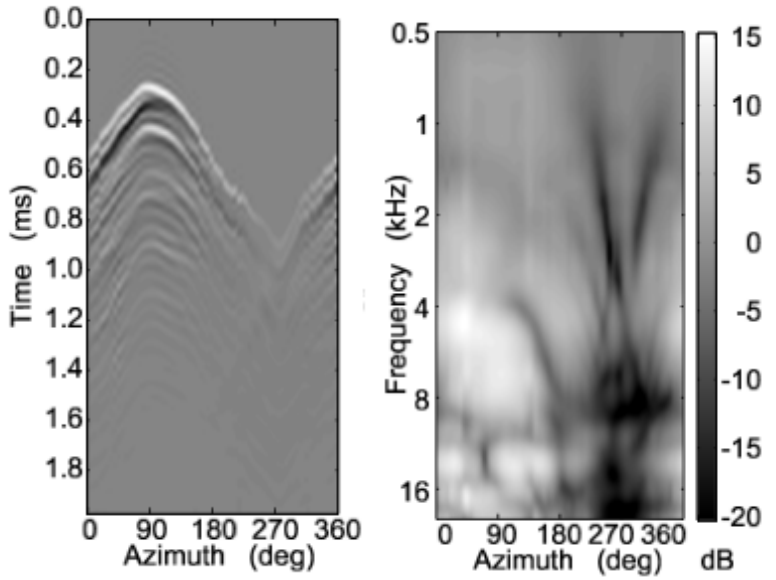

(a) hrir (b) HRTF

Figure 7: Hrir and HRTF for KEMAR's right ear. Each column represents an impulse response at a specified azimuth angle, and the colors of the plot show the strength of the responses. Many of the mechanisms involved in sound localizing can be seen from HRTFs and hrirs. Figure found in [13].

Figure 7(a) shows hrirs measured on the right ear (located at 90 degrees) of the KEMAR mannequin [11] [12]. Here, each column represents an impulse response at a specified azimuth angle, and the colors of the plot show the strength of the responses. The arrival time varies as the source moves closer to and further away from the ear, and several echoes can be observed after the initial

pulse. The effect of head shadow is also visible, as the response grows weaker when the angle approaches 270 degrees.

Figure 7(b) displays the magnitude responses of the HRTFs that correspond to the impulse responses in 7(a). Also here, the head shadow can be observed, since the magnitudes are smaller around 270 degrees. The plot shows that a resonance around 5 kHz exists, and a "pinna notch" can be seen around 9 kHz.

When measuring sets of HRTFs, every direction of interest has to be considered. This demands for special equipment, and includes time-consuming measurement procedures. Research has shown that use of individualized HRTFs give fewer front/back reversals, and also improves localization ability [41] [42]. Because of this, efforts to simplify the process have been made, e.g by developing more efficient measurement techniques, interpolation of databases that already exist, numerical methods, and by use of physical and structural filter models. More information about these simplification methods can be found in [21].

6.3 Interaural coordinate system

For the rest of this report, the interaural coordinate system will be used (see figure 8), unless otherwise is stated. The angles on the left hand side are considered negative, and the angles on the right hand side positive. Variation in elevation is not included in the study.

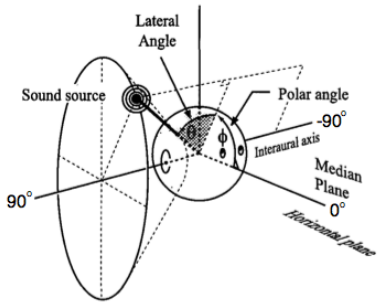

Figure 8: Interaural coordinate system. The angles on the left hand side are considered negative, and the angles on the right hand side are considered positive. Figure found in [38].

6.4 Sphere radius

Kuhn studied ITD in the azimuthal plane [31], and found that measured ITDs in many cases correspond well to calculated values for sound incidence on a rigid sphere. One advantage of modeling the head as a sphere is that it is possible to adapt the sphere radius to the head dimensions of the subjects, thus allowing for customization. The chosen head radius will affect localization performance, and should be carefully selected. Algazi, Avendano and Duda [38] found that the best predictors for the head radius that gives the smallest amount of localization error are the head width and the head depth ($\frac{x_1}{2}$ and $\frac{x_3}{2}$ in figure 9)

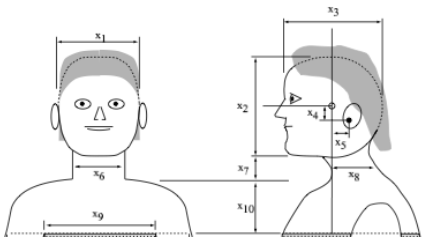

Figure 9: Anthropometric measures. Figure found in [13].

Consequently, the following formula is used to calculate the "optimal" sphere radius (in mm)

$$r_{opt} = 0.51 \cdot \frac{x_1}{2} + 0.18 \cdot \frac{x_3}{2} + 32 \tag{1}$$

6.5 The system

The QuietPro Intelligent Hearing System is a communication and hearing protection device produced by Nacre AS, Norway. The system consists of a digital signal processing unit and two earplugs, and was originally developed for military purposes. Sound from the environment is captured by a microphone on the outside of the earplugs, and played back to the user via a loudspeaker located on the inside. When the sound level exceeds a certain threshold, the system blocks out the noise that is considered harmful. This happens if the impulse or the average level exceeds a certain threshold, and the system monitors the environment automatically. Active noise reduction is also provided, to achieve large attenuation. On the inside of the earplugs, a microphone is located, allowing for radio communication between users in noisy conditions. In the current experiment, only the earplugs will be examined.

The frequency responses of the earplugs were measured using a Coupler ear simulator. 0.1 volt rms white noise was applied, and the set-up is shown in figure 10. The measurement chain was calibrated, and the following instruments were used:

- Rohde & Schwarz audio analyzer, HJ 2043
- Patch panel
- Brüel & Kjær microphone type 4190, 1054924
- Brüel & Kjær microphone preamplifier type 2619, 545579
- Brüel & Kjær measurement amplifier type 2636, CB 4046
- Coupler ear simulator type 4157, 1054924
- Brüel & Kjær calibrator type 4231

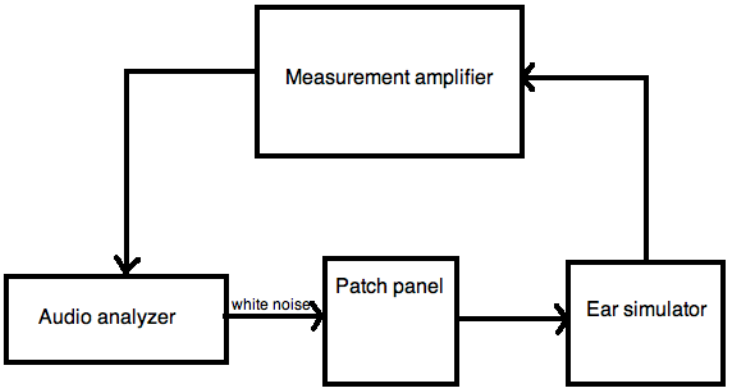

Figure 10: Set-up for measuring frequency responses of the ear plugs.

The resulting frequency responses are shown in figure 11.

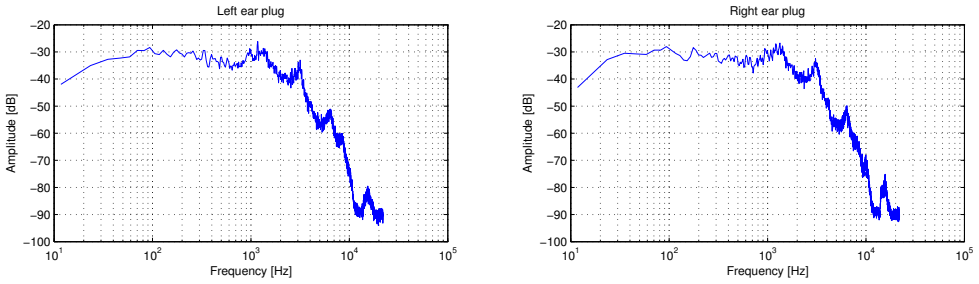

(a) Left (b) Right

Figure 11: Frequency responses for the earplugs used in the experiment.

7 The structural model

As mentioned in section 6.2.4, HRTFs can be represented by a combination of filters, where the different components correspond to anatomical structures. This representation method was first introduced by Genuit [40]. Structural models are relatively simple, and it is possible to adjust the model parameters to individual listeners. This makes it an attractive approach, which has provided promising results [27] [9].

Typically, reflections from different directions are ignored, as well as interaction effects. However, it has been shown that a good approximation of the KEMAR HRTF can be obtained as the product of the mannequin without a pinna attached and a HRTF that accounts for the effect of the pinna alone (often referred to as a PRTF) [22].

Modeling of the pinna is a challenging task, since it requires great level of detail, and large person-to-person variations exist. Attempts have been made to connect features in the PRTF to anthropometry [43] [15] [44], and recently a PRTF database has been made publicly available [45].

The model presented has the structure shown in figure 12 (shoulder reflections are excluded) and was developed in [9].

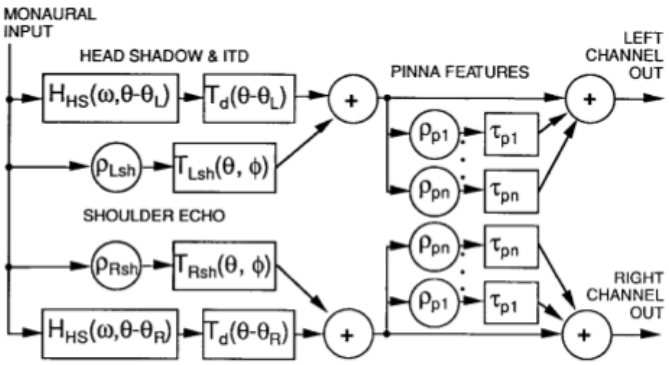

Figure 12: Structural model. Figure found in [9].

7.1 Interaural time difference

Normalized frequency can be defined as

$$\mu = \frac{\omega a}{c} \tag{2}$$

Here c is the speed of sound (343 $\frac{m}{s}$), and a is the effective head radius.

For frequencies where μ>1, the difference between the time the wave arrives at the observation point and the time it would arrive at the center of the sphere in a free field, ΔT, can be approximated by

$$\Delta T(\theta) = \begin{cases} -\frac{a}{c}cos(\theta) & if 0 \leq |\theta| < \frac{\pi}{2} \\ \frac{a}{c}(|\theta| - \frac{\pi}{2}) & if \frac{\pi}{2} \leq |\theta| < \pi \end{cases} \tag{3}$$

[32]. θ is the angle between a ray from the center of the sphere to the sound source and a ray from the center of the sphere to the observation point.

As $\mu \to 0$, the relative delay increases to a value that is about 50 % larger than the value this frequency independent formula predicts.

In order to keep the delays causal, a factor of $\frac{a}{c}$ was added for the implementation, giving

$$T_d(\theta) = \begin{cases} \frac{a}{c} - \frac{a}{c}cos(\theta) & if 0 \leq |\theta| < \frac{\pi}{2} \\ \frac{a}{c} + \frac{a}{c}(|\theta| - \frac{\pi}{2}) & if \frac{\pi}{2} \leq |\theta| < \pi \end{cases} \tag{4}$$

7.2 Interaural level difference

To get an ITD that exhibits proper behavior also for lower frequencies, and to include the effects of head shadowing, the following head shadow filter was implemented:

$$H_H(\omega, \theta) = \frac{1 + j\frac{\alpha\omega}{2\omega_0}}{1 + j\frac{\omega}{2\omega_0}}, \quad 0 \leq \alpha(\theta) \leq 2 \tag{5}$$

where f is frequency, $\omega = 2\pi f$, $\omega_0 = \frac{c}{a}$ and

$$\alpha(\theta) = (1 + \frac{\alpha_{min}}{2}) + (1 - \frac{\alpha_{min}}{2})cos(\frac{\theta}{\theta_{min}}180°) \tag{6}$$

It is the value of α that determines the shape of the frequency response. When $\alpha < 1$ higher frequencies are damped, and when $\alpha = 2$ a 6 dB increase can be observed in the same region (see figure 13(b)).

Figure 13(a) shows the frequency response of an ideal, rigid sphere plotted against μ, and figure 13(b) gives the frequency response of the filter with the values α_{min}=0.1 and $\theta_{min} = 150°$. These values for α_{min} and θ_{min} were used in the study.

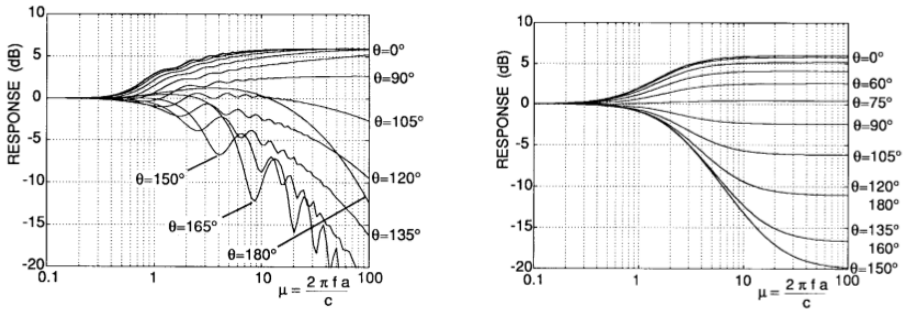

(a) Ideal rigid sphere

(b) Filter given by equation 5 and 6

Figure 13: There is good correspondence between the two frequency responses. Figures found in [9].

As can be seen from figure 13(a) and 13(b), there is good correspondence between the two responses.

The group delay becomes

$$T_g = \frac{1 - \alpha}{2\omega_0} = \frac{1}{2}(\frac{a}{c})(1 - \alpha) \tag{7}$$

as $\omega \to 0$.

At $\theta = 0°$, this filter gives a 50 % larger low-frequency delay than the delay calculated by (3).

Together with the ITD, the resulting filter becomes

$$H_H(\omega, \theta) = \frac{1 + j\frac{\alpha(\theta - \theta_{ear})\omega}{2\omega_0}}{1 + j\frac{\omega}{2\omega_0}} e^{-j\omega T_d(\theta - \theta_{ear})} \tag{8}$$

where T_d is given by (4) and θ_{ear} is the angle the ear is located.

7.3 Pinna model

The effect of the pinna is approximated with series of scaled and reflected main pulses. These reflections are modeled by FIR-filters, and described by a time delay, τ_{pn}, and a reflection coefficient, ρ_{pn}.

7.4 Duda and Brown's approach

Informal listening tests conducted in [9] indicated that the reflection coefficients could be assigned constant values without significantly affecting the final result.

The time delays τ_{pn} were computed by the following formula

$$\tau_{pn}(\theta, \phi) = A_n cos(\tfrac{\theta}{2}) sin[D_n(90° - \phi)] + B_n, \quad -90° \leq \theta \leq 90°, \quad -90° \leq \phi \leq 90° \tag{9}$$

A_n, B_n and D_n are the constants for the n'th reflection, θ is azimuth angle and ϕ is elevation.

Table 1: Values for coefficients in Duda and Brown's study

n	ρ_{pn}	A_n	B_n	D_{n1}	D_{n2}
2	0.5	1	2	1	0.85
3	-1	5	4	0.5	0.35
4	0.5	5	7	0.5	0.35
5	-0.25	5	11	0.5	0.35
6	0.25	5	13	0.5	0.35

Brown and Duda included five reflections in the study in [9]. The coefficients were determined by inspecting the subject's own measured impulse responses. It turned out that D_n was the only coefficient that needed adjustment. D_{n1} was used for two of the subjects, whereas D_{n2} was used for the last person. All the values are given in table 1. This method is tested in one of the conditions in the listening test in the current study, but only with the coefficients A_n, B_n and D_{n1}.

7.5 Alternative approach

Although Brown and Duda's approach is appealing, there is one major draw-back. Measured impulse responses are required to determine the coefficients used in the model. One of the remaining tasks is to link the values to anthropometric measures, e.g. dimensions of the ear. An attempt at doing this was made by studying hrirs found in the CIPIC database [13], and compare with corresponding ears.

7.5.1 Finding delays and reflection coefficients

33 of the subjects were included in this theoretical study, and only left ears were examined. Elevation angle was set to 0°, since only azimuthal dependence was studied. For 25 angles ranging from −80° to 80°, number of samples (τ_{pn}) from the main pulse to the first six following tops or bottoms were counted, and reflection coefficients ($\rho_{pn} = \frac{A_n}{A_1}$, where A_n is the amplitude of the n'th top or bottom and A_1 is the amplitude of the main pulse) were calculated.

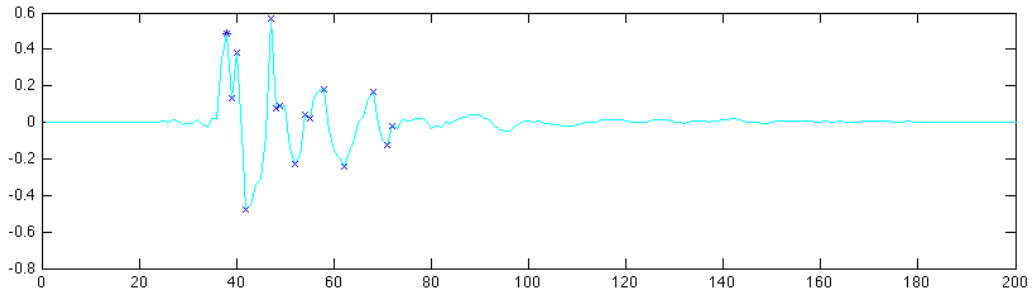

Figure 14: Head related impulse responses (plotted against number of samples) were inspected visually before the tops and bottoms were selected. '*' marks the main pulse, and 'x' shows the tops and bottoms found. In this case reflection 1, 2, 3, 4, 7 and 10 were chosen, to preserve the overall shape of the curve.

7.5.2 Reflection delays

Two different equations were explored to relate τ_{pn} to θ, one trigonometric and one polynomial.

In equation (9), τ_{pn} is a function of both azimuth and elevation, but in the current study the elevation was held constant. So in fact, only two coefficients for each reflection needed to be determined. In the following these two coefficients are denoted A_{tn} and B_{tn}, giving the expression $\tau_{pn} = A_{tn}cos\frac{\theta}{2} + B_{tn}$.

Various τ_{pn}s were plotted against θ, and there seemed to be a decent fit between the data points and curves on the form $A\theta^2$+$B\theta$+C. Because of this As, Bs and Cs for second degree polynomials were calculated. These coefficients are called A_{pn}, B_{pn} and C_{pn}.

The goal was to find the coefficients that resulted in the smallest error (ϵ) when all angles were considered.

$$\epsilon = \sqrt{\sum_{i=1}^{25}(\tau_i - \hat{\tau}_i)^2} \tag{10}$$

Here τ_i is the actual number of samples and $\hat{\tau}_i$ is the estimated number of samples for the i'th angle.

First the coefficients were allowed to vary freely, but based on the observation that the total error changed very little after a certain point, the range shown in table 2 was finally chosen. The coefficients could take on any value inside this interval, and the best combinations were saved.

Table 2: Range for selected coefficients. The coefficients could take on any value inside this interval, and the combinations resulting in smallest error were saved.

	A_{tn}	B_{tn}	A_{pn}	B_{pn}	C_{pn}
Minimum value	-40	0	-3	-2	0
Maximum value	0	80	10	10	20
Step size	0.1	0.1	0.1	0.1	0.1

This gave 198 sets of coefficients (33 subjects and six reflections). Figure 15 shows the data points plotted together with the two curves found for the third reflection of subject 3. The coefficients are A_{tn}=-12.2, B_{tn}=17.1, A_{pn}=1.5, B_{pn}=1, C_{pn}=4.9.

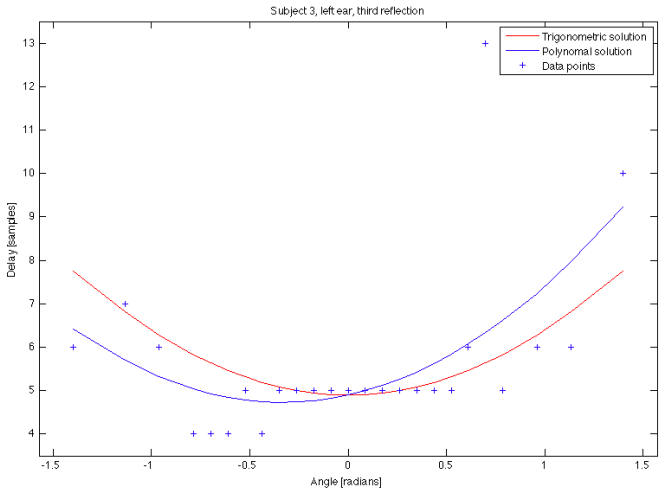

Figure 15: Data points with fitted curves. $\epsilon_{polynomal} = 7.77$, $\epsilon_{trigonometric} = 8.6$ [samples]

In general, the polynomial equation produced results with smaller errors than the trigonometric equation. This may be due to the fact that it is not dependent on symmetric variation around the center, as the trigonometric function is. An example of when the polynomial equation gives a more accurate result is shown in figure 16. Also, the error increased with reflection order.

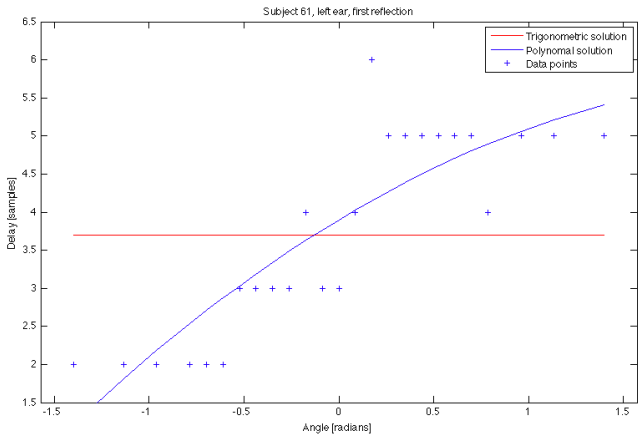

Figure 16: In general, the polynomial equation produced results with smaller errors than the trigonometric equation. In this case $\epsilon_{polynomal} = 3.17$ and $\epsilon_{trigonometric} = 6.4$ [samples].

Table 3 shows mean $\epsilon_{trigonometric}$ and $\epsilon_{polynomial}$ for the 33 subjects.

Table 3: Mean ϵ as function of method and reflection order

Reflection	$\epsilon_{trigonometric}$	$\epsilon_{polynomial}$
1	4.84	4.35
2	6.45	5.71
3	7.49	5.94
4	10.37	7.85
5	12.72	9.94
6	12.86	9.71

After finding the coefficients, attempts to relate them to ear dimensions were made. The ear measures for the selected subjects were found in the CIPIC database, and figure 17 shows the available quantities.

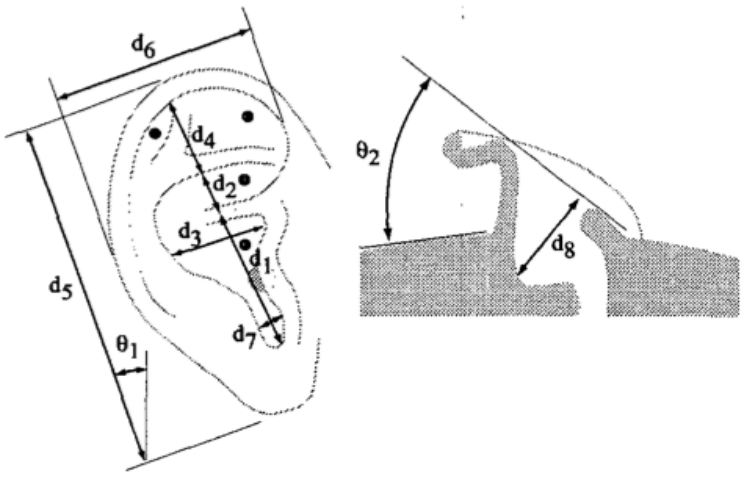

Figure 17: Ear dimensions available in the CIPIC database. Figure found in [13].

In addition to testing the connection between the coefficients and d3, d6 and d8 alone, the quantities $\frac{d3}{d1}$, d1· d3· d8, $\frac{d6}{d5}$, $\frac{d3}{d1+d2+d4}$, $\frac{d6}{d1+d2+d4}$ and $\frac{d3}{d6}$ were examined. Unfortunately, no relationship was detected. Some of the resulting normalized plots are shown in figure 18(a) - 18(e).

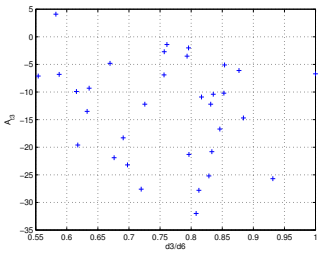

(a) A_{t3} plotted against $\frac{d_3}{d_6}$

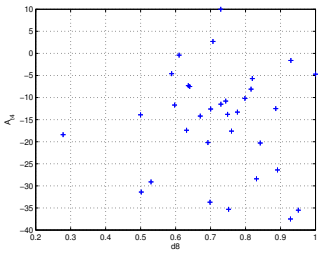

(b) A_{t4} plotted against d_8

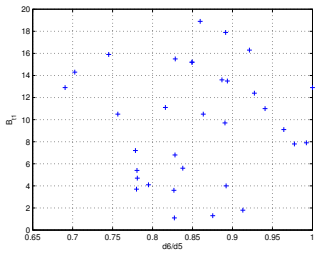

(c) B_{t1} plotted against $\frac{d_6}{d_5}$

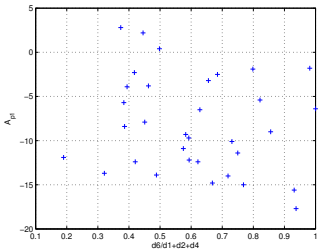

(d) A_{p1} plotted against $\frac{d_6}{d_1+d_2+d_4}$

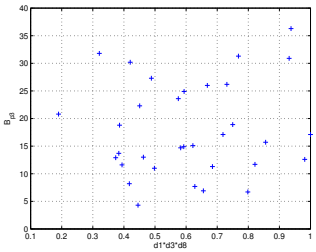

(e) B_{p3} plotted against $d_1 \cdot d_3 \cdot d_8$

Figure 18: Coefficients plotted against ear dimensions shown in figure. No relation was found between the coefficients and anthropometric measures. 17

Since the attempt to relate the coefficients to ear dimensions gave discouraging results, the mean values and standard deviations for the τs were calculated. These results are shown in figure 19.

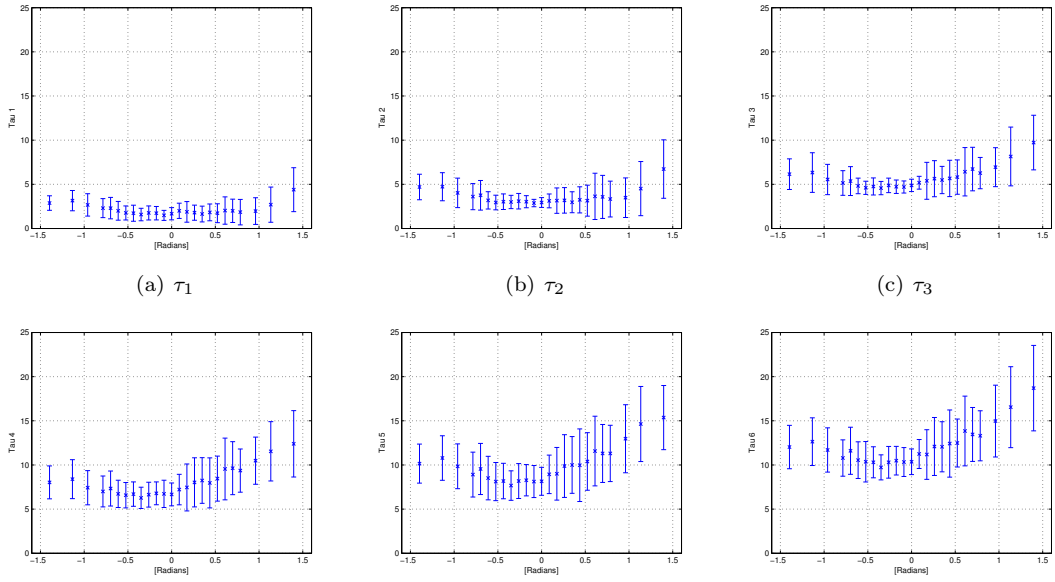

(a) τ_1 (b) τ_2 (c) τ_3

(d) τ_4 (e) τ_5 (f) τ_6

Figure 19: Mean reflection delays and standard deviations

The results are asymmetric around zero degrees, especially for reflections of higher order. Because of this, second degrees polynomials were found (as before) to approximate the data. The resulting coefficients and errors are displayed in table 4.

Table 4: Coefficients and errors for τ approximation

Reflection	A	B	C	ϵ_τ
1	1	0	1.6	1.46
2	1.3	0.2	2.9	1.68
3	1.5	1	5	1.27
4	1.9	1.6	7.1	1.77
5	2.5	1.8	8.7	2.52
6	2.5	2	10.9	2.30

The polynomials correspond well to the mean values. This is shown in figure 20.

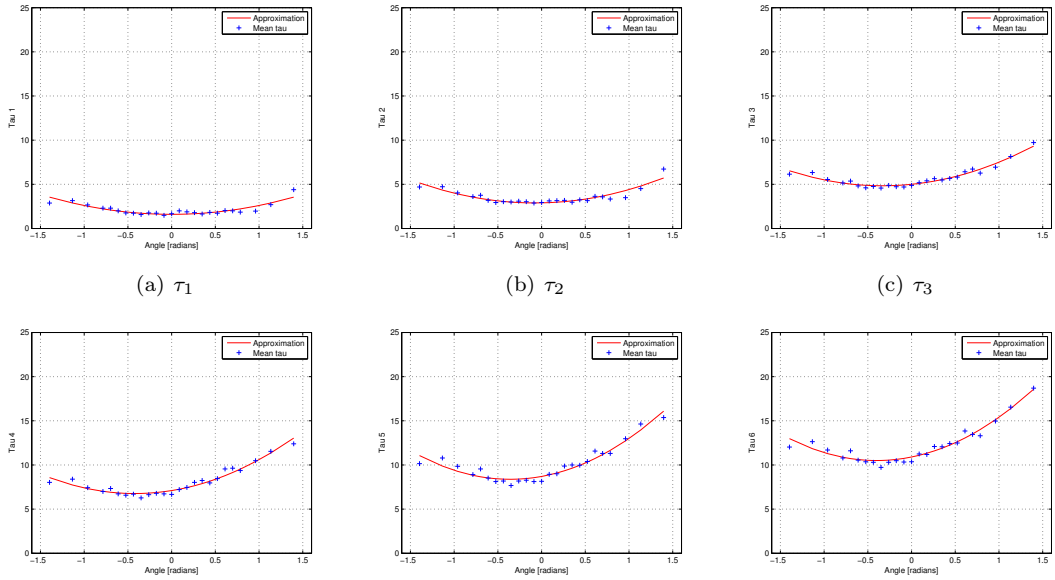

(a) τ_1 (b) τ_2 (c) τ_3

(d) τ_4 (e) τ_5 (f) τ_6

Figure 20: Mean reflection delays and polynomial approximations. There is a good fit between the data and the approximations.

This is the response for the left ear only. In order to find the results for the right ear, it was assumed that the head is symmetrical, and that these relations are valid for the right ear as well. The responses had to be mirrored around 0 degrees, and this was done simply by multiplying the $B_{pn}s$ with -1.

7.5.3 Reflection coefficients

A similar analysis was carried out for the reflection coefficients, but no attempts were made to relate them to anthropometric measures. Instead, the mean values and standard deviations were calculated right away, and their azimuthal dependence was explored.

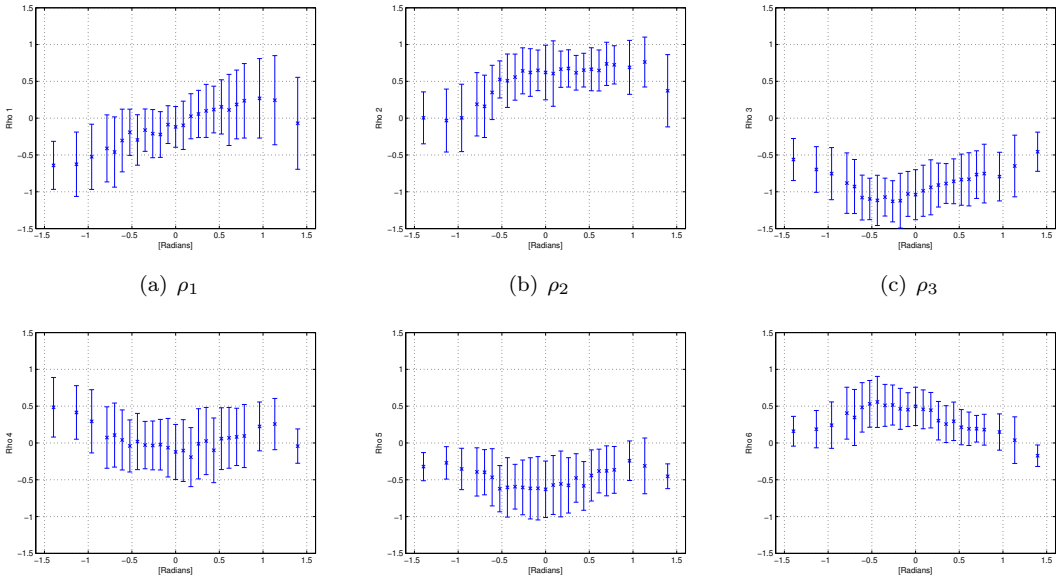

(a) ρ_1 (b) ρ_2 (c) ρ_3

(d) ρ_4 (e) ρ_5 (f) ρ_6

Figure 21: Mean reflection coefficients and standard deviations

As seen in figure 21(a)-21(f), the mean values could be approximated with second degrees polynomials.

The resulting coefficients and errors are given in table 5, and figure 22(a)-22(f) shows the results.

Table 5: Coefficients and errors for ρ approximation

Reflection	A	B	C	ϵ_ρ
1	-0.1	0.3	-0.1	0.48
2	-0.2	0.3	0.6	0.48
3	0.3	0.1	-1	0.43
4	0.2	-0.1	0	0.52
5	0.2	0	-0.6	0.46
6	-0.2	-0.1	0.4	0.37

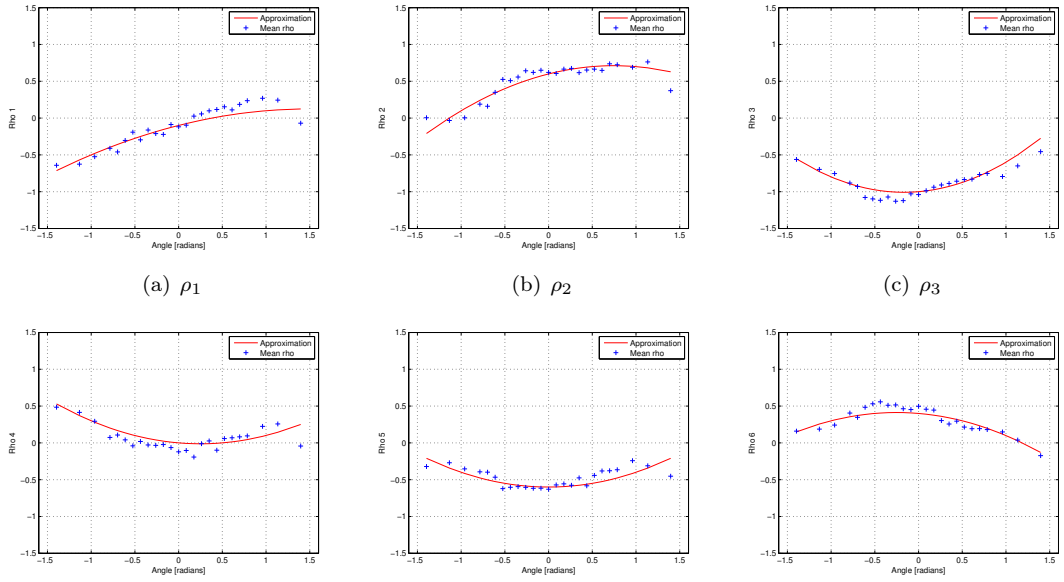

(a) ρ_1 (b) ρ_2 (c) ρ_3

(d) ρ_4 (e) ρ_5 (f) ρ_6

Figure 22: Mean reflection coefficients and polynomial approximations.

To find responses for the right ear, the B values were multiplied with -1, as in the case for the polynomial approximation for the reflection delays.

8 Analytical solution

The other model presented is simply the analytical solution of the wave equation for a plane wave incident on a rigid sphere, and is given by

$$p_{sphere} = p_0 \Sigma_{l=0}^{N} (2l+1) i^l j_l(kr) P_l(cos\theta) + \Sigma_{l=0}^{N} A_l h_l(kr) P_l(cos\theta) \tag{11}$$

where j_l is the spherical Bessel function, P_l is the Legrende function of order l, i is $\sqrt{-1}$,

$$A_l = -p_0 (2l+1) i^l \frac{l j_{l-1}(ka) - (l+1) j_{l+1}(ka)}{l h_{l-1}(ka) - (l+1) h_{l+1}(ka)} \tag{12}$$

and H_l is the spherical Hankel function of the first kind of order l.

This was derived by Lord Rayleigh in [35]. In section 7.2, responses for various incidence angles are shown in figure 13(a).

9 Methods

In the sound localization experiment, seven simulation methods were tested on 14 subjects. One stimulus consisted of three short noise bursts that were presented to the participants via the QuietPro earplugs. The subjects' task was to identify the sound source location. Each condition included 33 stimuli, and additional four test stimuli were provided, to make sure the subjects were ready and had completely understood the instructions. This resulted in a total of 235 series of noise bursts for each person. The test session lasted about one hour, and included measuring head dimensions, as well as performing the localization test. However, six subjects needed to come back for an additional session, after an error was discovered.

Prior to the experiment, an audiometry was performed, to check for hearing damage.

9.1 Subjects

14 subjects in the age range from 23 to 27 years were selected to participate in the experiment. This group included three females and eleven males. The subjects will be referred to as subject 1 to 14 for the rest of the report.

Before the experiment, a pure-tone audiometry for 125 Hz, 250 Hz, 500 Hz, 1 kHz, 2 kHz, 4 kHz and 8 kHz was conducted on every subject. The instructions for the procedure are found in [29].

Two criterions were stated. The subjects should not display a difference of more than 15 dB in the two measured hearing thresholds, and not exceed a hearing threshold of more than 20 dB above the minimum audibility curve for any of the frequencies tested.

Results from the audiometry are found in appendix A.

Subject 2 has normal hearing for the frequency range from 125 Hz to 4 kHz, but at 8 kHz a hearing loss of 40 dB on the left ear, and 25 dB on the right ear is observed. For subject 8, at 8 kHz, the hearing threshold is 30 dB above the minimum audibility curve the left hand side, and 25 on the right. Subject 11 displays a 20 dB difference between the left (20 dB) and the right (0 dB) ear at 1 kHz. All the subjects are still included in the study, in order to ensure a good statistical foundation.

Each person was supposed to complete a one-hour session that covered necessary preparations, as well as the localization test. However, after six sessions were finished, an error in the code for two of the conditions (low-pass filtered an unfiltered "average" pinna model developed in section 7.5) was discovered, and these subjects had to come back and perform another test. This time, the session lasted between 15 and 20 minutes. This included subject 2, 4, 7, 8, 9 and 11.

9.2 Stimuli

The stimuli consisted of three 150 ms noise bursts with 100 ms silence between. Generally, broad band noise provides good localization accuracy. To avoid an overemphasis of high frequency content, pink noise was applied instead of white noise.

The sound level was measured using the same equipment as when obtaining the frequency responses of the earplugs. The maximum RMS value averaged over 0.1 s was 81 dB for both ear plugs. The results were consistent when the measurement was repeated.

9.3 Experimental set-up.

The listening tests were conducted in the Aura lab at NTNU. 36 paper sheets were placed with 10 degrees spacing in a circle with a radius of two meters. The sheets were numbered from 1 (directly in front) to 36 (10 degrees to the left), and placed on top of loudspeakers and chairs, or hung on microphone stands. The subjects were seated in the middle of the ring, looking straight forward. Figure 23 shows a sketch of the experimental set-up.

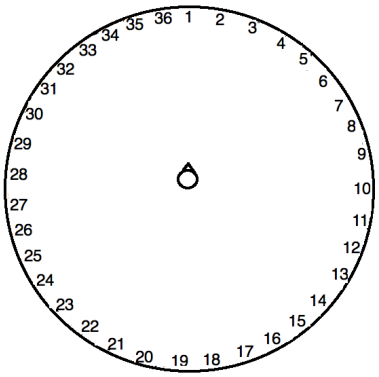

Figure 23: Experimental set-up. Each number indicates a possible sound direction.

The noise bursts were generated by Matlab on a MacBook 5,1, and presented to the participants via QuietPro ear plugs. A patch panel was used to send the signals to the earplugs. The set-up is shown in figure 24.

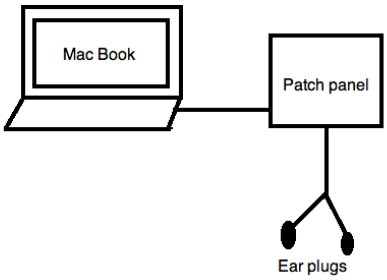

Figure 24: Generation and presentation of stimuli

9.4 Experimental conditions

The theoretical foundation for the simulation methods was presented in section 7 and 8. Low-pass filtering at 8 kHz was applied in two conditions, since this will happen when the DSP unit in the QuietPro system is included in the signal chain.

Analytical solution of the wave equation for a plane wave incident on a rigid sphere was the first method explored (see section 8), and resulted in two experimental conditions. One version was tested without modifications, and the other was low-pass filtered.

The second approach was based on the structural model developed by Brown and Duda in [9] (details are given in section 7), where the time difference between the two ears was calculated using equation 3. The response of sound scattering on a rigid sphere was imitated by the pole-zero filter to account for the interaural level difference.

Performance of the "average" pinna model developed in section 7.5 was tested, along with the pinna model applied for two subjects in [9]. This resulted in seven experimental conditions:

1. Analytical solution of the wave equation
2. Low-pass filtered version of analytical solution of the wave equation
3. Time delay
4. Time delay and head filter
5. Time delay, head filter and pinna filter (Duda‘s version)
6. Time delay, head filter and pinna filter (version found from CIPIC database)
7. Low-pass filtered version of time delay, head filter and pinna filter (version found from CIPIC database)

In the following, the term "spherical model" refers to the analytical solution of the wave equation. Hopefully, this will not be a confusing denotation, although all the models in some ways are "spherical". The pinna model developed from the CIPIC database will be called "alternative pinna model". The time delay and head shadow filter are included in both versions of the pinna models.

9.5 Experimental procedure

Before the listening tests, the required head dimensions were measured (see equation 1) using three rulers attached as shown in figure 25. The ear angle was found by using a piece of string and a pen. The ear locations were marked before measuring the string length around the head. The total length was divided by 360, and the result multiplied by the distances from the front to the ears. The mid point of the ear canal was chosen as the point defining "ear angle". The results were used as input to the models, and Matlab calculated the individualized impulse responses for all simulation methods.

After the measurements, an inspection of the ears was carried out, to determine correct size of the foam plugs.

Before the test started, the subjects were instructed to at all times keep their gaze at paper number 1 during playback. After the stimulus was done, the participants were free to turn their heads to see the number on the paper in the perceived sound direction.

The participants kept the Mac Book in their laps. They gave responses by typing in the number found on the note located in the registered sound direction. The answers were saved in Matlab, along with "correct" source angle.

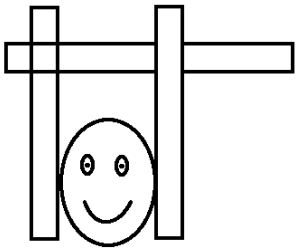

Figure 25: Equipment used for obtaining head dimensions.

Subject 2,4,7,8, 9, 11 and 12 received the stimuli in the following order:

1. Time delay and head filter
2. Duda's pinna model
3. Low-pass spherical (analytical)
4. Time delay
5. Alternative pinna model
6. Low-pass alternative pinna model
7. Spherical (analytical)

All these participants, except subject 12, had to come back for the additional test session. In this case the low-pass filtered version of the alternative pinna model was presented before the unfiltered alternative pinna model.

The rest of the subject were exposed to the stimuli in following order:

1. Alternative pinna model
2. Low-pass spherical (analytical)
3. Time delay
4. Time delay and head filter
5. Spherical (analytical)
6. Duda's pinna model
7. Low-pass alternative pinna model

The sounds were presented in blocks of 33, i.e all stimuli belonging to the same simulation method were presented sequentially, but the angles were randomly chosen. Once presented, It was not possible to repeat the stimuli. All simulated directions were located in front of the subjects, and

included the following angles: ±80, ±60, ±40, ±20, ±10 and 0 degrees. No breaks were scheduled, but the subjects controlled the progress themselves by requesting the next noise sequence.

9.6 Statistical analysis

To see if statistically significant differences existed between the simulation methods, two different statistical analyses were conducted. In the first, comparisons of responses for each angle were made. This was done to examine where differences are most pronounced. In the second analysis, total error was investigated, serving as a measure of overall performance.

To compare the means, analysis of variance (ANOVA) was performed in SPSS [52]. Conducting several t-tests would increase the chances of committing a type I error, i.e falsely reject the null hypothesis that no differences between mean errors exist.

However, for the results to be valid, the following requirements must be fulfilled:

- Response variable have to be normally distributed
- Samples need to be independent
- Population variances must be equal

Because of this, Levene's test of homogeneity was applied prior to the analyses. The test statistic is defined as

$$W = \frac{(N-k)\Sigma_{i=1}^{k} N_i (Z_{i\cdot} - Z_{\cdot\cdot})^2}{(k-1)\Sigma_{i=1}^{N_i}(Z_{ij} - Z_{i\cdot})^2} \tag{13}$$

Here W is the result of the test, k is the number of groups, N is the total number of samples, N_i is the number os samples in the ith group, Y_{ij} is the value of the jth sample from the ith group, $Z_{ij} = |Y_{ij} - \overline{Y}_i|$, $\overline{Y}_i$ is a mean of ith group, $Z_{\cdot\cdot} = \frac{1}{N}\Sigma_{i=1}^{k}\Sigma_{j=1}^{N_i} Z_{ij}$ is the mean of all Z_{ij} and $Z_i = \frac{1}{N_i}\Sigma_{j=1}^{N_i} Z_{ij}$ is the mean of the Z_{ij} for group i [39].

If the variances were found unequal, a Welch test was conducted. This is an approximate test of equality of means, and the condition of homoscedasticity does not have to be fulfilled to get reliable results. In the case of equal variances, the ANOVA was applied.

The criterion for equal variances also applied to the post-hoc tests. When a statistically significant result (α<0.05) was discovered by either of the first tests, it was interesting to find out which of the simulation conditions were involved. For this purpose, multiple comparison tests were carried out. These tests check for statistically significant differences between the means of all groups. In the case of equal variance, a Tukey's honestly significant difference test was conducted. For unequal variances, a Games-Howell test was applied. More information about the calculation algorithms can be found in the "help" feature of [52].

10 Analysis and Results

In this section, the results from the experiments will be presented. First, the effects of source reversals are discussed. One of the subjects was eliminated from the analysis, and the reason for this is explained in detail. It will also become clear why special care in interpreting some of the data is required.

In the final part, the results from the two statistical analyses are given.

10.1 Left/right confusion

A left/right confusion occurs when a simulated sound from the right is perceived as coming from the left, or vice versa. Left/right reversals were observed in all experimental conditions, and turned out to be highly dependent on person and applied simulation method.

Table 6: Left/right confusion for each subject.

Subject number	1	2	3	4	5	6	7	8	9	10	11	12	13	14
Low-pass filtered alternative pinna	1	6	3	0	7	0	0	0	0	0	0	0	0	3
Time delay	0	0	3	1	1	0	0	1	0	0	0	1	2	0
Low-pass filtered spherical model	0	0	0	0	0	0	0	3	5	0	0	0	0	0
Duda's pinna	0	0	3	1	0	0	0	0	0	0	0	0	0	0
Spherical model	0	0	1	0	0	0	0	0	6	0	0	0	0	0
Alternative pinna	0	15	0	0	4	0	0	0	0	0	0	0	1	1
Time delay + head shadow filter	0	0	0	0	3	0	0	0	0	1	0	0	1	0
Total	1	21	10	2	15	0	0	4	11	1	0	1	4	4

As can be seen in table 6, subject 2 experienced 21 left/right reversals, and 15 of them occurred in the alternative pinna model. Visual inspection of the data indicated that the person was completely unable to localize the sound direction correctly. In addition to a large number of left/right confusions, sources simulated in front were perceived as far off to the side.

One explanation to this may be found by inspecting this subject's audiogram. A hearing loss of 45 dB at 8 kHz is reported for the left ear, and 25 dB for the right. This may be the reason for the poor performance. It is rather surprising that a large effect also can be seen in the low-pass filtered model, as the subject has a rather normal hearing threshold (10 and 5 dB above the minimum audibility curve for the left and right ear, respectively) at 4 kHz.

Similar behavior can be observed for subject 5, but to a smaller extent. This person reported a total of four left/right confusions in the alternative pinna model, and seven in the low-pass filtered version. However, subject 5 has no significant hearing loss in the high-frquency area.

Since left/right confusions may be the result of regular localization inaccuracy, it is plausible to assume that this effect is most pronounced for angles close to zero degrees. If a simulated source direction of 10 degrees results in a response at -10 degrees, there is only 20 degrees difference between the two directions. This is indeed the case for most simulation conditions (see appendix C for angular distribution of left/right confusions in every method), and it indicates that the subjects to some extent are capable of identifying correct source directions. In the alternative pinna and the low-pass filtered alternative pinna model, subject 2 experienced 57 % of the confusions for angles with an absolute value of 40 degrees or more.

Based on this, subject 2 is eliminated from the rest of the analysis, as the responses in these two conditions seem to be randomly chosen. Another explanation could be that this person possesses ears that deviate from the "average" to such an extent that correct localization with

the alternative pinna method is impossible, but based on the large differences observed in the audiogram this seems unlikely.

Figure 26 shows the angular distribution of left/right confusions in the experiment, with and without subject 2.

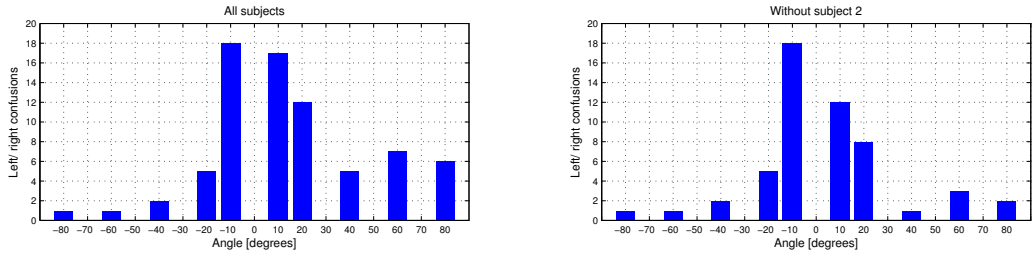

(a) All subjects

(b) Subject 2 removed

Figure 26: Left/right confusions as a function of simulated source direction, with and without subject 2.

10.2 Front/back confusion

The other type of source reversal encountered in the study is called front/back confusion, and is a common and well-documented phenomenon [9]. If the simulated sound direction is 10 degrees, but the source is perceived to be located at e.g 160, 170 or 180 degrees, it is an instance of front/back confusion. This is also the case if the simulated sound is supposed to come from behind, but the subject thinks that it arises from the front.

As earlier mentioned, all the simulated source directions were located in front of the subject. In order to quantify the degree of front/back confusion a method introduces, one approach could be to count all the responses with magnitudes greater than 90 degrees. However, for large incidence angles, the same effect that was discussed for left/right confusions at angles close to zero degrees applies. If a subject thinks a sound comes from the back, it might be because the person is unable to localize the sound direction correctly, and it is impossible to know whether this is due to front/back confusion or just "regular" localization inaccuracy.

Figure 27(a)-27(f) show all given responses for angles on the left hand side in the experimental condition with the analytical spherical head model. For zero and -10 degrees (figure 27(a) and 27(b)), distinct groups of responses are observed, and it is easy to separate localization error from front/back confusion. For -20 and -40 degrees (figure 27(c) and 27(d)), the groups seem to have moved closer together, and for -60 to -80 (figure 27(e) and 27(f)) degrees they completely overlap.

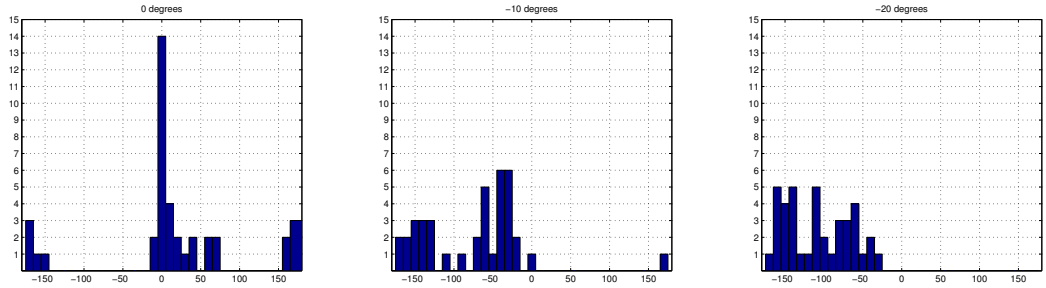

(a) 0 degrees (b) -10 degrees (c) -20 degrees

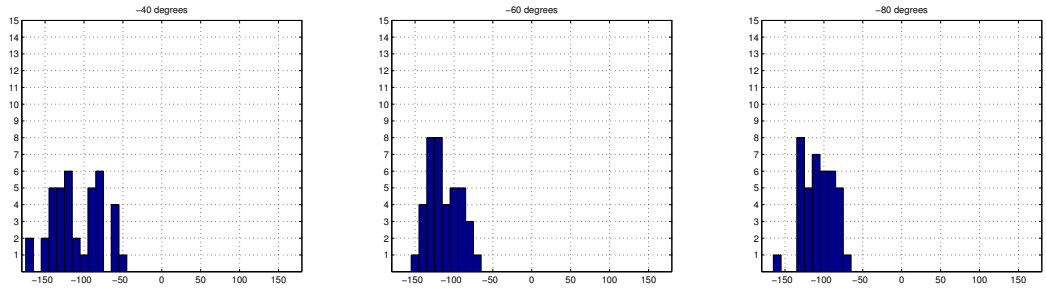

(d) -40 degrees (e) - 60 degrees (f) -80 degrees

Figure 27: Histograms showing given responses for all angles in the spherical method. Front/back confusions are clearly distinguished from regular localization "blur" for small angles. For large angles, the two areas overlap, and it is impossible to separate one effect from the other. Only the left hand side is shown, since both sides display similar behavior.

The consequence of this is that angles with absolute value greater than or equal to 60 degrees are eliminated from the analysis of front/back confusion. It could be argued that the groups in -20 and -40 degrees also are too closely spaced, but at 40 degrees, the non-overlapping area is 50 degrees. This means that localization errors up to 50 degrees both for the reversed and the unreversed version are included. There is a sliding transition from two groups to one, and the boundary at 40 degrees is only introduced to be able to analyze the results. Although some mistakes may occur, it is assumed that the main effects can be captured at these angles. Consequently, for angles ranging from -40 to 40 degrees, the responses with absolute values above 90 degrees are considered front/back reversals.

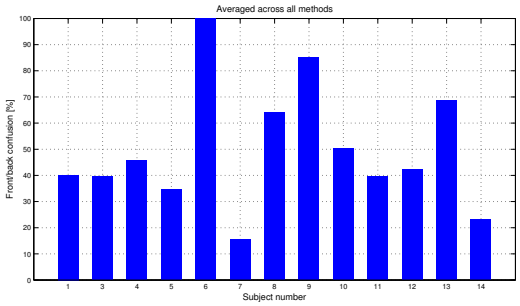

(a) Subject

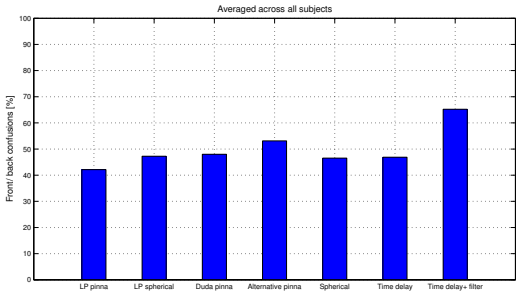

(b) Method

Figure 28: Total front/back confusion

Figure 28 shows front/back confusions as a function of subject and simulation method. Clearly, there is large variation between the different individuals (figure 28(a)). Subject 6 perceived all the sounds as coming from behind, whereas subject 7 experienced this for about 15 percent of the stimuli. These are the extreme values, and the majority of the subjects are located in the range from 30 to 70 percent.

Also when examining front/back confusion as a function of chosen method, variation is observable (see figure 28(b)). The low-pass filtered pinna model has the lowest amount, around 42 percent. For the case with head shadow filter and time delay, the share of sounds perceived from the back is as high as 65 percent. The remaining methods display front/back confusion for 45 to 55 percent of the responses. This is a large number, and clearly, it is hard to discriminate front from back. Since the share is located around 50 % it can be assumed that the subjects, at least to to some degree, were guessing when deciding between the two directions.

10.3 Scatter plots

For simulated source angles at ±40, ±20, ±10 and zero degrees, localization accuracy will be examined after front/back confusion is removed. This is done by converting the responses in the back to the corresponding angles in the frontal hemisphere (e.g a response at -160 degrees becomes -20 degrees, and a response at 150 degrees becomes 30 degrees). Thus, only angles ranging from -90 to 90 degrees will be considered. The remaining responses (at ±60 and ±80 degrees) are left unaltered, unless otherwise is stated.

A scatter plot shows the relation between given and "correct" responses. Scatter plots for all the subjects in each condition are displayed in figure 29. The sizes of the dots reflect number of responses, and the red line marks "correct" answer.

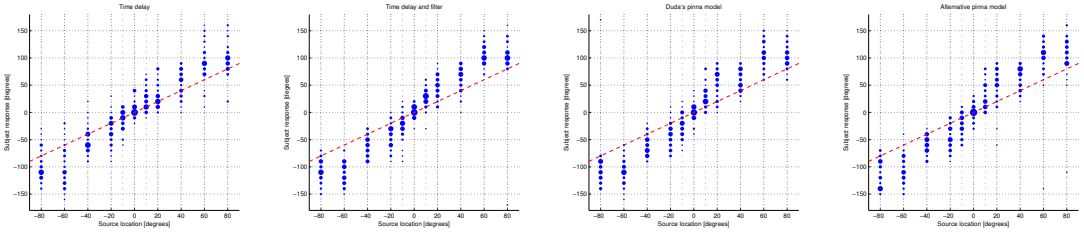

(a) Time delay (b) Time delay and filter (c) Duda's pinna model (d) Alternative pinna model

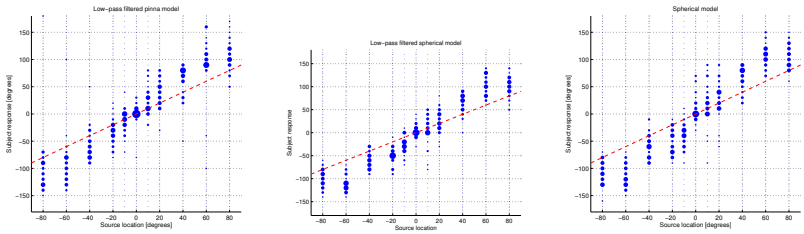

(e) Low-pass filtered alternative version (f) Low-pass filtered spherical model (g) Spherical model

Figure 29: Scatter plots for all conditions. The red line indicates "correct" responses, and the sizes of the blue dots reflect number of given responses. Perceived source location is often found further to the side (i.e to the left on the left hand side, and to the right on the right hand side) than the simulated source location. Note that front/back reversals are removed for simulated source angles between -40 and 40 degrees.

Generally, there is good correspondence between simulated direction and responses at zero degrees. Apparently, it is harder to differentiate between the other incidence angles, and there is a tendency to perceive sources further to the side than what is simulated. In the negative half of the plots, the majority of the responses can be found below the red line. To the contrary, most responses in the positive half are located above the line.

10.4 Localization error

Localization error is defined as response - simulated direction on the left hand side and for zero degrees ($-90<\theta\leq 0$), and simulated direction - response on the right hand side ($0<\theta\leq 90$). A positive localization error indicates that the absolute value of the perceived angle is smaller than the simulated angle, and a negative error reveals the opposite. For zero degrees, a response to the right leads to a positive error, and a response to the left gives a negative value. Two definitions are necessary, because of the chosen coordinate system, and since the filters are symmetric around zero degrees (it is assumed that they perform equally well on both sides). Consequently, if a negative error was defined as e.g a response to the left of simulated source direction, the responses would most likely cancel out, and resulting mean error become zero degrees.

10.4.1 Personal localization error

Mean localization error with standard deviation for every subject in each condition are displayed in figure 30. In this analysis, responses for ± 60 and ± 80 degrees are excluded, since degree of front/back confusion is unknown (see section 10.2). Responses for zero degrees are also left out, since they would affect the mean value of localization error.

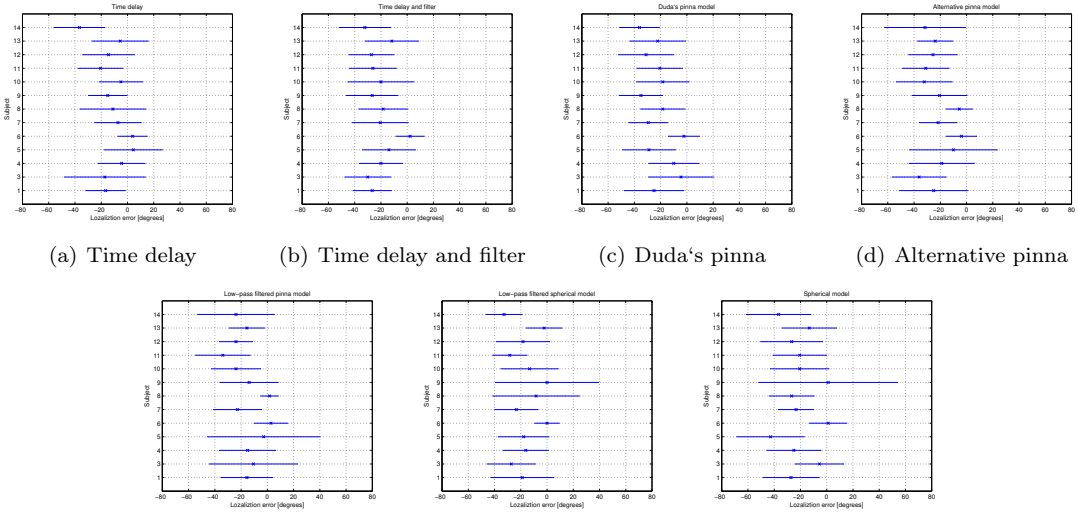

(a) Time delay (b) Time delay and filter (c) Duda's pinna (d) Alternative pinna

(e) Low-pass filtered pinna (f) Low-pass filtered spherical model (g) Spherical model

Figure 30: Average localization error for every subject

The majority of the subjects display negative mean values, as expected from the results in section 10.3. Large variations in localization ability exist, and it is apparent that a person's performance depends on presented method. Subject 9 has the biggest standard deviation for both conditions involving the spherical model, with a maximum of more than 50 degrees for the unfiltered version. However, for e.g the method with time delay and filter, there is little difference between this person and the other subjects. Subject 6 stands out as a good "localizer", with mean errors close to zero degrees and relatively small standard deviations in all the methods.

10.4.2 Intersubject variability

Since localization performance varied across subjects, it was interesting to examine how consistent they were in giving responses. If a person had judged a stimulus to come from one direction, would the same person respond in the same manner the next time the sound was presented?

In the first part of the investigation, the three responses for ± 40, ± 20 and ± 10 degrees in each method were grouped together (after front/back confusions were removed), and means and variances were calculated. Responses for zero degrees were again left out, to avoid affecting the mean value. This gave a total of 42 (6 angles $\cdot$ 7 methods $= 42$ values) means and variances. In table 7 the mean of these values are found ("Mean" and "Variance 1") together with corresponding standard deviations ("Std 1"). The mean value shows the tendency to perceive stimuli closer to (positive mean) or further away from (negative mean) zero degrees than the simulated source direction. The mean variance is a measure of consistency between the subject's responses.

In the second part, simulated source direction at ± 60 and ± 80 degrees were examined, and only variances ("Variance 2") were considered. As before, a low value indicates consistency, but now a high value can reveal source reversals in the responses given for the same angle, since front/back confusions are preserved. For most subjects, the second variance is smaller than the first, but for subject 4 and 5, an increase is observed.

Table 7: Intersubject variability

Subject	Mean	Variance 1	Std 1	Variance 2	Std 2
1	-22.14	263.49	16.23	227.21	15.07
3	-18.73	532.54	23.08	379.59	19.48
4	-15.63	335.71	18.32	695.24	26.37
5	-15.95	681.75	26.11	2027.90	45.03
6	0.56	39.68	6.30	34.01	5.83
7	-21.19	236.51	15.38	116.33	10.79
8	-12.38	394.44	19.86	178.23	13.35
9	-15.71	320.63	17.91	210 .20	14.50
10	-19.05	269.84	16.43	67.35	8.21
11	-25.87	318.25	17.84	74.83	8.65
12	-23.89	211.90	14.56	91.16	9.55
13	-13.49	175.40	13.24	123.13	11.10
14	-32.86	373.02	19.31	100.68	10.03

In both conditions, subject 5 displays most variation in given responses. This is also the person with the highest number of left/right confusions, since subject 2 was removed from the analysis. It may be assumed that this subject is inconsistent when discriminating front from back, due to the high variance in the second part. The majority have average standard deviations in the range from 10 to 24 degrees, which means there probably is a random component involved in their decision making.

Subject 6 shows remarkable consistency, and is also the subject with smallest deviation (0.56 degrees to the right) from "correct" values. It is interesting to note that this is the only person with 100 % front/back reversals. The other subjects have mean values ranging from -12 to -33 degrees.

10.4.3 Method variability

A similar analysis as the one described as part one in section 10.4.2 was conducted for the separate methods as well. The three responses for each angle in each model were grouped together, and the means and variances were calculated. This resulted in a total of 78 means and variances for each method (6 angles $\cdot$ 13 participants = 78 values). The mean of these values are shown in table 8 with corresponding standard deviations.

Table 8: Method variability

	Mean	Variance	Resulting standard devation
Low-pass filtered alternative pinna model	-6.22	446.15	21.12
Time delay	-6.27	238.00	15.43
Low-pass filtered spherical model	-5.04	96.74	9.84
Duda‘s pinna model	-5.64	293.47	17.13
Spherical model	-5.45	143.12	11.96
Alternative pinna model	-6.13	144.29	12.01
Time delay and head shadow filter	-6.78	130.54	11.43

There is little variation in the mean values found in each method, with only two degrees separating the smallest and largest deviation from simulated source direction. The low-pass filtered alternative pinna model has the largest standard deviation (21.12 degrees), whereas the lowest value is found in the low-pass filtered spherical model (9.84 degrees).

10.5 Statistical analysis

Two statistical analyses were carried out in SPSS [52], in order to evaluate the performance of the methods. First, responses for each angle were compared, and then total error (eliminating angular dependence) was examined. However, in order to include ±60 and ±80 degrees, some assumptions were made.

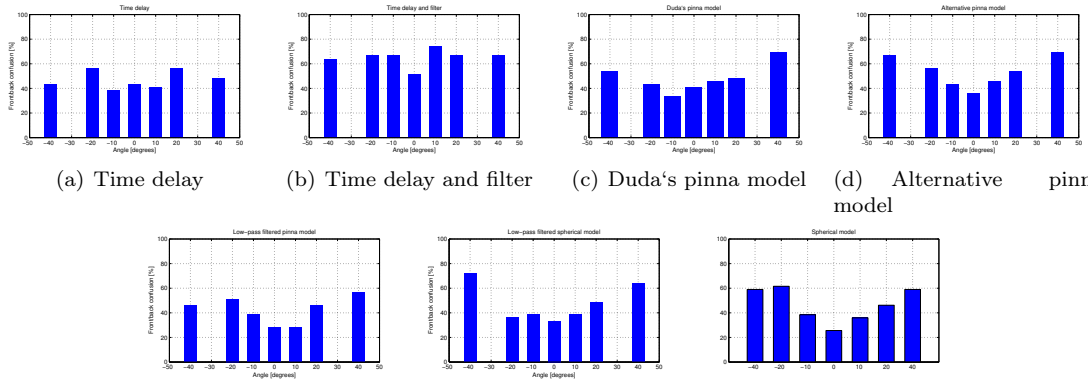

(a) Time delay (b) Time delay and filter (c) Duda's pinna model (d) Alternative pinna model

(e) Low-pass filtered alternative pinna model (f) Low-pass filtered spherical model (g) Spherical model

Figure 31: Front/back confusion as a function of angle

Figure 31 shows total front/back confusion for every angle in each method. As there was no obvious way to predict number of front/back confusions for larger angles, the mean of the values at ±40 degrees was found. Then the corresponding number of responses were randomly chosen from ±60 and ±80 degrees, and considered front/back confusions. The resulting values are found in table 9.

Table 9: Calculated front/back confusion for ±60 and ±80 degrees

	Front/back confusion [%]
Low-pass filtered alternative pinna model	50.8
Time delay	46.2
Low-pass filtered spherical model	67.9
Duda's pinna model	61.5
Spherical model	59.0
Alternative pinna model	68.0
Time delay and head shadow filter	65.4

10.6 Angular dependence of localization error

As earlier described, a Levene's test of homogeneity of variances was conducted for every angle, to see if the responses from the groups had significantly different variances. This was done to determine if an ANOVA could be applied, or a Welch test should be carried out instead. A significance level of α=0.05 was chosen. Table 10 shows the result for every angle. Significant values were found for -80, -60, 0 and 10 degrees.

Table 10: Levene's statistic

Angle	Levene's statistic	p value
-80	F(6,266)=3.05	0.007
-60	F(6,265)=2.769	0.013
-40	F(6,266)=1.314	0.251
-20	F(6,266)=1.77	0.105
-10	F(6,266)=0.417	0.867
0	F(6,266)= 3.665	0.002
10	F(6.266)= 2.513	0.022
20	F(6,266)=1.158	0.329
40	F(6,266)=0.888	0.504
60	F(6,264)=1.399	0.215
80	F(6,266)=0.279	0.946

After determining appropriate approach, it was time to see if statistically significant differences in mean error existed. As can be seen from table 11, this was the case for certain angles. Post-hoc tests were carried out only for statistically significant different results, i.e -20,-10,10, 20 and 80 degrees.

Table 11: Results from ANOVA and Welch test

Angle	Method	F	p value
-80	Welch	F(6,117.222)=1.455	0.2
-60	Welch	F(6,116.746)=1.683	0.131
-40	ANOVA	F(6,266)= 1.095	0.365
-20	ANOVA	F(6,266)=4.265	0.00...
-10	ANOVA	F(6,266)=8.086	0.00...
0	Welch	F(6,117.554)=1.56	0.165
10	Welch	F(6,117.589)=2.798	0.014
20	ANOVA	F(6,266)=6.681	0.00...
40	ANOVA	F(6,266)=1.032	0.405
60	ANOVA	F(6,264)=1.854	0.089
80	ANOVA	F(6,266)=2.225	0.041

For -20, -10, 20 and 80 degrees a Tukey HSD test was conducted, since the first test applied was an ANOVA. The only direction with a statistically significant result found in the Welch's test was 10 degrees, so for these responses a Games-Howell test was applied.

Table 12 shows the results from this analysis. Also here only statistically significant results are included. The rest of the analysis can be found in appendix E.

Table 12: Results from the post-hoc tests. For -20, -10, 20 and 80 degrees a Tukey HSD test was conducted, and for 10 degrees a Games-Howell test was carried out.

Angle	Method 1	Mean 1 ± st.d [deg]	Method 2	Mean 2 ± st.d [deg]	p value
-20	LP pinna	-14.62 ± 21.74	LP spherical	-31.03 ± 17.29	0.017
-20	LP pinna	-14.62 ± 21.74	Spherical	-31.03 ± 22.10	0.017
-20	Time delay	-13.03 ± 24.83	LP spherical	-31.03 ± 17.29	0.006
-20	Time delay	-13.03 ± 24.83	Spherical	-31.03 ± 22.10	0.006
-10	LP pinna	-2.56 ± 19.43	LP spherical	-16.15 ± 18.01	0.041
-10	LP pinna	-2.56 ± 19.43	Spherical	-28.97 ± 20.49	0.00....
-10	Time delay	-2.82 ± 17.16	LP spherical	-16.15 ± 18.01	0.048
-10	Duda's pinna	-14.10 ± 20.09	Spherical	-28.97 ± 20.49	0.017
-10	Alternative pinna	-12.82 ± 19.86	Spherical	-28.97 ± 20.49	0.006
-10	Time delay	-2.82 ± 17.16	Spherical	-28.97 ± 20.49	0.00...
-10	Time delay + filter	-14.87 ± 22.46	Spherical	-28.97 ± 20.49	0.029
10	LP spherical	1.28 ± 29.04	Duda's pinna	-19.49 ± 21.02	0.01
10	LP spherical	1.28 ± 29.04	Alternative pinna	-20.51 ± 24.49	0.01
10	LP spherical	1.28 ± 29.04	Time delay + filter	-16.67 ± 16.75	0.023
20	LP spherical	-5.13 ± 22.35	Duda's pinna	-32.82 ± 25.23	0.00...
20	LP spherical	-5.13 ± 22.35	Alternative pinna	-29.23 ± 32.15	0.001
20	LP spherical	-5.13 ± 22.35	Time delay + filter	-25.9 ± 20.48	0.009
20	Spherical	-8.46 ± 32.24	Duda's pinna	-32.82 ± 25.23	0.001
20	Spherical	-8.46 ± 32.24	Alternative pinna	-29.23 ± 32.15	0.009
20	Time delay	-11.79 ± 23.16	Duda's pinna	-32.82 ± 25.23	0.008
80	Time delay + filter	0.77 ± 27.28	Alternative pinna	17.95 ± 17.95	0.023

As seen in table 12 statistically significant differences exist for certain directions. It could be expected that the methods would perform equally well for angles with the same absolute value, but this was not the case.

Figure 32(a)-32(g) show the average results for all conditions plotted together with 95 % confidence intervals.

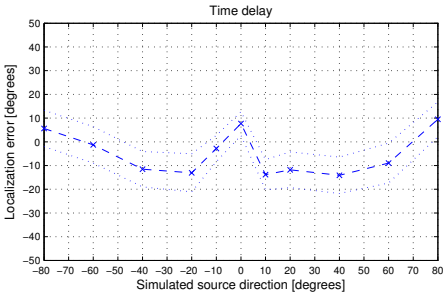

(a) Time delay

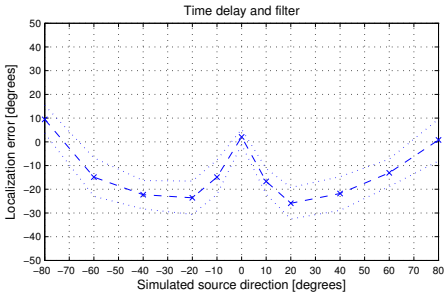

(b) Time delay and filter

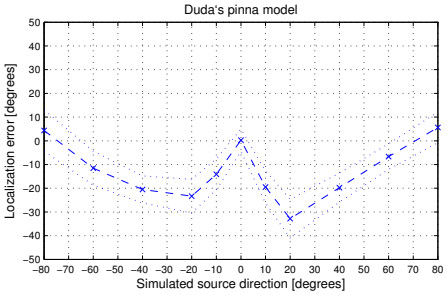

(c) Duda's pinna model

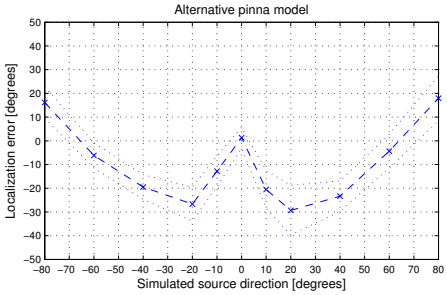

(d) Alternative pinna model

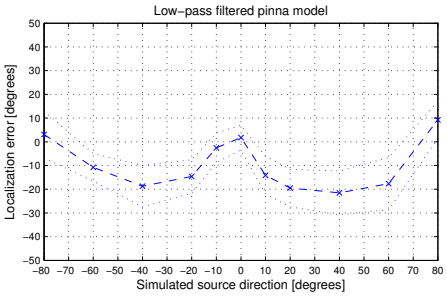

(e) Low-pass filtered alternative pinna model

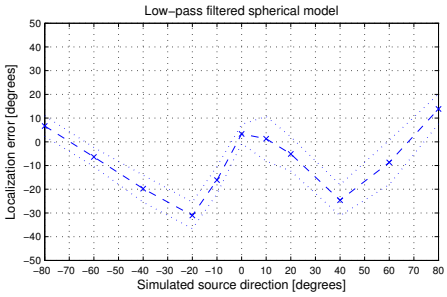

(f) Low-pass filtered spherical model

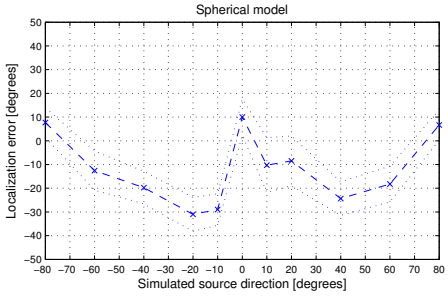

(g) Spherical model

Figure 32: Mean values for every angle plotted with 95% confidence intervals

10.7 Total error

The goal of the experiment was to determine whether any of the simulation conditions gave overall significantly better results than the other approaches. This was investigated by examining total error in every method.

If the angles in this analysis had been the same as in the analysis described in section 10.4.3, the same mean values would have been obtained (except small deviations, due to removed outliers). However, in the final analysis, all the responses except for the ones given for zero degrees were included. For angles ranging from -40 to 40 degrees, all front/back confusions were inverted, whereas for -80, -60, 60 and 80 degrees, responses treated as front/back confusions were randomly chosen, as described in section 10.5.

Table 13: Mean, standard deviation and standard error for total error in every method.

Method	N	Mean	Standard deviation	Standard error
Low-pass filtered alternative pinna model	388	-10.70	27.12	1.38
Low-pass filtered spherical model	389	-9.0	24.27	1.23
Duda‘s pinna model	390	-13.82	23.96	1.21
Alternative pinna model	390	-10.85	27.59	1.40
Spherical model	390	-13.92	27.53	1.39
Time delay	390	-6.23	24.02	1.22
Time delay and head shadow filter	390	-14.28	23.56	1.19

The Levene‘s test of homogeneity of variances indicated that the variances of the groups were unequal ($F(6,2720)=2.692$, $p<0.05$), so a Welch test was applied to check if a statistically significant difference between the methods existed. The test gave a positive result (Welch's $F(6,1208,268) = 5.859$, $p< 0.05$), and a Games-Howell post-hoc test was conducted to further investigate the differences.

According to this post-hoc test, there is a statistically significant difference in the mean error between the model with time delay only (-6.23±24.02 degrees) compared to the spherical model (-13.92±27.53 degrees, p=0.001), Duda's pinna model(-13.82±23.96, p=0.000...) and the model with time delay and head filter (-14.28±23.56, p=0.000...). There is also a statistical difference between the low-pass filtered spherical model (-9.0±24.27 degrees) and the model with time delay and filter (-14.28± 23.56 degrees, p=0.034). There are no statistically significant differences between the other methods. Figure 33 shows mean values plotted together with 95% confidence intervals. The rest of the results from the analysis can be found in appendix E.

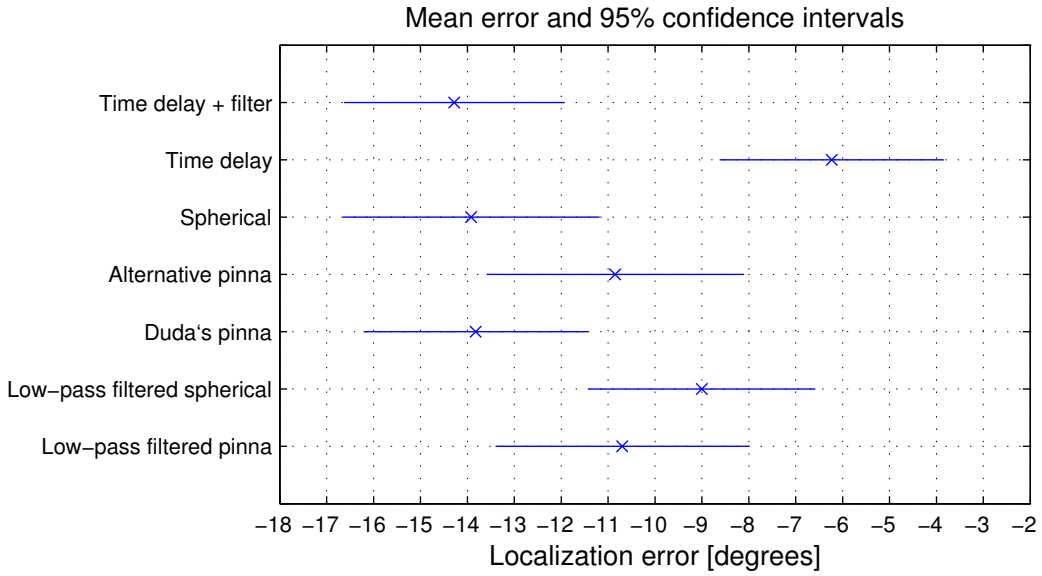

Figure 33: Mean total error with 95 % confidence intervals. The approach with mean value closest to zero degrees is also the "simplest" simulation method, and involves just a time delay. This method performs statistically significant better (α=0.05) than the method with time delay and filter, the analytical spherical model and Duda's pinna model.

11 Discussion

This section provides possible explanations for the observed results from the previous chapters. Potential sources of error in the experimental design are identified, and suggestions for further studies are given. Some practical implications of the findings are also explored.

11.1 Theoretical study

Although it was not possible to relate features in the hrirs to pinna dimensions, some interesting results were obtained. The mean value of the reflection coefficients were not independent of azimuth angle, but could be well approximated with second degree polynomials. However, the perceptual relevance of this is unclear.

Accuracy in describing the time delays seems crucial in order to achieve better localization ability, and applying an "average" model does not enhance model performance. In fact, by inspecting figure 32, it may seem like the extra information leads to a higher degree of confusion. However, a significant quality reduction occurred when introducing the head shadow filter, and since this is included in all the conditions involving pinna models, it is hard to separate the effects.

11.2 Left/right confusion

Left/right confusions were observed in all experimental conditions, and since the time delay alone should provide enough information to distinguish left from right, this is an unexpected result. Subject 2 was removed from the analysis, due to very poor performance in two conditions, probably resulting from significantly different hearing thresholds at 8 kHz. Of the remaining participants, subject 5 experienced the largest amount of left/right confusion, with a share of 6.5%. As previously mentioned, this is also the person that displayed the highest level of variance in both conditions in section 10.4.2, which indicates that the responses to some degree were randomly chosen. The high number of left/right confusion in both versions of the alternative pinna model is reflected by large standard deviations in figure 30(d) and 30(e).

Some of the left/right confusions may be explained as regular localization inaccuracy. It was expected that many of these source reversals would occur for angles with small absolute values. This is true for all conditions, except for the approaches including the alternative pinna model. In appendix C, angular dependence of left/right confusions for every method are shown.

Subject 2 was completely unable to determine source location in the alternative pinna model, and had also trouble localizing in the low-pass filtered version. It can be assumed that some important information has not been perceived, and very different hearing thresholds will especially affect ILD cues.

After subject 2 was removed, some instances of left/right confusions for incidence angles with large absolute values remained. Reasons for this are unknown, but it may be suspected that the subjects in some cases were distracted or unfocused when the sound was played. They were asked to assess 235 stimuli, which is a rather high number, and it was not possible to repeat the stimuli. Other explanations may be misleading ITDs, due to inaccurate estimations, or contradicting time delays and spectral cues.

11.3 Front/back confusion

A high level of front/back confusion occurred in the study, and a number of the participants reported that they were guessing when deciding between the two directions. Some also perceived the sound as coming from the inside of their head.

As mentioned in section 9, the subjects were not allowed to move their head while the stimuli were presented, eliminating an instinctive and effective way to determine source location. Thus, the participants had to fully depend on spectral information to resolve front/back ambiguities. As Langendijk and Bronkhorst [16] study showed, the frequency range from 8-16 kHz is important in this process. Inspection of the ear plugs' frequency responses reveals that the high-frequency area is significantly damped (30 dB or more for frequencies above 8 kHz compared to the response at 1 kHz, see section 6.5). It can be assumed that the attenuation of information in this range may be one of the causes for the large number of source reversals.

It has earlier been shown that only a small contribution of high-frequency content can enhance localization performance. This was investigated in [50] for speech signals, and it was found that even after a 40 dB attenuation, the 8 to 16 kHz frequency band provided some localization information. Highly accurate modeling techniques are required to capture these features, and in this study no attempts for customization of pinna models were made. Consequently, it can be expected that the subjects experienced presence of unfamiliar high-frequency information, which might have caused front/back confusion.

Some subjects seemed to have a strong preference for one direction. An obvious example is subject 6, who perceived all the sounds as coming from behind. There is reason to believe that the stimuli included spectral information that corresponds well to this persons localization cues for sources in the back.

Another factor that is hard to control is the effect of previously presented stimuli. A few of the participants said that once they had located a stimulus e.g from the front, there was a tendency to continue perceiving this direction, until they "remembered" that the sounds were presented independently.

11.4 Localization accuracy and consistency

For most subjects, mean localization error is located between zero and -30 degrees, with variable standard deviations (figure 30). This confirms the finding of many other studies [41] [42] [47], that people are best at localizing when listening through their own ears. Better accuracy could have been expected if the HRTFs were measured, instead of estimated. Even if the "optimal" radius of a sphere for this purpose can be found, there is no guarantee that a sphere in fact is a good representation of a head.

Subject 9 experienced a number of left/right confusions in both conditions of the analytical spherical method, and displays the largest standard deviation in figure 30. However, from the analysis in section 10.4.2, it can be seen that the consistency between the responses is similar to what is observed for most of the other subjects. In table 7, subject 5 has the largest variance, and it can be assumed that a spherical head model does not provide necessary localization cues for this person. Subject 6 showed overall good localization performance (figure 30), and displayed a high level of consistency in the responses, compared to the other participants (table 7).

The method that was shown to provide highest consistency was the low-pass filtered spherical model, with a standard deviation of 9.84 degrees. However, low-pass filtering the alternative pinna model, caused the variance to increase considerably. This again shows that even small contributions of frequencies above 8 kHz can affect the localization process, also for azimuthal angles.

11.5 Angular dependence of localization error

In figure 32, the tendency to assume angles located too far to the sides is evident, as almost all the curves display negative values for angles between -10 and -60 degrees, and 10 and 60 degrees . At -80 and 80 degrees the opposite effect is seen, and the subjects seem to become "conservative" in their estimations. The results for angles with absolute values larger than 40 degrees should, however, be considered less certain, since degree of front/back confusion was only estimated.

Best localization ability is in most cases found at zero degrees, where the confidence intervals are small, and mean values located close to zero degrees. For the model with time delay and the analytical spherical model, simulated sources at zero degrees are perceived as slightly to the right.

Almost all statistically significant differences discovered are located between -20 and 20 degrees, i.e at small incidence angles. This is the area where humans have best localization ability, and it can be assumed that ambiguous cues will have larger effect on localization performance here than further to the sides, where angular resolution naturally is poorer.

It was expected that most of the methods would function equally well for both sides, but this is not always the case. The most obvious examples are the two versions of the analytical spherical model, that seem to work better for small incidence angles to the right than the left. Some differences can be observed in other conditions as well. In section 10.4.2 it was concluded that all the subjects to a certain degree were guessing when determining source direction, and some of the variation may be explained by lack of consistency in the given answers.

11.6 Total error

The method that stands out when inspecting figure 33 includes just a time delay, and this outcome might be a little surprising. However, the model does not provide results that are statistically significant better than the results from neither of the versions of the alternative pinna model nor the low-pass filtered spherical model.

The addition of a head shadow filter to the time delay reduces the model's performance. Since the time delay is the same in both conditions, it can be assumed that the degrading factor is found in the sound spectrum. One possible explanation could be that diffraction of a plane wave around a rigid sphere is not an optimal way to represent sound propagation around a human head. Indeed, the unfiltered analytical spherical model displays similar results as the model with time delay and head shadow filter. The statistical analysis revealed that no significant improvement was achieved by including the alternative pinna model, and adding Duda's pinna model did not affect the outcome noteworthy either.

Very little difference exist between the low-pass filtered and the unfiltered alternative pinna model. However, for the spherical model, larger variations can be observed, and the addition of a low-pass filter seems to enhance the performance. Although there is no statistically significant difference between the two analytical models, the low-pass filtered version perform statistically significant better than the time delay and filter model.

11.7 Practical implications

From the results in the previous sections it is apparent that auralization in the QuietPro system is possible with the methods explored in this study. Localization performance will, however, be affected. This is most likely due to inaccuracies in the simulation models, but also limitations in the signal's bandwidth.

The method with just a time delay was found statistically significant better than three other approaches, and being the simplest model explored, this may seem like a good choice for achieving directionality. Some of the other models performed better regarding consistency between the answers, but the differences are rather small. When inspecting figure 32, it becomes clear that the method with time delay is the only approach with mean absolute errors located less than 15 degrees from zero for all simulated directions.

In the experiment, front/back confusions were encountered many times. Some participants said it was hard to tell the difference between the two directions, and that they felt uncertain in their decision making. However, there is a strong coupling between the sight and the hearing, and it can be assumed that the degree of front/back confusion would significantly decrease if the sound source had been visible. In many practical applications, this condition will be fulfilled (e.g when speaking to another person nearby), and the user will have no trouble detecting source location.

It should also be noted that none of the subjects had previously worn QuietPro earplugs, and that the experimental setting was unfamiliar to them. There is a possibility that localization performance might have been improved if more sessions had been carried out. Most of the subjects who completed the experiment two times did not perform noticeably better the second time. An improvement can be observed for subject 8 (in the two alternative pinna conditions in figure 7), but this may also be a coincidence.

11.8 Sources of errors in the experimental design

In this section, a few issues regarding the experimental design are discussed.

One obvious source of error is that the subjects only were instructed to look directly ahead, but there was nothing preventing them from moving the head during the experiment. This would severely affect perceived source direction, since head tracking was not implemented in the current design. The subjects also had to turn around in order to see the numbers on the papers, and this might have lead to small variations in head orientation from one trial to the next.

As seen in section 6.5 the earplugs introduce their own frequency responses, and high frequencies are significantly damped. The cues located in the this area might have been hard to perceive, or even inaudible, and an equalization should have been carried out to compensate for this. Frequency content located in lower areas may also have been affected, since the responses are non-flat.

It may seem like a sphere is not the best way to represent the shape of the head, but it is also important to consider the accuracy of the input values of the models. Exact measurements of head dimensions are hard to obtain. For instance, it is not straight-forward to locate the exact mid-point of the back of the head (when measuring ear location), and the device used to find head dimensions introduces small uncertainties. If the estimated head size is too small, the range of azimuth angles the subject is able to localize will decrease. Conversely, the subject will find it difficult to perceive the direction of the sound source if the calculated head size gives ITD cues that are much larger than what the person normally experiences [19]. As mentioned in section 6.2, the angular resolution in frontal direction is as high as one degree, which corresponds to an ITD of 10 μs. [32]. So, only a small deviation from the person's own head measures will be perceivable.

The notes showing the numbers in the frontal hemisphere were standing on loudspeakers, whereas the rest were held up by microphone stands and placed on top of chairs. This resulted in a more

homogenous visual impression in the front than in the back. The effect this has on localization ability is unknown, but in this context, it can be mentioned that the person that gave the most consistent responses of all the subjects, is the one with 100% front/back reversals. The set-up was identical for all conditions, so if any disturbance was introduced, it was the same for every method tested.

The effect of having two test sessions is uncertain. Ideally, all subjects should have conducted the procedure only once. The subjects' abilities to concentrate may have differed from the first time to the next, as well as degree of experienced fatigue or stress. Since it was not possible to repeat the stimuli, it was crucial that the subjects paid attention the whole time during the sessions.These are factors that will affect the results, but unfortunately are hard to control. In addition, the fact that they had already attended this type of experiment before, and the difference in time it took to complete the sessions, may have influenced their performance.

Finally, the importance of randomizing the stimuli should be emphasized, although this was done in the experiment. As mentioned in section 11.3, the previous stimuli influence the perception of the next, and this is also true when it comes to discriminating incidence angles close to zero degrees from those further to the sides. One of the subjects even stated that this was one of the most important factors in the decision making.

11.9 Suggestions for further studies

A natural extension of the current study is to include elevation effects in future models. For this purpose, accurate representation of the features found in PRTFs will be especially important.

It is assumed that at the time delays for reflections found in hrirs are affected by dimensions of the outer ear. One reason that the theoretical investigation failed to discover any relation could be that the impulse responses in the CIPIC database also includes effects of the head. It would be interesting to study the influence of the pinna alone, and this is possible with the database given in [45]. This database was not considered in the current study, since it only contains PRTFs in the median plane (see figure 8).

Another important step is to implement a head tracking system. Head tracking and dynamic updating of the sound signals allow the participants to move around during playback, which is advantageous for avoiding the feeling of a sound source placed inside the head, and almost eliminates localization errors [37]. For use in the QuietPro system, it is also necessary to include a feature that monitors the position of the other users, in order to select correct pairs of hrirs. One example of an implementation algorithm for a head tracking system can be found in [48].

It could also be interesting to see if other modeling techniques would provide more accurate results. As earlier mentioned, there are many possible approaches, ranging from interpolation of a few measured directions [49], finding the "best fit" from an existing database [47] and numerical solution of the wave equation [51], to name a few. Still, the method that has been proven most effective is the use of individualized HRTFs.

12 Conclusion

The purpose of the study was to examine if auralization in the QuietPro system is possible and which limitations exist. To do this, different simulation methods with varying degree of complexity were tested and presented via the system's earplugs. All models originated from two main approaches, both based on the assumption that the head can be approximated by a rigid sphere. In total, seven conditions were examined.

The results reveal that the subjects in general were able to perceive simulated sound direction. However, localization ability was significantly reduced compared to what can be expected for normal hearing conditions. For all angles except ± 80 degrees, there was a tendency to perceive the sound sources located further to the sides than what was simulated, and this effect was seen in all the models. Best localization ability was in many cases found at zero degrees.

A high level of front/back reversals occurred in all conditions, and it can be assumed that this was due to missing or ambiguous information in the frequency area above 8 kHz. Some subjects reported that they felt like the sound came from the inside of their head. The implementation of a functional auralization feature in the QuietPro system will require the inclusion of head-tracking, since the users move around. This is known to reduce front/back confusions, and can provide enhanced externalization. A visible sound source will also decrease number of source reversals.

A model's complexity is not always a good predictor of accuracy of the results it produces, and this was clearly shown in the experiment. For a pinna model to be effective, the parameters need to be carefully adjusted to the specific subject.

Simply introducing a time delay gave statistically significant better results than applying the same time delay together with a head shadow filter, using a method that included the pinna model developed in [9] and analytically solve the wave equation for a plane wave incident on a rigid sphere.

Since the model with time delay is the simplest method to implement, and also provided promising results, this is the recommended simulation approach for use in the QuietPro system. However, in this context a few factors that might have influenced the analysis have to be be mentioned. Equalization to compensate for the frequency responses of the earplugs was not performed, and this affected especially the high-frequency area. It should also be noted that the analysis of total error rests on the validity of the assumptions made about front/back confusions. It can be assumed that the outcome would have been different if the actual number of front/back reversals to a large extent differ from the estimated values.

In this study, only localization in the horizontal plane was considered, and a simple time delay turned out to be sufficient to approximately localize the source direction. However, if elevation effects later will be included, it can be assumed that a greater level of detail is required. The issue of developing perceptually satisfactory models occupies many researchers, but to this date, best performance is achieved by use of individualized HRTFs.

A Audiograms

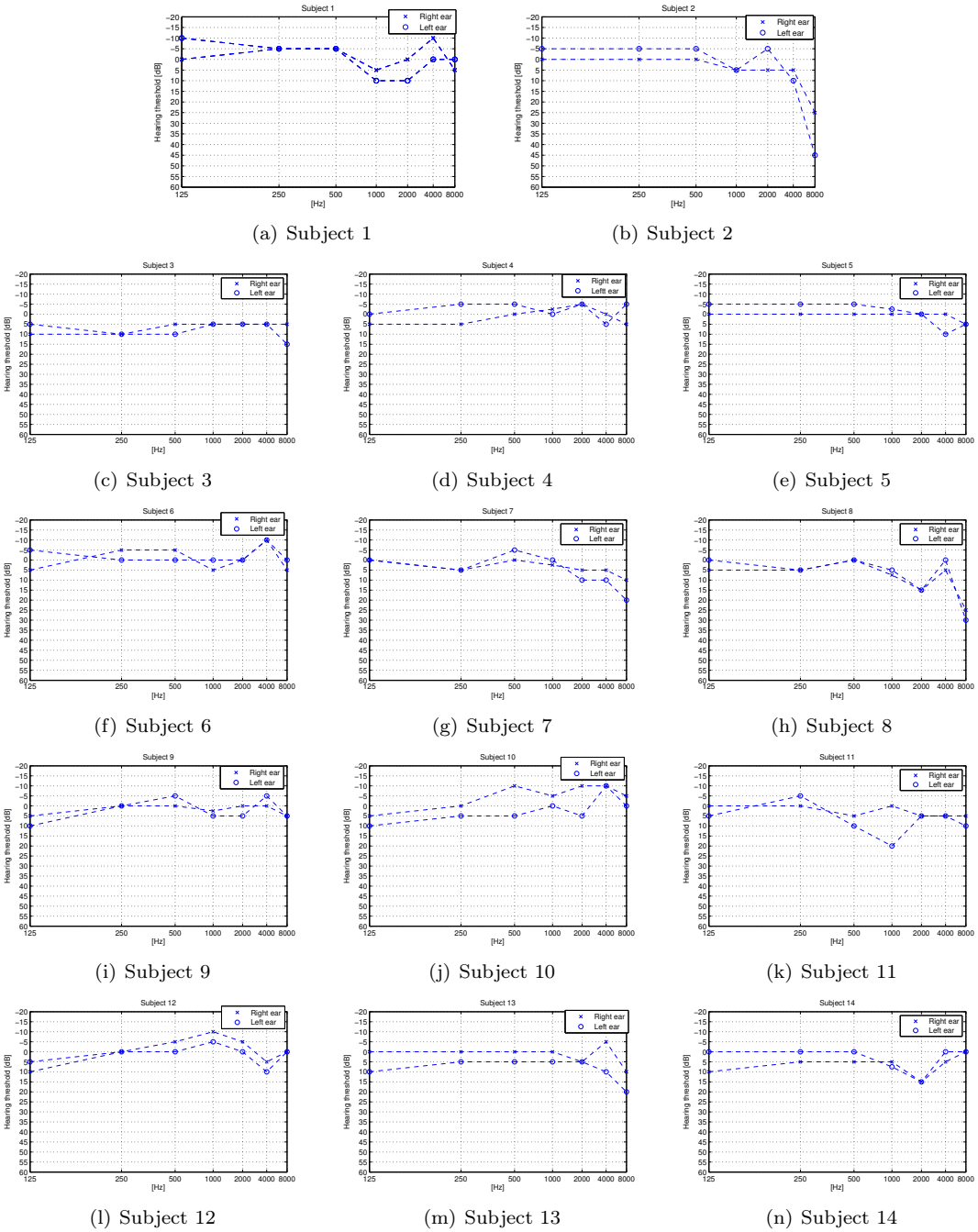

(a) Subject 1 (b) Subject 2

(c) Subject 3 (d) Subject 4 (e) Subject 5

(f) Subject 6 (g) Subject 7 (h) Subject 8

(i) Subject 9 (j) Subject 10 (k) Subject 11

(l) Subject 12 (m) Subject 13 (n) Subject 14

Figure 34: Audiogram

B Front/back confusion

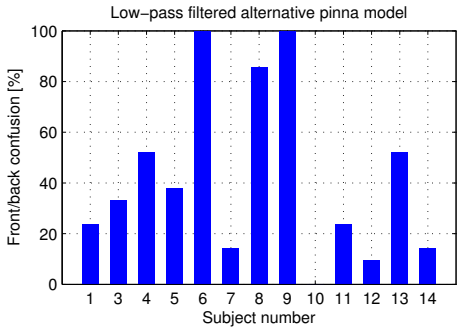

(a) Low-pass filtered pinna model

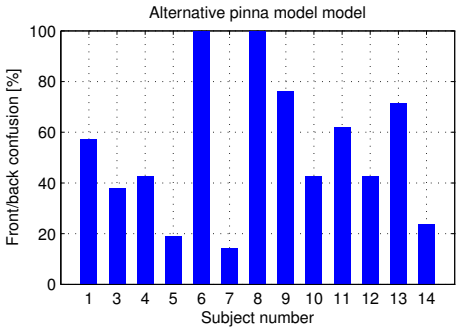

(b) Alternative pinna model

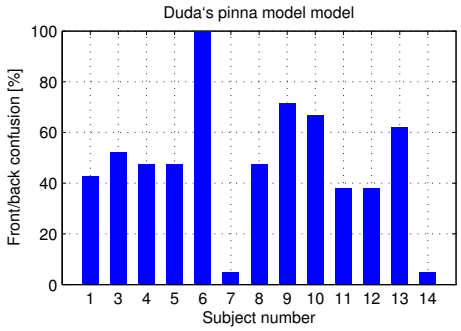

(c) Duda‘s pinna model

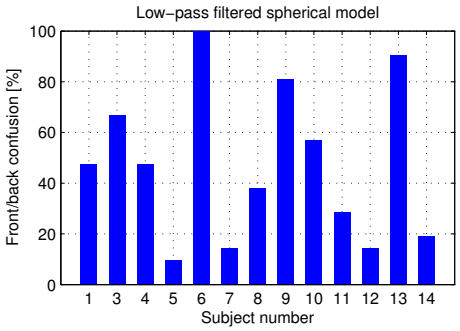

(d) Low-pass filtered spherical model

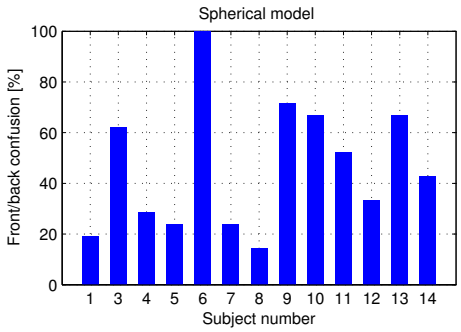

(e) Spherical model

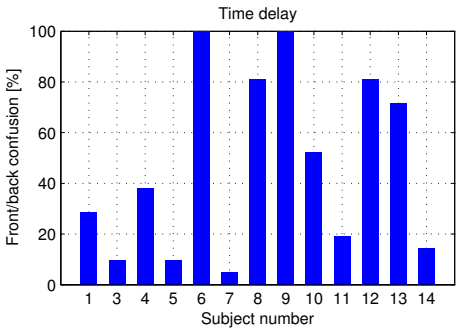

(f) Time delay

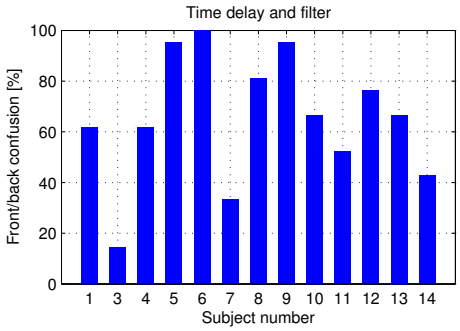

(g) Time delay and filter

Figure 35: Front/back confusion for every subject

C Left/right confusion

Subject 2 is included in this analysis.

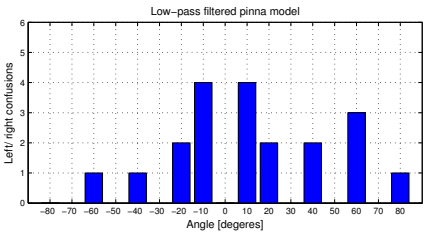

(a) Low-pass filtered pinna model

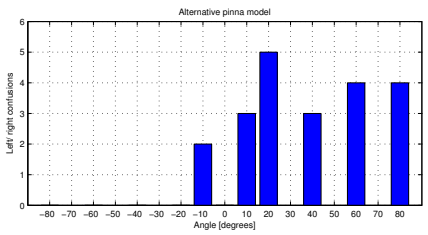

(b) Alternative pinna model

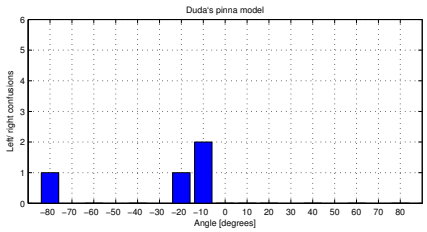

(c) Duda‘s pinna model

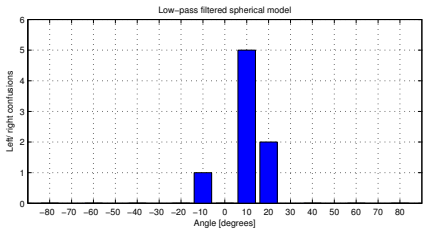

(d) Low-pass filtered spherical model

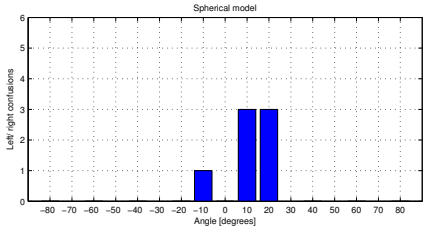

(e) Spherical model

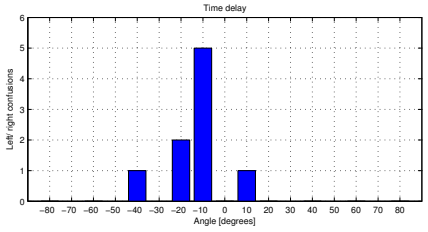

(f) Time delay

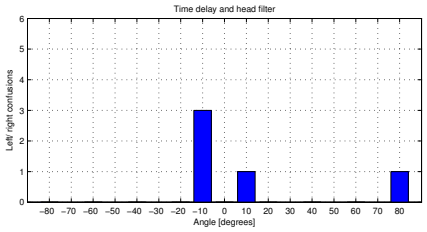

(g) Time delay and filter

Figure 36: Left/right confusion for every angle

D MATLAB

In this section, only some of the code is given. The rest can be found in the zip file.

```
%%%%%%%%%%%%%%%%%%%%%%%%%%%%%%%%%%%%%%%%%%%%
%%% Find coefficients, brute force %%%
%%%%%%%%%%%%%%%%%%%%%%%%%%%%%%%%%%%%%%%%%%%%

%function[final_A final_B final_D error final_Ap final_Bp final_Cp errorp]=Brute_force(n)
%clear all;clc;
error=inf;errorp=inf;


theta=[-80 -65 -55 -45 -40 -35 -30 -25 -20 -15 -10 -5 0 5 10 15 20 25 30 35 40 45 55 65 80]*pi/180;
%n=[1 4 3 5 2 3 4 5 6 7 6 8 9 5 4 3 2 5 3 4 6 8 3 4 5];
%n=sin(pi/6)*cos(theta/2)+2;

final_svar=zeros(198,8);

%%%%%%%%%%%%%%%%%%%%%%%%%%%%%%%%%%%%%%%%%%%%%%%%%%%%%%%%%%%%%%%%%%%%%%%%%%%%%%%%%%%%%%
A1=-40.0;An=0;
B1=0;Bn=80;


dA=0.1;dB=0.1;

Ap1=-3;Apn=10;
Bp1=-2; Bpn=10;
Cp1=0;Cpn=20;

dpA=0.1;dpB=0.1;dpC=0.1;


for gag = 1:1:length(Hele)
n=Hele(gag,:);
error=inf;errorp=inf;

%%%%%%%%%%%%%%%%%%%%%%%%%%%%%%%%%%%%
%%% Trigonometric approach %%%
%%%%%%%%%%%%%%%%%%%%%%%%%%%%%%%%%%%%


for A=A1:dA:An
    for B=B1:dB:Bn

                Y=A*cos(theta/2)+B;
                P=sqrt(sum((Y-n).^2));

                 if (P < error)

                    final_A=A;
                    final_B=B;

                    error=P;    %Absolute error in samples


        end
    end
end


final_svar(gag,1)=final_A;
final_svar(gag,2)=final_B;
final_svar(gag,4)=error;

% svar=final_A*cos(theta/2).*sin(final_D*pi/2)+final_B;
% svarp=final_Ap*(theta).^2+final_Bp*(theta)+final_Cp;
%
% figure(1)
%
% plot(theta,svar,'r',theta,svarp,'b')
% hold on
% plot(theta,n,'+')
% legend('Trigonometric solution','Polynomal solution', 'Data points')
% axis([-pi/2 pi/2 min(n)-0.5 max(n)+0.5])
% ylabel('Delay [samples]')
% xlabel('Angle [degrees]')
```

```
74 % hold off
75 end
```

MATLAB/Brute_force_n_ref2.m

```
 1 function [y_pinna_l y_pinna_r]=generate_time_pinna_filter(a,theta_s,theta_ear_l,
       theta_ear_r)
 2
 3 x=importdata('Pinknoise3.mat');
 4
 5 %  a=8;
 6 %  theta_s=-90;
 7 %  theta_ear_r=90;
 8 %  theta_ear_l=-90;
 9
10 a=a/100;
11
12 %source angle in degrees, assuming positive to the right and negative to the left
13
14
15 c=343;
16
17 %%%%%%%%%%%%%%%%%%%%%%%%%%%%%%%%%%%%%%%%%%%%%%%%%%%%%%%%%%%%%%%%%%%%%%%%%%%%%%%
18 %Finding Td(angle between source and ear) for both ears
19
20
21 theta_r=theta_ear_r-theta_s;
22 theta_l=theta_ear_l-theta_s;
23
24 if(abs(theta_r)<=180)
25     theta_r=abs(theta_r);
26
27 else
28     theta_r=360-abs(theta_r);
29 end
30
31
32 if(abs(theta_l)<=180)
33     theta_l=abs(theta_l);
34
35 else
36     theta_l=360-abs(theta_l);
37 end
38 %%%%%%%%%%%%%%%%%%%%%%%%%%%%%%%%%%%%%%%%%%%%%%%%%%%%%%%%%%%%%%%%%%%%%%%%%%%%%%%
39
40 %Find Td
41
42 if(theta_r<90 && theta_r>=0)
43
44     theta_r=(theta_r*pi)/180;        %Radians
45     Td_r=(a/c)-(a/c)*cos(theta_r);
46
47 else
48     theta_r=(theta_r*pi)/180;        %Radians
49     Td_r=(a/c)+((a/c)*(abs(theta_r)-(pi/2)));
50 end
51
52
53 if(theta_l<90 && theta_l>=0)
54
55     theta_l=(theta_l*pi)/180;
56     Td_l=(a/c)-(a/c)*cos(theta_l);
57
58 else
59     theta_l=(theta_l*pi)/180;
60     Td_l=(a/c)+((a/c)*(abs(theta_l)-(pi/2)));
61 end
62
63
64 %%%%%%%%%%%%%%%%%%%%%%%%%%%%%%%%%%%%%%%%%%%%%%%%%%%%%%%%%%%%%%%%%%%%%%%%%%%%%%%
65 %Constants
66
67  Nfft=1024;
68  Fs=44100;
69
70  f=(0:Nfft/2)*(Fs/Nfft);
71  f=transpose(f);
72  w=2*pi*f;
73
```

```
w0=c/a;
alpha_min=0.1;


theta_min=(150*pi)/180;    %Radians
theta_earl=-(100*pi)/180;
theta_earr=(100*pi)/180;


%%%%%%%%%%%%%%%%%%%%%%%%%%%%%%%%%%%%%%%%%%%%%%%%%%%%%%%%%%%%%%%%%%%%%%%%%%%%%%%%

%Calculate the two alphaes and filters
alpha_r=(1+(alpha_min/2))+(1-(alpha_min/2))*cos(((theta_r*pi)/theta_min));
alpha_l=(1+(alpha_min/2))+(1-(alpha_min/2))*cos(((theta_l*pi)/theta_min));

HH_L=((1+((alpha_l*w)/(2*w0))*1j)./(1+(w/(2*w0))*1j)).*exp(-1j*w*Td_l);
HH_R=((1+((alpha_r*w)/(2*w0))*1j)./(1+(w/(2*w0))*1j)).*exp(-1j*w*Td_r);

%%%%%%%%%%%%%%%%%%%%%%%%%%%%%%%%%%%%%%%%%%%%%%%%%%%%%%%%%%%%%%%%%%%%%%%%%%%%%%%%
%Plot filters in frequency domain
%
% figure(1)
% subplot(2,1,1)
% semilogx(20*log10(abs(HH_L)))
% %xlabel('f')
% ylabel('dB')
% %axis([0 21000 -25 20])
% title('Head filter, left')
%
% subplot(2,1,2)
% semilogx(20*log10(abs(HH_R)))
% %xlabel('f')
% ylabel('dB')
% %axis([0 21000 -25 20])
% title('Head filter, right')
%%%%%%%%%%%%%%%%%%%%%%%%%%%%%%%%%%%%%%%%%%%%%%%%%%%%%%%%%%%%%%%%%%%%%%%%%%%%%%%%
% Transform to time domain
hh_l = real(ifft(2*HH_L,Nfft));
hh_r = real(ifft(2*HH_R,Nfft));

% figure(1)
% subplot(2,1,1)
% plot(hh_l)
% subplot(2,1,2)
% plot(hh_r)


%%%%%%%%%%%%%%%%%%%%%%%%%%%%%%%%%%%%%%%%%%%%%%%%%%%%%%%%%%%%%%%%%%%%%%%%%%%%%%%
%Pinna model
%Set variables, left

theta_s=theta_s*pi/180; %Radians

n1_l=theta_s^2+1.6;
rho1_l=-0.1*(theta_s^2)+0.3*theta_s-0.1;

[nsamples1_l delay1_l]=interpolate_pinna(hh_l,n1_l);
delay1_l=delay1_l*rho1_l;


%%%%%%%%%%%%%%%%%%%%%%%%%%%%%%%%%%%%%%%%%%%%%%%%%%%%%%%%%%%%%%%%%%%%%%%%%%%%%%%

n2_l=1.3*(theta_s^2)+0.2*theta_s+2.9;
rho2_l=-0.2*(theta_s^2)+0.3*theta_s+0.6;

[nsamples2_l delay2_l]=interpolate_pinna(hh_l,n2_l);
delay2_l=delay2_l*rho2_l;

%%%%%%%%%%%%%%%%%%%%%%%%%%%%%%%%%%%%%%%%%%%%%%%%%%%%%%%%%%%%%%%%%%%%%%%%%%%%%%%%

n3_l=1.5*(theta_s^2)+theta_s+5;
rho3_l=0.3*(theta_s^2)+0.1*theta_s-1;

[nsamples3_l delay3_l]=interpolate_pinna(hh_l,n3_l);
delay3_l=delay3_l*rho3_l;

%%%%%%%%%%%%%%%%%%%%%%%%%%%%%%%%%%%%%%%%%%%%%%%%%%%%%%%%%%%%%%%%%%%%%%%%%%%%%%%%

n4_l=1.9*(theta_s^2)+1.6*theta_s+7.1;
rho4_l=0.2*(theta_s^2)-0.1*theta_s;
```

```
[nsamples4_l delay4_l]=interpolate_pinna(hh_l,n4_l);
delay4_l=delay4_l*rho4_l;

%%%%%%%%%%%%%%%%%%%%%%%%%%%%%%%%%%%%%%%%%%%%%%%%%%%%%%%%%%%%%%%%%%%%%%%%%%%%%%
n5_l=2.5*(theta_s^2)+1.8*theta_s+8.7;
rho5_l=0.2*(theta_s^2)-0.6;

[nsamples5_l delay5_l]=interpolate_pinna(hh_l,n5_l);
delay5_l=delay5_l*rho5_l;

%%%%%%%%%%%%%%%%%%%%%%%%%%%%%%%%%%%%%%%%%%%%%%%%%%%%%%%%%%%%%%%%%%%%%%%%%%%%%%

n6_l=2.5*(theta_s^2)+2*theta_s+10.9;
rho6_l=-0.2*(theta_s^2)-0.1*theta_s+0.4;

[nsamples6_l delay6_l]=interpolate_pinna(hh_l,n6_l);
delay6_l=delay6_l*rho6_l;

%%%%%%%%%%%%%%%%%%%%%%%%%%%%%%%%%%%%%%%%%%%%%%%%%%%%%%%%%%%%%%%%%%%%%%%%%%%%%%

hh_pinna_l1=zeros(length(hh_l)+nsamples6_l,1);

hh_pinna_l1(1:length(hh_l),1)=hh_pinna_l1(1:length(hh_l),1)+hh_l(:,1); %Main signal

hh_pinna_l1(1:length(delay1_l),1)=hh_pinna_l1(1:length(delay1_l),1)+delay1_l(:,1); %
    First echo

hh_pinna_l1(1:length(delay2_l),1)=hh_pinna_l1(1:length(delay2_l),1)+delay2_l(:,1);

hh_pinna_l1(1:length(delay3_l),1)=hh_pinna_l1(1:length(delay3_l),1)+delay3_l(:,1);

hh_pinna_l1(1:length(delay4_l),1)=hh_pinna_l1(1:length(delay4_l),1)+delay4_l(:,1);

hh_pinna_l1(1:length(delay5_l),1)=hh_pinna_l1(1:length(delay5_l),1)+delay5_l(:,1);

hh_pinna_l1(1:length(delay6_l),1)=hh_pinna_l1(1:length(delay6_l),1)+delay6_l(:,1);
%%%%%%%%%%%%%%%%%%%%%%%%%%%%%%%%%%%%%%%%%%%%%%%%%%%%%%%%%%%%
%Set variables, right

n1_r=theta_s^2+1.6;
rho1_r=-0.1*(theta_s^2)-0.3*theta_s-0.1;

[nsamples1_r delay1_r]=interpolate_pinna(hh_r,n1_r);
delay1_r=delay1_r*rho1_r;


%%%%%%%%%%%%%%%%%%%%%%%%%%%%%%%%%%%%%%%%%%%%%%%%%%%%%%%%%%%%%%%%%%%%%%%%%%%%%%

n2_r=1.3*(theta_s^2)-0.2*theta_s+2.9;
rho2_r=-0.2*(theta_s^2)-0.3*theta_s+0.6;

[nsamples2_r delay2_r]=interpolate_pinna(hh_r,n2_r);
delay2_r=delay2_r*rho2_r;


%%%%%%%%%%%%%%%%%%%%%%%%%%%%%%%%%%%%%%%%%%%%%%%%%%%%%%%%%%%%%%%%%%%%%%%%%%%%

n3_r=1.5*(theta_s^2)-theta_s+5;
rho3_r=0.3*(theta_s^2)-0.1*theta_s-1;

[nsamples3_r delay3_r]=interpolate_pinna(hh_r,n3_r);
delay3_r=delay3_r*rho3_r;

%%%%%%%%%%%%%%%%%%%%%%%%%%%%%%%%%%%%%%%%%%%%%%%%%%%%%%%%%%%%%%%%%%%%%%%%%%%%%

n4_r=1.9*(theta_s^2)-1.6*theta_s+7.1;
rho4_r=0.2*(theta_s^2)+0.1*theta_s;

[nsamples4_r delay4_r]=interpolate_pinna(hh_r,n4_r);
delay4_r=delay4_r*rho4_r;

%%%%%%%%%%%%%%%%%%%%%%%%%%%%%%%%%%%%%%%%%%%%%%%%%%%%%%%%%%%%%%%%%%%%%%%%%%%%%

n5_r=2.5*(theta_s^2)-1.8*theta_s+8.7;
rho5_r=0.2*(theta_s^2)-0.6;

[nsamples5_r delay5_r]=interpolate_pinna(hh_r,n5_r);
delay5_r=delay5_r*rho5_r;

```

```
%%%%%%%%%%%%%%%%%%%%%%%%%%%%%%%%%%%%%%%%%%%%%%%%%%%%%%%%%%%%%%%%%%%%%%%%%%%%%%%%

n6_r=2.5*(theta_s^2)-2*theta_s+10.9;
rho6_r=-0.2*(theta_s^2)+0.1*theta_s+0.4;

[nsamples6_r delay6_r]=interpolate_pinna(hh_r,n6_r);
delay6_r=delay6_r*rho6_r;

%%%%%%%%%%%%%%%%%%%%%%%%%%%%%%%%%%%%%%%%%%%%%%%%%%%%%%%%%%%%%%%%%%%%%%%%%%%%%%%%


hh_pinna_r1=zeros(length(hh_r)+nsamples6_r,1);

hh_pinna_r1(1:length(hh_r),1)=hh_pinna_r1(1:length(hh_r),1)+hh_r(:,1); %Main signal

hh_pinna_r1(1:length(delay1_r),1)=hh_pinna_r1(1:length(delay1_r),1)+delay1_r(:,1); %First echo

hh_pinna_r1(1:length(delay2_r),1)=hh_pinna_r1(1:length(delay2_r),1)+delay2_r(:,1);

hh_pinna_r1(1:length(delay3_r),1)=hh_pinna_r1(1:length(delay3_r),1)+delay3_r(:,1);

hh_pinna_r1(1:length(delay4_r),1)=hh_pinna_r1(1:length(delay4_r),1)+delay4_r(:,1);

hh_pinna_r1(1:length(delay5_r),1)=hh_pinna_r1(1:length(delay5_r),1)+delay5_r(:,1);

hh_pinna_r1(1:length(delay6_r),1)=hh_pinna_r1(1:length(delay6_r),1)+delay6_r(:,1);
%%%%%%%%%%%%%%%%%%%%%%%%%%%%%%%%%%%%%%%%%%%%%%%%%%%%%%%%%%%%%%%%%%%%%%%%%%%%%%%%

t=0.005;



hh_pinna_l=zeros(ceil(t*Fs),1);
hh_pinna_r=zeros(ceil(t*Fs),1);

if(length(hh_pinna_r) > length(hh_pinna_r1))
hh_pinna_r(1:length(hh_pinna_r1),1)=hh_pinna_r(1:length(hh_pinna_r1),1)+hh_pinna_r1(:,1);
elseif(length(hh_pinna_r1) > length(hh_pinna_r))
hh_pinna_r(:,1)=hh_pinna_r1(1:length(hh_pinna_r),1)+hh_pinna_r(:,1);
end


if(length(hh_pinna_l) > length(hh_pinna_l1))
hh_pinna_l(1:length(hh_pinna_l1),1)=hh_pinna_l(1:length(hh_pinna_l1),1)+hh_pinna_l1(:,1);
elseif(length(hh_pinna_l1) > length(hh_pinna_l))
hh_pinna_l(:,1)=hh_pinna_l1(1:length(hh_pinna_l),1)+hh_pinna_l(:,1);
end


y_pinna_l=conv(x,hh_pinna_l);
y_pinna_r=conv(x,hh_pinna_r);
```

MATLAB/generate_time_pinna_filter.m

```
%Plot svar -80 deg
degrees=[-180:10:170];

choise=no2_all_sorted_sphere3;

%Matrise med alle grader nedover i tre kolonner
%-80

for i=1:3
    temp(:,i)=choise(i,:);
end

%-60

for i=4:6
    temp(:,i)=choise(i,:);
end

%-40

for i=7:9
    temp(:,i)=choise(i,:);
```

```
end

%-20
for i=10:12
    temp(:,i)=choise(i,:);
end

%-10
for i=13:15
    temp(:,i)=choise(i,:);
end

%0
for i=16:18
    temp(:,i)=choise(i,:);
end

%10
for i=19:21
    temp(:,i)=choise(i,:);
end

%20
for i=22:24
    temp(:,i)=choise(i,:);
end

%40
for i=25:27
    temp(:,i)=choise(i,:);
end

%60
for i=28:30
    temp(:,i)=choise(i,:);
end

%80
for i=31:33
    temp(:,i)=choise(i,:);
end


m80deg=[temp(:,1);temp(:,2);temp(:,3)];
m60deg=[temp(:,4);temp(:,5);temp(:,6)];
m40deg=[temp(:,7);temp(:,8);temp(:,9)];
m20deg=[temp(:,10);temp(:,11);temp(:,12)];
m10deg=[temp(:,13);temp(:,14);temp(:,15)];
m0deg=[temp(:,16);temp(:,17);temp(:,18)];
p10deg=[temp(:,19);temp(:,20);temp(:,21)];
p20deg=[temp(:,22);temp(:,23);temp(:,24)];
p40deg=[temp(:,25);temp(:,26);temp(:,27)];
p60deg=[temp(:,28);temp(:,29);temp(:,30)];
p80deg=[temp(:,31);temp(:,32);temp(:,33)];



figure(1)
hist(m80deg,degrees)
axis([-180 180 0 15])
title('-80 degrees')
grid on
set(gca,'YTick',1:15);

figure(2)
hist(m60deg,degrees)
axis([-180 180 0 15])
title('-60 degrees')
grid on
set(gca,'YTick',1:15);

figure(3)
hist(m40deg,degrees)
axis([-180 180 0 15])
title('-40 degrees')
grid on
set(gca,'YTick',1:15);

figure(4)
hist(m20deg,degrees)
```

```
axis([-180 180 0 15])
title('-20 degrees')
grid on
set(gca,'YTick',1:15);

figure(5)
hist(m10deg,degrees)
axis([-180 180 0 15])
title('-10 degrees')
grid on
set(gca,'YTick',1:15);

figure(6)
hist(m0deg,degrees)
axis([-180 180 0 15])
title('0 degrees')
grid on
set(gca,'YTick',1:15);

figure(7)
hist(p10deg,degrees)
axis([-180 180 0 15])
title('10 degrees')
grid on
set(gca,'YTick',1:15);

figure(8)
hist(p20deg,degrees)
axis([-180 180 0 15])
title('20 degrees')
grid on
set(gca,'YTick',1:15);

figure(9)
hist(p40deg,degrees)
axis([-180 180 0 15])
title('40 degrees')
grid on
set(gca,'YTick',1:15);

figure(10)
hist(p60deg,degrees)
axis([-180 180 0 15])
title('60 degrees')
grid on
set(gca,'YTick',1:15);

figure(11)
hist(p80deg,degrees)
axis([-180 180 0 15])
title('80 degrees')
grid on
set(gca,'YTick',1:15);
```

MATLAB/Make_hist_fb3.m

```
fasit=[-80 -80 -80 -60 -60 -60 60 60 60 80 80 80];
fasit=transpose(fasit);

error_LP_pinna=zeros(12,13);
error_LP_sphere=zeros(12,13);
error_duda_pinna=zeros(12,13);
error_pinna=zeros(12,13);
error_sphere=zeros(12,13);
error_time=zeros(12,13);
error_time_filter=zeros(12,13);


for i=3:4
    for j=1:6
error_LP_pinna(j,i)=no2_all_sorted_LP_pinna3_pr(j,i)-fasit(j);
    end

    for j=7:12
        error_LP_pinna(j,i)=fasit(j)-no2_all_sorted_LP_pinna3_pr(j,i);
    end


```

```
end

for i=4
 for j=1:6
error_LP_sphere(j,i)=no2_all_sorted_LP_sphere3_pr(j,i)-fasit(j);
    end

    for j=7:12
        error_LP_sphere(j,i)=fasit(j)-no2_all_sorted_LP_sphere3_pr(j,i);
    end

end

for i=4
for j=1:6
error_duda_pinna(j,i)=no2_all_sorted_duda_pinna3_pr(j,i)-fasit(j);
    end


    for j=7:12
        error_duda_pinna(j,i)=fasit(j)-no2_all_sorted_duda_pinna3_pr(j,i);
    end

end

for i=4
for j=1:6
error_pinna(j,i)=no2_all_sorted_pinna3_pr(j,i)-fasit(j);
    end


    for j=7:12
        error_pinna(j,i)=fasit(j)-no2_all_sorted_pinna3_pr(j,i);
    end

end

for i=4
for j=1:6
error_sphere(j,i)=no2_all_sorted_sphere3_pr(j,i)-fasit(j);
    end

    for j=7:12
        error_sphere(j,i)=fasit(j)-no2_all_sorted_sphere3_pr(j,i);
    end

end

for i=4
for j=1:6
error_time(j,i)=no2_all_sorted_time3_pr(j,i)-fasit(j);
    end

    for j=7:12
        error_time(j,i)=fasit(j)-no2_all_sorted_time3_pr(j,i);
    end

end

for i=4
   for j=1:6
error_time_filter(j,i)=no2_all_sorted_time_filter3_pr(j,i)-fasit(j);
    end

    for j=7:12
        error_time_filter(j,i)=fasit(j)-no2_all_sorted_time_filter3_pr(j,i);
    end

end

%%%%%%%%%%%%%%%%%%%%%%%%%%%%%%%%%%%%%%%%%%%%%%%%
%Lage mean og varianse matrise 6*13

mean_LP_pinna=find_mean_of_three32(error_LP_pinna);
mean_LP_sphere=find_mean_of_three32(error_LP_sphere);
mean_duda_pinna=find_mean_of_three32(error_duda_pinna);
mean_pinna=find_mean_of_three32(error_pinna);
mean_sphere=find_mean_of_three32(error_sphere);
mean_time=find_mean_of_three32(error_time);
mean_time_filter=find_mean_of_three32(error_time_filter);
```

```
104
105 var_LP_pinna=find_var_of_three32(error_LP_pinna);
106 var_LP_sphere=find_var_of_three32(error_LP_sphere);
107 var_duda_pinna=find_var_of_three32(error_duda_pinna);
108 var_pinna=find_var_of_three32(error_pinna);
109 var_sphere=find_var_of_three32(error_sphere);
110 var_time=find_var_of_three32(error_time);
111 var_time_filter=find_var_of_three32(error_time_filter);
112
113 %%%%%%%%%%%%%%%%%%%%%%%%%%%%%%%%%%%%%%%%%%%%%%%%%%%%%%%%%%%%%%%%%%%%%%%
114 %Make 1 colonne, to find mean mean and mean variance
115
116 tot_mean_LP_pinna=make_colonne32(mean_LP_pinna);
117 tot_mean_LP_sphere=make_colonne32(mean_LP_sphere);
118 tot_mean_duda_pinna=make_colonne32(mean_duda_pinna);
119 tot_mean_pinna=make_colonne32(mean_pinna);
120 tot_mean_sphere=make_colonne32(mean_sphere);
121 tot_mean_time=make_colonne32(mean_time);
122 tot_mean_time_filter=make_colonne32(mean_time_filter);
123
124 tot_var_LP_pinna=make_colonne32(var_LP_pinna);
125 tot_var_LP_sphere=make_colonne32(var_LP_sphere);
126 tot_var_duda_pinna=make_colonne32(var_duda_pinna);
127 tot_var_pinna=make_colonne32(var_pinna);
128 tot_var_sphere=make_colonne32(var_sphere);
129 tot_var_time=make_colonne32(var_time);
130 tot_var_time_filter=make_colonne32(var_time_filter);
131
132 %%%%%%%%%%%%%%%%%%%%%%%%%%%%%%%%%%%%%%%%%%%%%%%%%%%%%%%%%%%%%%%%%%%%%%%
133
134 mean_mean=zeros(7,1);
135 mean_mean(1)=mean(tot_mean_LP_pinna);
136 mean_mean(2)=mean(tot_mean_LP_sphere);
137 mean_mean(3)=mean(tot_mean_duda_pinna);
138 mean_mean(4)=mean(tot_mean_pinna);
139 mean_mean(5)=mean(tot_mean_sphere);
140 mean_mean(6)=mean(tot_mean_time);
141 mean_mean(7)=mean(tot_mean_time_filter);
142
143 mean_var=zeros(7,1);
144 mean_var(1)=mean(tot_var_LP_pinna);
145 mean_var(2)=mean(tot_var_LP_sphere);
146 mean_var(3)=mean(tot_var_duda_pinna);
147 mean_var(4)=mean(tot_var_pinna);
148 mean_var(5)=mean(tot_var_sphere);
149 mean_var(6)=mean(tot_var_time);
150 mean_var(7)=mean(tot_var_time_filter);
151
152 save('Method_var_3','mean_mean','mean_var')
153
154 a=mean_var
155 b=sqrt(mean_var)
```

MATLAB/Intermethodvariability3_high.m

```
1  fasit=[-40 -40 -40 -20 -20 -20 -10 -10 -10 10 10 10 20 20 20 40 40 40];
2  fasit=transpose(fasit);
3
4  error_LP_pinna=zeros(18,13);
5  error_LP_sphere=zeros(18,13);
6  error_duda_pinna=zeros(18,13);
7  error_pinna=zeros(18,13);
8  error_sphere=zeros(18,13);
9  error_time=zeros(18,13);
10 error_time_filter=zeros(18,13);
11
12
13 for i=1:13
14     for j=1:9
15 error_LP_pinna(j,i)=no2_all_sorted_LP_pinna3_pr(j,i)-fasit(j);
16     end
17
18     for j=10:18
19         error_LP_pinna(j,i)=fasit(j)-no2_all_sorted_LP_pinna3_pr(j,i);
20     end
21
22
23
24 end
```

```

for i=1:13
 for j=1:9
error_LP_sphere(j,i)=no2_all_sorted_LP_sphere3_pr(j,i)-fasit(j);
    end

    for j=10:18
        error_LP_sphere(j,i)=fasit(j)-no2_all_sorted_LP_sphere3_pr(j,i);
    end

end

for i=1:13
for j=1:9
error_duda_pinna(j,i)=no2_all_sorted_duda_pinna3_pr(j,i)-fasit(j);
    end


    for j=10:18
        error_duda_pinna(j,i)=fasit(j)-no2_all_sorted_duda_pinna3_pr(j,i);
    end

end

for i=1:13
for j=1:9
error_pinna(j,i)=no2_all_sorted_pinna3_pr(j,i)-fasit(j);
    end


    for j=10:18
        error_pinna(j,i)=fasit(j)-no2_all_sorted_pinna3_pr(j,i);
    end

end

for i=1:13
for j=1:9
error_sphere(j,i)=no2_all_sorted_sphere3_pr(j,i)-fasit(j);
    end

    for j=10:18
        error_sphere(j,i)=fasit(j)-no2_all_sorted_sphere3_pr(j,i);
    end

end

for i=1:13
for j=1:9
error_time(j,i)=no2_all_sorted_time3_pr(j,i)-fasit(j);
    end

    for j=10:18
        error_time(j,i)=fasit(j)-no2_all_sorted_time3_pr(j,i);
    end

end

for i=1:13
   for j=1:9
error_time_filter(j,i)=no2_all_sorted_time_filter3_pr(j,i)-fasit(j);
    end

    for j=10:18
        error_time_filter(j,i)=fasit(j)-no2_all_sorted_time_filter3_pr(j,i);
    end

end

%%%%%%%%%%%%%%%%%%%%%%%%%%%%%%%%%%%%%%%%%%%%%%
%Lage mean og varianse matrise 6*13

mean_LP_pinna=find_mean_of_three3(error_LP_pinna);
mean_LP_sphere=find_mean_of_three3(error_LP_sphere);
mean_duda_pinna=find_mean_of_three3(error_duda_pinna);
mean_pinna=find_mean_of_three3(error_pinna);
mean_sphere=find_mean_of_three3(error_sphere);
mean_time=find_mean_of_three3(error_time);
mean_time_filter=find_mean_of_three3(error_time_filter);

```

```
var_LP_pinna=find_var_of_three3(error_LP_pinna);
var_LP_sphere=find_var_of_three3(error_LP_sphere);
var_duda_pinna=find_var_of_three3(error_duda_pinna);
var_pinna=find_var_of_three3(error_pinna);
var_sphere=find_var_of_three3(error_sphere);
var_time=find_var_of_three3(error_time);
var_time_filter=find_var_of_three3(error_time_filter);

%%%%%%%%%%%%%%%%%%%%%%%%%%%%%%%%%%%%%%%%%%%%%%%%%%%%%%%%%%%%
%Make 1 colonne, to find mean mean and mean variance

tot_mean_LP_pinna=make_colonne3(mean_LP_pinna);
tot_mean_LP_sphere=make_colonne3(mean_LP_sphere);
tot_mean_duda_pinna=make_colonne3(mean_duda_pinna);
tot_mean_pinna=make_colonne3(mean_pinna);
tot_mean_sphere=make_colonne3(mean_sphere);
tot_mean_time=make_colonne3(mean_time);
tot_mean_time_filter=make_colonne3(mean_time_filter);

tot_var_LP_pinna=make_colonne3(var_LP_pinna);
tot_var_LP_sphere=make_colonne3(var_LP_sphere);
tot_var_duda_pinna=make_colonne3(var_duda_pinna);
tot_var_pinna=make_colonne3(var_pinna);
tot_var_sphere=make_colonne3(var_sphere);
tot_var_time=make_colonne3(var_time);
tot_var_time_filter=make_colonne3(var_time_filter);

%%%%%%%%%%%%%%%%%%%%%%%%%%%%%%%%%%%%%%%%%%%%%%%%%%%%%%%%%%%

mean_mean=zeros(7,1);
mean_mean(1)=mean(tot_mean_LP_pinna);
mean_mean(2)=mean(tot_mean_LP_sphere);
mean_mean(3)=mean(tot_mean_duda_pinna);
mean_mean(4)=mean(tot_mean_pinna);
mean_mean(5)=mean(tot_mean_sphere);
mean_mean(6)=mean(tot_mean_time);
mean_mean(7)=mean(tot_mean_time_filter);

mean_var=zeros(7,1);
mean_var(1)=mean(tot_var_LP_pinna);
mean_var(2)=mean(tot_var_LP_sphere);
mean_var(3)=mean(tot_var_duda_pinna);
mean_var(4)=mean(tot_var_pinna);
mean_var(5)=mean(tot_var_sphere);
mean_var(6)=mean(tot_var_time);
mean_var(7)=mean(tot_var_time_filter);

save('Method_var_3','mean_mean','mean_var')
```

MATLAB/Intermethodvariability3.m

```
%%%Finne personlig feil, over alle hoyttalere

fasit=[-40 -40 -40 -20 -20 -20 -10 -10 -10 10 10 10 20 20 20 40 40 40];

fasit=transpose(fasit);
error=zeros(18,13);

method=no2_all_sorted_time3_pr;


%Left side
for i=1:13
    error(1:9,i)=method(7:15,i)-fasit(1:9,1);
end


%Right side
for i=1:13
    error(10:18,i)=fasit(10:18,1)-method(19:27,i);
end

mean_error=mean(error);
std_error=sqrt(var(error));

subject=1:13;

plot(mean_error,subject, 'x')
hold on
```

```
for i=1:13
    xx=[i i];
    yy=[mean_error(i)-std_error(i) mean_error(i)+std_error(i)];
    plot(yy,xx)
    hold on
end


grid on
xlabel('Lozaliztion error [degrees]')
ylabel('Subject')
title('Time delay')
set(gca, 'Ygrid','On');
set(gca,'YTick',1:13);
axis([-80 80 0 14])
```

MATLAB/personlig_feil3.m

```
function pressurematrix = SCATTponspherefromfar(kvec,a,norder,thetavec)
% SCATTponspherefromfar calculates the sound pressure on a rigid sphere
% for a number of frequencies and a number of incidence angles.
% Plane wave incidence of amplitude 1 is assumed.
%
% Input parameters:
%   kvec            Array of wave numbers to compute the result for
%   a               The sphere radius, in meters
%   norder          The highest order in the truncate summation
%                   Recommended start value: 50
%   thetavec        Array of incidence angles to compute the result for,
%                   in radians.
%
% Output parameters:
%   pressurematrix  Matrix of complex pressures. Size [nfreqs,nangles].
%
% Peter Svensson and Mark Poletti 2007
%
% pressurematrix = SCATTponspherefromfar(kvec,a,norder,thetavec);

if kvec(1) == 0,
   computedc = 1;
   kvec = kvec(2:end);
else
    computedc = 0;
end

nfreqs = length(kvec);
nangles = length(thetavec);

pressurematrix = zeros(nfreqs,nangles);
nvec = [0:norder].';
kRvec = kvec(:).'*a;
costheta = cos(thetavec(:));

onesvec1 = ones(1,nangles);
onesvec2 = ones(1,nfreqs);
onesvec3 = ones(norder+1,1);

% One would believe that it would be faster to use the fact that we need
% to compute the difference between Bessel functions of order n+0.5 and
% n-0.5,
% which means that "n+0.5" could be the "n-0.5" for the next n, so to say.
% But, such an alternative formulation does not seem to be any faster!
% That alternative formulation would be:
% nveconeextra = [0:norder+1].';
% Bbig = besselj(nveconeextra-0.5,kRvec) + i*bessely(nveconeextra-0.5,kRvec);
% Bbig = Bbig(:,1:N+1) - Bbig(:,2:N+2)./kRvec(onesvec3,:).';
% multfac = sqrt(pi/2./kRvec);
% Bbig = Bbig.*multfac(onesvec3,:).';

Bbig = besselj(nvec+0.5,kRvec) + i*bessely(nvec+0.5,kRvec);
Bbig = Bbig.*(nvec(:,onesvec2)+1).'./kRvec(onesvec3,:).';
Bbig = besselj(nvec-0.5,kRvec) + i*bessely(nvec-0.5,kRvec) -Bbig;
multfac = sqrt(pi/2./kRvec);
Bbig = Bbig.*multfac(onesvec3,:).';

ncalcsvec = (2*nvec+1).*(-i).^nvec;
Bbig = ncalcsvec(:,onesvec2).'./Bbig;

for kn = 0:norder,
```

```
62      P = legendre(kn,costheta);
63      if kn > 0,
64          P = P(1,:);
65      else
66          P = P(:).';
67      end
68      addterm = Bbig(:,kn+1);
69      pressurematrix = pressurematrix + addterm(:,onesvec1).*P(onesvec2.',:);
70  end;
71
72  multfac = i./(kRvec.').^2;
73  pressurematrix = pressurematrix.*multfac(:,onesvec1);
74
75  if computedc == 1,
76     pressurematrix = [onesvec1;pressurematrix];
77  end
```

MATLAB/SCATTponspherefromfar.m

E Statistical analyses

```
 DATASET ACTIVATE DataSet28.
NEW FILE.
DATASET NAME DataSet38 WINDOW=FRONT.
DATASET ACTIVATE DataSet28.
DATASET CLOSE DataSet33.
DATASET ACTIVATE DataSet28.
DATASET CLOSE DataSet34.
DATASET ACTIVATE DataSet28.
DATASET CLOSE DataSet35.
DATASET ACTIVATE DataSet28.
DATASET CLOSE DataSet36.
DATASET ACTIVATE DataSet28.
DATASET CLOSE DataSet37.
DATASET ACTIVATE DataSet28.
DATASET CLOSE DataSet32.
DATASET ACTIVATE DataSet28.
DATASET CLOSE DataSet31.
DATASET ACTIVATE DataSet28.
DATASET CLOSE DataSet30.
DATASET ACTIVATE DataSet28.
DATASET CLOSE DataSet29.
DATASET ACTIVATE DataSet38.
DATASET CLOSE DataSet28.
ONEWAY Error BY Method
  /STATISTICS DESCRIPTIVES HOMOGENEITY WELCH
  /PLOT MEANS
  /MISSING ANALYSIS
  /POSTHOC=TUKEY GH ALPHA(0.05).
```

Oneway

Notes

Output Created		**11-JUN-2012 11:16:55**
Comments		
Input	**Active Dataset**	**DataSet38**
	Filter	**<none>**
	Weight	**<none>**
	Split File	**<none>**
	N of Rows in Working Data File	**2727**
Missing Value Handling	**Definition of Missing**	User-defined missing values are treated as missing.
	Cases Used	Statistics for each analysis are based on cases with no missing data for any variable in the analysis.
Syntax		ONEWAY Error BY Method /STATISTICS DESCRIPTIVES HOMOGENEITY WELCH /PLOT MEANS /MISSING ANALYSIS /POSTHOC=TUKEY GH ALPHA(0.05).
Resources	**Processor Time**	**00:00:00,45**
	Elapsed Time	**00:00:00,00**

[DataSet38]

Descriptives

Error

	N	Mean	Std. Deviation	Std. Error	95% Confidence Interval for Mean		Minimum	Maximum
					Lower Bound	Upper Bound		
LP_pinna	388	-10.6959	27.12361	1.37699	-13.4032	-7.9886	-100.00	100.00
LP_sphere	389	-8.9974	24.26810	1.23044	-11.4166	-6.5783	-70.00	100.00
Duda_pinna	390	-13.8205	23.96481	1.21351	-16.2064	-11.4347	-70.00	90.00
pinna	390	-10.8462	27.58584	1.39686	-13.5925	-8.0998	-70.00	150.00
sphere	390	-13.9231	27.53347	1.39421	-16.6642	-11.1819	-80.00	100.00
Time	390	-6.2308	24.01581	1.21609	-8.6217	-3.8398	-90.00	60.00
time_filter	390	-14.2821	23.56138	1.19308	-16.6277	-11.9364	-90.00	90.00
Total	2727	-11.2578	25.61629	.49054	-12.2197	-10.2959	-100.00	150.00

Test of Homogeneity of Variances

Error

Levene Statistic	df1	df2	Sig.
2.692	6	2720	.013

ANOVA

Error

	Sum of Squares	df	Mean Square	F	Sig.
Between Groups	20930.559	6	3488.426	5.367	.000
Within Groups	1767855.21	2720	649.947		
Total	1788785.77	2726			

Robust Tests of Equality of Means

Error

	Statistic[a]	df1	df2	Sig.
Welch	5.859	6	1208.268	.000

a. Asymptotically F distributed.

Post Hoc Tests

Multiple Comparisons

Dependent Variable: Error

	(I) Method	(J) Method	Mean Difference (I-J)	Std. Error	Sig.	95% Confidence Interval	
						Lower Bound	Upper Bound
Tukey HSD	LP_pinna	LP_sphere	-1.69845	1.82919	.968	-7.0955	3.6986
		Duda_pinna	3.12464	1.82802	.610	-2.2690	8.5183
		pinna	.15028	1.82802	1.000	-5.2434	5.5439
		sphere	3.22720	1.82802	.572	-2.1664	8.6208
		Time	-4.46511	1.82802	.181	-9.8587	.9285
		time_filter	3.58617	1.82802	.440	-1.8075	8.9798
	LP_sphere	LP_pinna	1.69845	1.82919	.968	-3.6986	7.0955
		Duda_pinna	4.82308	1.82684	.115	-.5671	10.2132
		pinna	1.84872	1.82684	.951	-3.5414	7.2389
		sphere	4.92565	1.82684	.100	-.4645	10.3158
		Time	-2.76666	1.82684	.736	-8.1568	2.6235
		time_filter	5.28462	1.82684	.059	-.1055	10.6748
	Duda_pinna	LP_pinna	-3.12464	1.82802	.610	-8.5183	2.2690
		LP_sphere	-4.82308	1.82684	.115	-10.2132	.5671
		pinna	-2.97436	1.82567	.663	-8.3611	2.4123
		sphere	.10256	1.82567	1.000	-5.2841	5.4893
		Time	-7.58974*	1.82567	.001	-12.9764	-2.2030
		time_filter	.46154	1.82567	1.000	-4.9252	5.8482
	pinna	LP_pinna	-.15028	1.82802	1.000	-5.5439	5.2434
		LP_sphere	-1.84872	1.82684	.951	-7.2389	3.5414
		Duda_pinna	2.97436	1.82567	.663	-2.4123	8.3611
		sphere	3.07692	1.82567	.626	-2.3098	8.4636
		Time	-4.61538	1.82567	.150	-10.0021	.7713
		time_filter	3.43590	1.82567	.492	-1.9508	8.8226
	sphere	LP_pinna	-3.22720	1.82802	.572	-8.6208	2.1664
		LP_sphere	-4.92565	1.82684	.100	-10.3158	.4645
		Duda_pinna	-.10256	1.82567	1.000	-5.4893	5.2841
		pinna	-3.07692	1.82567	.626	-8.4636	2.3098
		Time	-7.69231*	1.82567	.001	-13.0790	-2.3056
		time_filter	.35897	1.82567	1.000	-5.0277	5.7457
	Time	LP_pinna	4.46511	1.82802	.181	-.9285	9.8587
		LP_sphere	2.76666	1.82684	.736	-2.6235	8.1568
		Duda_pinna	7.58974*	1.82567	.001	2.2030	12.9764
		pinna	4.61538	1.82567	.150	-.7713	10.0021
		sphere	7.69231*	1.82567	.001	2.3056	13.0790
		time_filter	8.05128*	1.82567	.000	2.6646	13.4380
	time_filter	LP_pinna	-3.58617	1.82802	.440	-8.9798	1.8075
		LP_sphere	-5.28462	1.82684	.059	-10.6748	.1055
		Duda_pinna	-.46154	1.82567	1.000	-5.8482	4.9252
		pinna	-3.43590	1.82567	.492	-8.8226	1.9508
		sphere	-.35897	1.82567	1.000	-5.7457	5.0277
		Time	-8.05128*	1.82567	.000	-13.4380	-2.6646
Games-Howell	LP_pinna	LP_sphere	-1.69845	1.84664	.969	-7.1575	3.7606
		Duda_pinna	3.12464	1.83540	.615	-2.3012	8.5505
		pinna	.15028	1.96146	1.000	-5.6480	5.9485

Multiple Comparisons

Dependent Variable: Error

(I) Method	(J) Method	Mean Difference (I-J)	Std. Error	Sig.	95% Confidence Interval	
					Lower Bound	Upper Bound
	sphere	3.22720	1.95957	.652	-2.5655	9.0199
	Time	-4.46511	1.83711	.187	-9.8960	.9658
	time_filter	3.58617	1.82196	.436	-1.8000	8.9724
LP_sphere	LP_pinna	1.69845	1.84664	.969	-3.7606	7.1575
	Duda_pinna	4.82308	1.72817	.079	-.2855	9.9317
	pinna	1.84872	1.86151	.955	-3.6543	7.3517
	sphere	4.92565	1.85952	.113	-.5715	10.4228
	Time	-2.76666	1.72999	.683	-7.8806	2.3473
	time_filter	5.28462*	1.71389	.034	.2182	10.3510
Duda_pinna	LP_pinna	-3.12464	1.83540	.615	-8.5505	2.3012
	LP_sphere	-4.82308	1.72817	.079	-9.9317	.2855
	pinna	-2.97436	1.85036	.678	-8.4444	2.4957
	sphere	.10256	1.84836	1.000	-5.3616	5.5667
	Time	-7.58974*	1.71798	.000	-12.6682	-2.5113
	time_filter	.46154	1.70177	1.000	-4.5690	5.4921
pinna	LP_pinna	-.15028	1.96146	1.000	-5.9485	5.6480
	LP_sphere	-1.84872	1.86151	.955	-7.3517	3.6543
	Duda_pinna	2.97436	1.85036	.678	-2.4957	8.4444
	sphere	3.07692	1.97359	.709	-2.7571	8.9110
	Time	-4.61538	1.85205	.164	-10.0905	.8597
	time_filter	3.43590	1.83702	.501	-1.9948	8.8666
sphere	LP_pinna	-3.22720	1.95957	.652	-9.0199	2.5655
	LP_sphere	-4.92565	1.85952	.113	-10.4228	.5715
	Duda_pinna	-.10256	1.84836	1.000	-5.5667	5.3616
	pinna	-3.07692	1.97359	.709	-8.9110	2.7571
	Time	-7.69231*	1.85005	.001	-13.1615	-2.2232
	time_filter	.35897	1.83501	1.000	-5.0658	5.7837
Time	LP_pinna	4.46511	1.83711	.187	-.9658	9.8960
	LP_sphere	2.76666	1.72999	.683	-2.3473	7.8806
	Duda_pinna	7.58974*	1.71798	.000	2.5113	12.6682
	pinna	4.61538	1.85205	.164	-.8597	10.0905
	sphere	7.69231*	1.85005	.001	2.2232	13.1615
	time_filter	8.05128*	1.70361	.000	3.0153	13.0873
time_filter	LP_pinna	-3.58617	1.82196	.436	-8.9724	1.8000
	LP_sphere	-5.28462*	1.71389	.034	-10.3510	-.2182
	Duda_pinna	-.46154	1.70177	1.000	-5.4921	4.5690
	pinna	-3.43590	1.83702	.501	-8.8666	1.9948
	sphere	-.35897	1.83501	1.000	-5.7837	5.0658
	Time	-8.05128*	1.70361	.000	-13.0873	-3.0153

*. The mean difference is significant at the 0.05 level.

Homogeneous Subsets

Error

	Method	N	Subset for alpha = 0.05	
			1	2
Tukey HSD[a,b]	time_filter	390	-14.2821	
	sphere	390	-13.9231	
	Duda_pinna	390	-13.8205	
	pinna	390	-10.8462	-10.8462
	LP_pinna	388	-10.6959	-10.6959
	LP_sphere	389	-8.9974	-8.9974
	Time	390		-6.2308
	Sig.		.059	.150

Means for groups in homogeneous subsets are displayed.

a. Uses Harmonic Mean Sample Size = 389,570.

b. The group sizes are unequal. The harmonic mean of the group sizes is used. Type I error levels are not guaranteed.

Means Plots

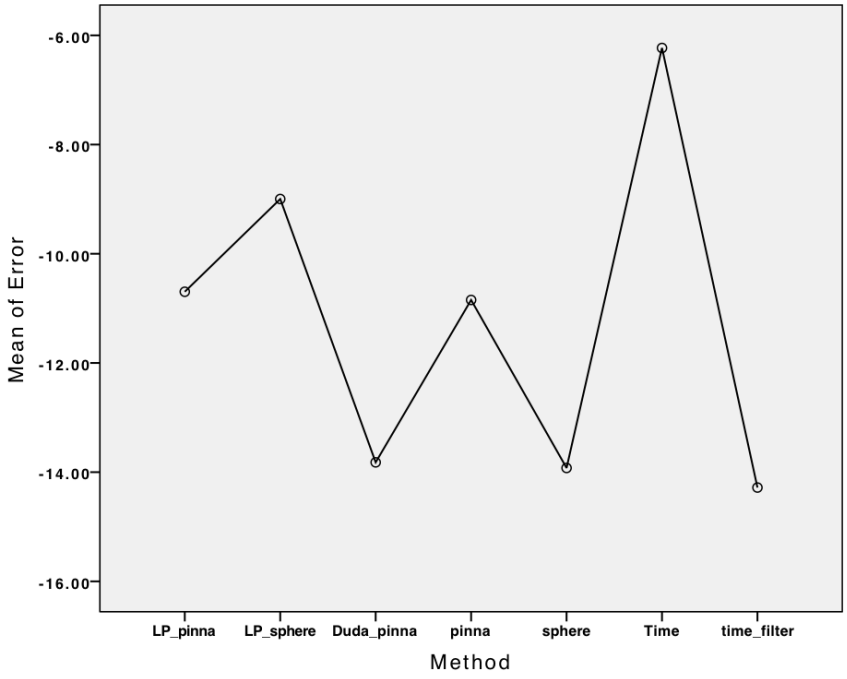

```
ONEWAY Angle BY Method
  /STATISTICS DESCRIPTIVES HOMOGENEITY WELCH
  /PLOT MEANS
  /MISSING ANALYSIS
  /POSTHOC=TUKEY GH ALPHA(0.05).
```

Oneway

Notes

Output Created		**10-JUN-2012 15:44:06**
Comments		
Input	**Data**	/Users/nordstoga_eide/Documents/SPSSInc/Each angle/m0.sav
	Active Dataset	**DataSet5**
	Filter	**<none>**
	Weight	**<none>**
	Split File	**<none>**
	N of Rows in Working Data File	**273**
Missing Value Handling	**Definition of Missing**	User-defined missing values are treated as missing.
	Cases Used	Statistics for each analysis are based on cases with no missing data for any variable in the analysis.
Syntax		ONEWAY Angle BY Method /STATISTICS DESCRIPTIVES HOMOGENEITY WELCH /PLOT MEANS /MISSING ANALYSIS /POSTHOC=TUKEY GH ALPHA(0.05).
Resources	**Processor Time**	**00:00:00,42**
	Elapsed Time	**00:00:01,00**

```
[DataSet5] /Users/nordstoga_eide/Documents/SPSSInc/Each angle/m0.sav
```

Descriptives

Angle

	N	Mean	Std. Deviation	Std. Error	95% Confidence Interval for Mean		Minimum	Maximum
					Lower Bound	Upper Bound		
LP_pinna	39	1.7949	16.03808	2.56815	-3.4041	6.9938	-80.00	30.00
LP_sphere	39	3.3333	12.42521	1.98963	-.6945	7.3611	-30.00	40.00
Duda_pinna	39	.2564	14.59762	2.33749	-4.4756	4.9884	-40.00	40.00
pinna	39	1.2821	13.79922	2.20964	-3.1911	5.7552	-30.00	30.00
Sphere	39	10.0000	23.50812	3.76431	2.3795	17.6205	-30.00	70.00
Time	39	7.6923	15.46840	2.47693	2.6780	12.7066	-20.00	40.00
Time_filter	39	2.0513	10.04712	1.60883	-1.2056	5.3082	-30.00	20.00
Total	273	3.7729	15.81301	.95705	1.8887	5.6571	-80.00	70.00

Test of Homogeneity of Variances

Angle

Levene Statistic	df1	df2	Sig.
3.665	6	266	.002

ANOVA

Angle

	Sum of Squares	df	Mean Square	F	Sig.
Between Groups	3111.355	6	518.559	2.125	.051
Within Groups	64902.564	266	243.995		
Total	68013.919	272			

Robust Tests of Equality of Means

Angle

	Statistic[a]	df1	df2	Sig.
Welch	1.560	6	117.554	.165

a. Asymptotically F distributed.

Post Hoc Tests

Multiple Comparisons

Dependent Variable: Angle

	(I) Method	(J) Method	Mean Difference (I-J)	Std. Error	Sig.	95% Confidence Interval	
						Lower Bound	Upper Bound
Tukey HSD	LP_pinna	LP_sphere	-1.53846	3.53731	.999	-12.0480	8.9711
		Duda_pinna	1.53846	3.53731	.999	-8.9711	12.0480
		pinna	.51282	3.53731	1.000	-9.9967	11.0224
		Sphere	-8.20513	3.53731	.239	-18.7147	2.3044
		Time	-5.89744	3.53731	.639	-16.4070	4.6121
		Time_filter	-.25641	3.53731	1.000	-10.7659	10.2531
	LP_sphere	LP_pinna	1.53846	3.53731	.999	-8.9711	12.0480
		Duda_pinna	3.07692	3.53731	.977	-7.4326	13.5865
		pinna	2.05128	3.53731	.997	-8.4582	12.5608
		Sphere	-6.66667	3.53731	.492	-17.1762	3.8429
		Time	-4.35897	3.53731	.881	-14.8685	6.1506
		Time_filter	1.28205	3.53731	1.000	-9.2275	11.7916
	Duda_pinna	LP_pinna	-1.53846	3.53731	.999	-12.0480	8.9711
		LP_sphere	-3.07692	3.53731	.977	-13.5865	7.4326
		pinna	-1.02564	3.53731	1.000	-11.5352	9.4839
		Sphere	-9.74359	3.53731	.089	-20.2531	.7659
		Time	-7.43590	3.53731	.354	-17.9454	3.0736
		Time_filter	-1.79487	3.53731	.999	-12.3044	8.7147
	pinna	LP_pinna	-.51282	3.53731	1.000	-11.0224	9.9967
		LP_sphere	-2.05128	3.53731	.997	-12.5608	8.4582
		Duda_pinna	1.02564	3.53731	1.000	-9.4839	11.5352
		Sphere	-8.71795	3.53731	.177	-19.2275	1.7916

Multiple Comparisons

Dependent Variable: Angle

	(I) Method	(J) Method	Mean Difference (I-J)	Std. Error	Sig.	95% Confidence Interval	
						Lower Bound	Upper Bound
		Time	-6.41026	3.53731	.541	-16.9198	4.0993
		Time_filter	-.76923	3.53731	1.000	-11.2788	9.7403
	Sphere	LP_pinna	8.20513	3.53731	.239	-2.3044	18.7147
		LP_sphere	6.66667	3.53731	.492	-3.8429	17.1762
		Duda_pinna	9.74359	3.53731	.089	-.7659	20.2531
		pinna	8.71795	3.53731	.177	-1.7916	19.2275
		Time	2.30769	3.53731	.995	-8.2018	12.8172
		Time_filter	7.94872	3.53731	.274	-2.5608	18.4582
	Time	LP_pinna	5.89744	3.53731	.639	-4.6121	16.4070
		LP_sphere	4.35897	3.53731	.881	-6.1506	14.8685
		Duda_pinna	7.43590	3.53731	.354	-3.0736	17.9454
		pinna	6.41026	3.53731	.541	-4.0993	16.9198
		Sphere	-2.30769	3.53731	.995	-12.8172	8.2018
		Time_filter	5.64103	3.53731	.686	-4.8685	16.1506
	Time_filter	LP_pinna	.25641	3.53731	1.000	-10.2531	10.7659
		LP_sphere	-1.28205	3.53731	1.000	-11.7916	9.2275
		Duda_pinna	1.79487	3.53731	.999	-8.7147	12.3044
		pinna	.76923	3.53731	1.000	-9.7403	11.2788
		Sphere	-7.94872	3.53731	.274	-18.4582	2.5608
		Time	-5.64103	3.53731	.686	-16.1506	4.8685
Games-Howell	LP_pinna	LP_sphere	-1.53846	3.24869	.999	-11.3944	8.3175
		Duda_pinna	1.53846	3.47264	.999	-8.9817	12.0586
		pinna	.51282	3.38791	1.000	-9.7544	10.7800
		Sphere	-8.20513	4.55691	.552	-22.0563	5.6460
		Time	-5.89744	3.56799	.649	-16.7043	4.9094
		Time_filter	-.25641	3.03046	1.000	-9.4820	8.9692
	LP_sphere	LP_pinna	1.53846	3.24869	.999	-8.3175	11.3944
		Duda_pinna	3.07692	3.06960	.952	-6.2264	12.3803
		pinna	2.05128	2.97340	.993	-6.9570	11.0595
		Sphere	-6.66667	4.25778	.704	-19.6730	6.3397
		Time	-4.35897	3.17707	.815	-13.9935	5.2755
		Time_filter	1.28205	2.55870	.999	-6.4767	9.0408
	Duda_pinna	LP_pinna	-1.53846	3.47264	.999	-12.0586	8.9817
		LP_sphere	-3.07692	3.06960	.952	-12.3803	6.2264
		pinna	-1.02564	3.21658	1.000	-10.7686	8.7173
		Sphere	-9.74359	4.43102	.311	-23.2352	3.7480
		Time	-7.43590	3.40573	.317	-17.7518	2.8800
		Time_filter	-1.79487	2.83764	.995	-10.4189	6.8291
	pinna	LP_pinna	-.51282	3.38791	1.000	-10.7800	9.7544
		LP_sphere	-2.05128	2.97340	.993	-11.0595	6.9570
		Duda_pinna	1.02564	3.21658	1.000	-8.7173	10.7686
		Sphere	-8.71795	4.36492	.427	-22.0230	4.5871
		Time	-6.41026	3.31929	.467	-16.4670	3.6464
		Time_filter	-.76923	2.73328	1.000	-9.0686	7.5302

Multiple Comparisons

Dependent Variable: Angle

(I) Method	(J) Method	Mean Difference (I-J)	Std. Error	Sig.	95% Confidence Interval	
					Lower Bound	Upper Bound
Sphere	LP_pinna	8.20513	4.55691	.552	-5.6460	22.0563
	LP_sphere	6.66667	4.25778	.704	-6.3397	19.6730
	Duda_pinna	9.74359	4.43102	.311	-3.7480	23.2352
	pinna	8.71795	4.36492	.427	-4.5871	22.0230
	Time	2.30769	4.50613	.999	-11.3978	16.0132
	Time_filter	7.94872	4.09370	.463	-4.6106	20.5080
Time	LP_pinna	5.89744	3.56799	.649	-4.9094	16.7043
	LP_sphere	4.35897	3.17707	.815	-5.2755	13.9935
	Duda_pinna	7.43590	3.40573	.317	-2.8800	17.7518
	pinna	6.41026	3.31929	.467	-3.6464	16.4670
	Sphere	-2.30769	4.50613	.999	-16.0132	11.3978
	Time_filter	5.64103	2.95355	.481	-3.3444	14.6264
Time_filter	LP_pinna	.25641	3.03046	1.000	-8.9692	9.4820
	LP_sphere	-1.28205	2.55870	.999	-9.0408	6.4767
	Duda_pinna	1.79487	2.83764	.995	-6.8291	10.4189
	pinna	.76923	2.73328	1.000	-7.5302	9.0686
	Sphere	-7.94872	4.09370	.463	-20.5080	4.6106
	Time	-5.64103	2.95355	.481	-14.6264	3.3444

Homogeneous Subsets

Angle

	Method	N	Subset for alpha = 0.05
			1
Tukey HSD[a]	Duda_pinna	39	.2564
	pinna	39	1.2821
	LP_pinna	39	1.7949
	Time_filter	39	2.0513
	LP_sphere	39	3.3333
	Time	39	7.6923
	Sphere	39	10.0000
	Sig.		.089

Means for groups in homogeneous subsets are displayed.

a. Uses Harmonic Mean Sample Size = 39,000.

Means Plots

```
ONEWAY Angle BY Method
  /STATISTICS DESCRIPTIVES HOMOGENEITY WELCH
  /PLOT MEANS
  /MISSING ANALYSIS
  /POSTHOC=TUKEY GH ALPHA(0.05).
```

Oneway

Notes

Output Created		**10-JUN-2012 15:38:37**
Comments		
Input	**Data**	/Users/nordstoga_eide/Documents/SPSSInc/Each angle/m10.sav
	Active Dataset	**DataSet4**
	Filter	**<none>**
	Weight	**<none>**
	Split File	**<none>**
	N of Rows in Working Data File	**273**
Missing Value Handling	**Definition of Missing**	User-defined missing values are treated as missing.
	Cases Used	Statistics for each analysis are based on cases with no missing data for any variable in the analysis.
Syntax		ONEWAY Angle BY Method /STATISTICS DESCRIPTIVES HOMOGENEITY WELCH /PLOT MEANS /MISSING ANALYSIS /POSTHOC=TUKEY GH ALPHA(0.05).
Resources	**Processor Time**	**00:00:00,50**
	Elapsed Time	**00:00:00,00**

```
[DataSet4] /Users/nordstoga_eide/Documents/SPSSInc/Each angle/m10.sav
```

Descriptives

Angle

	N	Mean	Std. Deviation	Std. Error	95% Confidence Interval for Mean		Minimum	Maximum
					Lower Bound	Upper Bound		
LP_pinna	**39**	**-2.5641**	**19.42840**	**3.11103**	**-8.8621**	**3.7339**	**-60.00**	**50.00**
LP_sphere	**39**	**-16.1538**	**18.00810**	**2.88360**	**-21.9914**	**-10.3163**	**-60.00**	**20.00**
Duda_pinna	**39**	**-14.1026**	**20.09424**	**3.21765**	**-20.6164**	**-7.5888**	**-60.00**	**30.00**
pinna	**39**	**-12.8205**	**19.86119**	**3.18034**	**-19.2588**	**-6.3823**	**-50.00**	**20.00**
Sphere	**39**	**-28.9744**	**20.49324**	**3.28155**	**-35.6175**	**-22.3312**	**-80.00**	**20.00**
Time	**39**	**-2.8205**	**17.16004**	**2.74781**	**-8.3832**	**2.7421**	**-50.00**	**20.00**
Time_filter	**39**	**-14.8718**	**22.46305**	**3.59697**	**-22.1535**	**-7.5901**	**-80.00**	**30.00**
Total	**273**	**-13.1868**	**21.18957**	**1.28245**	**-15.7116**	**-10.6620**	**-80.00**	**50.00**

Test of Homogeneity of Variances

Angle

Levene Statistic	df1	df2	Sig.
.417	6	266	.867

ANOVA

Angle

	Sum of Squares	df	Mean Square	F	Sig.
Between Groups	18804.396	6	3134.066	8.068	.000
Within Groups	103323.077	266	388.433		
Total	122127.473	272			

Robust Tests of Equality of Means

Angle

	Statistic[a]	df1	df2	Sig.
Welch	8.122	6	118.135	.000

a. Asymptotically F distributed.

Post Hoc Tests

Multiple Comparisons

Dependent Variable: Angle

	(I) Method	(J) Method	Mean Difference (I-J)	Std. Error	Sig.	95% Confidence Interval	
						Lower Bound	Upper Bound
Tukey HSD	LP_pinna	LP_sphere	13.58974*	4.46314	.041	.3295	26.8500
		Duda_pinna	11.53846	4.46314	.135	-1.7218	24.7987
		pinna	10.25641	4.46314	.249	-3.0038	23.5166
		Sphere	26.41026*	4.46314	.000	13.1500	39.6705
		Time	.25641	4.46314	1.000	-13.0038	13.5166
		Time_filter	12.30769	4.46314	.088	-.9525	25.5679
	LP_sphere	LP_pinna	-13.58974*	4.46314	.041	-26.8500	-.3295
		Duda_pinna	-2.05128	4.46314	.999	-15.3115	11.2089
		pinna	-3.33333	4.46314	.989	-16.5936	9.9269
		Sphere	12.82051	4.46314	.066	-.4397	26.0807
		Time	-13.33333*	4.46314	.048	-26.5936	-.0731
		Time_filter	-1.28205	4.46314	1.000	-14.5423	11.9782
	Duda_pinna	LP_pinna	-11.53846	4.46314	.135	-24.7987	1.7218
		LP_sphere	2.05128	4.46314	.999	-11.2089	15.3115
		pinna	-1.28205	4.46314	1.000	-14.5423	11.9782
		Sphere	14.87179*	4.46314	.017	1.6116	28.1320
		Time	-11.28205	4.46314	.154	-24.5423	1.9782
		Time_filter	.76923	4.46314	1.000	-12.4910	14.0295
	pinna	LP_pinna	-10.25641	4.46314	.249	-23.5166	3.0038
		LP_sphere	3.33333	4.46314	.989	-9.9269	16.5936
		Duda_pinna	1.28205	4.46314	1.000	-11.9782	14.5423
		Sphere	16.15385*	4.46314	.006	2.8936	29.4141

Multiple Comparisons

Dependent Variable: Angle

	(I) Method	(J) Method	Mean Difference (I-J)	Std. Error	Sig.	95% Confidence Interval	
						Lower Bound	Upper Bound
		Time	-10.00000	4.46314	.278	-23.2602	3.2602
		Time_filter	2.05128	4.46314	.999	-11.2089	15.3115
	Sphere	LP_pinna	-26.41026*	4.46314	.000	-39.6705	-13.1500
		LP_sphere	-12.82051	4.46314	.066	-26.0807	.4397
		Duda_pinna	-14.87179*	4.46314	.017	-28.1320	-1.6116
		pinna	-16.15385*	4.46314	.006	-29.4141	-2.8936
		Time	-26.15385*	4.46314	.000	-39.4141	-12.8936
		Time_filter	-14.10256*	4.46314	.029	-27.3628	-.8423
	Time	LP_pinna	-.25641	4.46314	1.000	-13.5166	13.0038
		LP_sphere	13.33333*	4.46314	.048	.0731	26.5936
		Duda_pinna	11.28205	4.46314	.154	-1.9782	24.5423
		pinna	10.00000	4.46314	.278	-3.2602	23.2602
		Sphere	26.15385*	4.46314	.000	12.8936	39.4141
		Time_filter	12.05128	4.46314	.102	-1.2089	25.3115
	Time_filter	LP_pinna	-12.30769	4.46314	.088	-25.5679	.9525
		LP_sphere	1.28205	4.46314	1.000	-11.9782	14.5423
		Duda_pinna	-.76923	4.46314	1.000	-14.0295	12.4910
		pinna	-2.05128	4.46314	.999	-15.3115	11.2089
		Sphere	14.10256*	4.46314	.029	.8423	27.3628
		Time	-12.05128	4.46314	.102	-25.3115	1.2089
Games-Howell	LP_pinna	LP_sphere	13.58974*	4.24190	.031	.7402	26.4393
		Duda_pinna	11.53846	4.47569	.147	-2.0176	25.0945
		pinna	10.25641	4.44894	.255	-3.2184	23.7312
		Sphere	26.41026*	4.52184	.000	12.7138	40.1067
		Time	.25641	4.15078	1.000	-12.3203	12.8331
		Time_filter	12.30769	4.75570	.145	-2.1041	26.7194
	LP_sphere	LP_pinna	-13.58974*	4.24190	.031	-26.4393	-.7402
		Duda_pinna	-2.05128	4.32070	.999	-15.1417	11.0391
		pinna	-3.33333	4.29298	.987	-16.3389	9.6723
		Sphere	12.82051	4.36849	.064	-.4163	26.0573
		Time	-13.33333*	3.98316	.021	-25.3980	-1.2687
		Time_filter	-1.28205	4.61013	1.000	-15.2627	12.6986
	Duda_pinna	LP_pinna	-11.53846	4.47569	.147	-25.0945	2.0176
		LP_sphere	2.05128	4.32070	.999	-11.0391	15.1417
		pinna	-1.28205	4.52414	1.000	-14.9845	12.4204
		Sphere	14.87179*	4.59585	.028	.9521	28.7915
		Time	-11.28205	4.23128	.122	-24.1059	1.5418
		Time_filter	.76923	4.82612	1.000	-13.8526	15.3911
	pinna	LP_pinna	-10.25641	4.44894	.255	-23.7312	3.2184
		LP_sphere	3.33333	4.29298	.987	-9.6723	16.3389
		Duda_pinna	1.28205	4.52414	1.000	-12.4204	14.9845
		Sphere	16.15385*	4.56980	.012	2.3128	29.9949
		Time	-10.00000	4.20297	.222	-22.7369	2.7369
		Time_filter	2.05128	4.80132	1.000	-12.4965	16.5990

Multiple Comparisons

Dependent Variable: Angle

(I) Method	(J) Method	Mean Difference (I-J)	Std. Error	Sig.	95% Confidence Interval	
					Lower Bound	Upper Bound
Sphere	LP_pinna	-26.41026*	4.52184	.000	-40.1067	-12.7138
	LP_sphere	-12.82051	4.36849	.064	-26.0573	.4163
	Duda_pinna	-14.87179*	4.59585	.028	-28.7915	-.9521
	pinna	-16.15385*	4.56980	.012	-29.9949	-2.3128
	Time	-26.15385*	4.28007	.000	-39.1278	-13.1799
	Time_filter	-14.10256	4.86895	.070	-28.8526	.6475
Time	LP_pinna	-.25641	4.15078	1.000	-12.8331	12.3203
	LP_sphere	13.33333*	3.98316	.021	1.2687	25.3980
	Duda_pinna	11.28205	4.23128	.122	-1.5418	24.1059
	pinna	10.00000	4.20297	.222	-2.7369	22.7369
	Sphere	26.15385*	4.28007	.000	13.1799	39.1278
	Time_filter	12.05128	4.52643	.123	-1.6836	25.7861
Time_filter	LP_pinna	-12.30769	4.75570	.145	-26.7194	2.1041
	LP_sphere	1.28205	4.61013	1.000	-12.6986	15.2627
	Duda_pinna	-.76923	4.82612	1.000	-15.3911	13.8526
	pinna	-2.05128	4.80132	1.000	-16.5990	12.4965
	Sphere	14.10256	4.86895	.070	-.6475	28.8526
	Time	-12.05128	4.52643	.123	-25.7861	1.6836

*. The mean difference is significant at the 0.05 level.

Homogeneous Subsets

Angle

	Method	N	Subset for alpha = 0.05		
			1	2	3
Tukey HSD[a]	Sphere	39	-28.9744		
	LP_sphere	39	-16.1538	-16.1538	
	Time_filter	39		-14.8718	-14.8718
	Duda_pinna	39		-14.1026	-14.1026
	pinna	39		-12.8205	-12.8205
	Time	39			-2.8205
	LP_pinna	39			-2.5641
	Sig.		.066	.989	.088

Means for groups in homogeneous subsets are displayed.

a. Uses Harmonic Mean Sample Size = 39,000.

Means Plots

```
 GET
  FILE='/Users/nordstoga_eide/Documents/SPSSInc/Each angle/m20.sav'.
DATASET NAME DataSet3 WINDOW=FRONT.
DATASET ACTIVATE DataSet3.
DATASET CLOSE DataSet2.
ONEWAY Angle BY Method
  /STATISTICS DESCRIPTIVES HOMOGENEITY WELCH
  /PLOT MEANS
  /MISSING ANALYSIS
  /POSTHOC=TUKEY GH ALPHA(0.05).
```

Oneway

Notes

Output Created		**10-JUN-2012 15:35:03**
Comments		
Input	**Data**	/Users/nordstoga_eide/Documents/SPSSInc/Each angle/m20.sav
	Active Dataset	**DataSet3**
	Filter	**<none>**
	Weight	**<none>**
	Split File	**<none>**
	N of Rows in Working Data File	**273**
Missing Value Handling	**Definition of Missing**	User-defined missing values are treated as missing.
	Cases Used	Statistics for each analysis are based on cases with no missing data for any variable in the analysis.
Syntax		ONEWAY Angle BY Method /STATISTICS DESCRIPTIVES HOMOGENEITY WELCH /PLOT MEANS /MISSING ANALYSIS /POSTHOC=TUKEY GH ALPHA(0.05).
Resources	**Processor Time**	**00:00:00,41**
	Elapsed Time	**00:00:00,00**

```
[DataSet3] /Users/nordstoga_eide/Documents/SPSSInc/Each angle/m20.sav
```

Descriptives

Angle

	N	Mean	Std. Deviation	Std. Error	95% Confidence Interval for Mean		Minimum	Maximum
					Lower Bound	Upper Bound		
LP_pinna	39	-14.6154	21.74568	3.48210	-21.6645	-7.5663	-60.00	40.00
LP_sphere	39	-31.0256	17.28931	2.76851	-36.6302	-25.4211	-70.00	10.00
Duda_pinna	39	-23.3333	21.92491	3.51080	-30.4406	-16.2261	-60.00	30.00
pinna	39	-26.6667	22.04461	3.52996	-33.8127	-19.5206	-70.00	10.00
Sphere	39	-31.0256	22.09964	3.53877	-38.1895	-23.8618	-70.00	10.00
Time	39	-13.0769	24.83142	3.97621	-21.1263	-5.0275	-70.00	50.00
Time_filter	39	-23.5897	21.70219	3.47513	-30.6248	-16.5547	-70.00	20.00
Total	273	-23.3333	22.52994	1.36357	-26.0178	-20.6488	-70.00	50.00

Test of Homogeneity of Variances

Angle

Levene Statistic	df1	df2	Sig.
1.770	6	266	.105

ANOVA

Angle

	Sum of Squares	df	Mean Square	F	Sig.
Between Groups	12117.949	6	2019.658	4.265	.000
Within Groups	125948.718	266	473.491		
Total	138066.667	272			

Robust Tests of Equality of Means

Angle

	Statistic[a]	df1	df2	Sig.
Welch	4.179	6	118.056	.001

a. Asymptotically F distributed.

Post Hoc Tests

Multiple Comparisons

Dependent Variable: Angle

	(I) Method	(J) Method	Mean Difference (I-J)	Std. Error	Sig.	95% Confidence Interval	
						Lower Bound	Upper Bound
Tukey HSD	LP_pinna	LP_sphere	16.41026*	4.92764	.017	1.7700	31.0505
		Duda_pinna	8.71795	4.92764	.570	-5.9223	23.3582
		pinna	12.05128	4.92764	.184	-2.5890	26.6916
		Sphere	16.41026*	4.92764	.017	1.7700	31.0505
		Time	-1.53846	4.92764	1.000	-16.1787	13.1018
		Time_filter	8.97436	4.92764	.535	-5.6659	23.6146
	LP_sphere	LP_pinna	-16.41026*	4.92764	.017	-31.0505	-1.7700
		Duda_pinna	-7.69231	4.92764	.707	-22.3326	6.9480
		pinna	-4.35897	4.92764	.975	-18.9992	10.2813
		Sphere	.00000	4.92764	1.000	-14.6403	14.6403
		Time	-17.94872*	4.92764	.006	-32.5890	-3.3084
		Time_filter	-7.43590	4.92764	.739	-22.0762	7.2044
	Duda_pinna	LP_pinna	-8.71795	4.92764	.570	-23.3582	5.9223
		LP_sphere	7.69231	4.92764	.707	-6.9480	22.3326
		pinna	3.33333	4.92764	.994	-11.3069	17.9736
		Sphere	7.69231	4.92764	.707	-6.9480	22.3326
		Time	-10.25641	4.92764	.367	-24.8967	4.3839
		Time_filter	.25641	4.92764	1.000	-14.3839	14.8967
	pinna	LP_pinna	-12.05128	4.92764	.184	-26.6916	2.5890
		LP_sphere	4.35897	4.92764	.975	-10.2813	18.9992
		Duda_pinna	-3.33333	4.92764	.994	-17.9736	11.3069
		Sphere	4.35897	4.92764	.975	-10.2813	18.9992
		Time	-13.58974	4.92764	.088	-28.2300	1.0505
		Time_filter	-3.07692	4.92764	.996	-17.7172	11.5634
	Sphere	LP_pinna	-16.41026*	4.92764	.017	-31.0505	-1.7700
		LP_sphere	.00000	4.92764	1.000	-14.6403	14.6403
		Duda_pinna	-7.69231	4.92764	.707	-22.3326	6.9480
		pinna	-4.35897	4.92764	.975	-18.9992	10.2813
		Time	-17.94872*	4.92764	.006	-32.5890	-3.3084
		Time_filter	-7.43590	4.92764	.739	-22.0762	7.2044
	Time	LP_pinna	1.53846	4.92764	1.000	-13.1018	16.1787
		LP_sphere	17.94872*	4.92764	.006	3.3084	32.5890
		Duda_pinna	10.25641	4.92764	.367	-4.3839	24.8967
		pinna	13.58974	4.92764	.088	-1.0505	28.2300
		Sphere	17.94872*	4.92764	.006	3.3084	32.5890
		Time_filter	10.51282	4.92764	.336	-4.1275	25.1531
	Time_filter	LP_pinna	-8.97436	4.92764	.535	-23.6146	5.6659
		LP_sphere	7.43590	4.92764	.739	-7.2044	22.0762
		Duda_pinna	-.25641	4.92764	1.000	-14.8967	14.3839
		pinna	3.07692	4.92764	.996	-11.5634	17.7172
		Sphere	7.43590	4.92764	.739	-7.2044	22.0762
		Time	-10.51282	4.92764	.336	-25.1531	4.1275
Games-Howell	LP_pinna	LP_sphere	16.41026*	4.44855	.008	2.9184	29.9021
		Duda_pinna	8.71795	4.94476	.577	-6.2584	23.6943
		pinna	12.05128	4.95839	.200	-2.9664	27.0689

Multiple Comparisons

Dependent Variable: Angle

(I) Method	(J) Method	Mean Difference (I-J)	Std. Error	Sig.	95% Confidence Interval	
					Lower Bound	Upper Bound
	Sphere	16.41026*	4.96467	.023	1.3736	31.4470
	Time	-1.53846	5.28538	1.000	-17.5539	14.4770
	Time_filter	8.97436	4.91951	.536	-5.9255	23.8742
LP_sphere	LP_pinna	-16.41026*	4.44855	.008	-29.9021	-2.9184
	Duda_pinna	-7.69231	4.47105	.605	-21.2537	5.8691
	pinna	-4.35897	4.48612	.958	-17.9670	9.2490
	Sphere	.00000	4.49306	1.000	-13.6295	13.6295
	Time	-17.94872*	4.84509	.007	-32.6708	-3.2266
	Time_filter	-7.43590	4.44310	.636	-20.9109	6.0391
Duda_pinna	LP_pinna	-8.71795	4.94476	.577	-23.6943	6.2584
	LP_sphere	7.69231	4.47105	.605	-5.8691	21.2537
	pinna	3.33333	4.97859	.994	-11.7454	18.4121
	Sphere	7.69231	4.98484	.718	-7.4054	22.7900
	Time	-10.25641	5.30433	.465	-26.3284	5.8156
	Time_filter	.25641	4.93986	1.000	-14.7051	15.2179
pinna	LP_pinna	-12.05128	4.95839	.200	-27.0689	2.9664
	LP_sphere	4.35897	4.48612	.958	-9.2490	17.9670
	Duda_pinna	-3.33333	4.97859	.994	-18.4121	11.7454
	Sphere	4.35897	4.99836	.976	-10.7797	19.4976
	Time	-13.58974	5.31704	.155	-29.6997	2.5202
	Time_filter	-3.07692	4.95350	.996	-18.0798	11.9260
Sphere	LP_pinna	-16.41026*	4.96467	.023	-31.4470	-1.3736
	LP_sphere	.00000	4.49306	1.000	-13.6295	13.6295
	Duda_pinna	-7.69231	4.98484	.718	-22.7900	7.4054
	pinna	-4.35897	4.99836	.976	-19.4976	10.7797
	Time	-17.94872*	5.32289	.019	-34.0761	-1.8213
	Time_filter	-7.43590	4.95978	.744	-22.4578	7.5860
Time	LP_pinna	1.53846	5.28538	1.000	-14.4770	17.5539
	LP_sphere	17.94872*	4.84509	.007	3.2266	32.6708
	Duda_pinna	10.25641	5.30433	.465	-5.8156	26.3284
	pinna	13.58974	5.31704	.155	-2.5202	29.6997
	Sphere	17.94872*	5.32289	.019	1.8213	34.0761
	Time_filter	10.51282	5.28079	.429	-5.4890	26.5146
Time_filter	LP_pinna	-8.97436	4.91951	.536	-23.8742	5.9255
	LP_sphere	7.43590	4.44310	.636	-6.0391	20.9109
	Duda_pinna	-.25641	4.93986	1.000	-15.2179	14.7051
	pinna	3.07692	4.95350	.996	-11.9260	18.0798
	Sphere	7.43590	4.95978	.744	-7.5860	22.4578
	Time	-10.51282	5.28079	.429	-26.5146	5.4890

*. The mean difference is significant at the 0.05 level.

Homogeneous Subsets

```
 GET
  FILE='/Users/nordstoga_eide/Documents/SPSSInc/Each angle/m40.sav'.
DATASET NAME DataSet2 WINDOW=FRONT.
DATASET CLOSE DataSet1.
ONEWAY Angle BY Method
  /STATISTICS DESCRIPTIVES HOMOGENEITY WELCH
  /PLOT MEANS
  /MISSING ANALYSIS
  /POSTHOC=TUKEY GH ALPHA(0.05).
```

Oneway

Notes

Output Created		**10-JUN-2012 15:25:45**
Comments		
Input	**Data**	/Users/nordstoga_eide/Documents/SPSSInc/Each angle/m40.sav
	Active Dataset	**DataSet2**
	Filter	**<none>**
	Weight	**<none>**
	Split File	**<none>**
	N of Rows in Working Data File	**273**
Missing Value Handling	**Definition of Missing**	User-defined missing values are treated as missing.
	Cases Used	Statistics for each analysis are based on cases with no missing data for any variable in the analysis.
Syntax		ONEWAY Angle BY Method /STATISTICS DESCRIPTIVES HOMOGENEITY WELCH /PLOT MEANS /MISSING ANALYSIS /POSTHOC=TUKEY GH ALPHA(0.05).
Resources	**Processor Time**	**00:00:00,45**
	Elapsed Time	**00:00:00,00**

[DataSet2] /Users/nordstoga_eide/Documents/SPSSInc/Each angle/m40.sav

Descriptives

Angle

	N	Mean	Std. Deviation	Std. Error	95% Confidence Interval for Mean		Minimum	Maximum
					Lower Bound	Upper Bound		
LP_pinna	39	-18.7179	26.96777	4.31830	-27.4599	-9.9760	-50.00	90.00
LP_sphere	39	-19.7436	17.54501	2.80945	-25.4310	-14.0562	-50.00	10.00
Duda_pinna	39	-20.5128	17.61410	2.82051	-26.2227	-14.8030	-50.00	20.00
pinna	39	-19.4872	16.05070	2.57017	-24.6902	-14.2841	-50.00	10.00
Sphere	39	-19.7436	21.08718	3.37665	-26.5793	-12.9079	-50.00	30.00
Time	39	-11.5385	23.00326	3.68347	-18.9953	-4.0817	-50.00	60.00
Time_filter	39	-22.3077	18.41932	2.94945	-28.2785	-16.3368	-50.00	10.00
Total	273	-18.8645	20.43174	1.23658	-21.2990	-16.4300	-50.00	90.00

Test of Homogeneity of Variances

Angle

Levene Statistic	df1	df2	Sig.
1.314	6	266	.251

ANOVA

Angle

	Sum of Squares	df	Mean Square	F	Sig.
Between Groups	2737.729	6	456.288	1.095	.365
Within Groups	110810.256	266	416.580		
Total	113547.985	272			

Robust Tests of Equality of Means

Angle

	Statistic[a]	df1	df2	Sig.
Welch	.929	6	117.921	.477

a. Asymptotically F distributed.

Post Hoc Tests

Multiple Comparisons

Dependent Variable: Angle

	(I) Method	(J) Method	Mean Difference (I-J)	Std. Error	Sig.	95% Confidence Interval	
						Lower Bound	Upper Bound
Tukey HSD	LP_pinna	LP_sphere	1.02564	4.62202	1.000	-12.7066	14.7579
		Duda_pinna	1.79487	4.62202	1.000	-11.9374	15.5271
		pinna	.76923	4.62202	1.000	-12.9630	14.5015
		Sphere	1.02564	4.62202	1.000	-12.7066	14.7579
		Time	-7.17949	4.62202	.712	-20.9118	6.5528
		Time_filter	3.58974	4.62202	.987	-10.1425	17.3220
	LP_sphere	LP_pinna	-1.02564	4.62202	1.000	-14.7579	12.7066
		Duda_pinna	.76923	4.62202	1.000	-12.9630	14.5015
		pinna	-.25641	4.62202	1.000	-13.9887	13.4759
		Sphere	.00000	4.62202	1.000	-13.7323	13.7323
		Time	-8.20513	4.62202	.566	-21.9374	5.5271
		Time_filter	2.56410	4.62202	.998	-11.1682	16.2964
	Duda_pinna	LP_pinna	-1.79487	4.62202	1.000	-15.5271	11.9374
		LP_sphere	-.76923	4.62202	1.000	-14.5015	12.9630
		pinna	-1.02564	4.62202	1.000	-14.7579	12.7066
		Sphere	-.76923	4.62202	1.000	-14.5015	12.9630
		Time	-8.97436	4.62202	.455	-22.7066	4.7579
		Time_filter	1.79487	4.62202	1.000	-11.9374	15.5271
	pinna	LP_pinna	-.76923	4.62202	1.000	-14.5015	12.9630
		LP_sphere	.25641	4.62202	1.000	-13.4759	13.9887
		Duda_pinna	1.02564	4.62202	1.000	-12.7066	14.7579
		Sphere	.25641	4.62202	1.000	-13.4759	13.9887
		Time	-7.94872	4.62202	.603	-21.6810	5.7836
		Time_filter	2.82051	4.62202	.996	-10.9118	16.5528
	Sphere	LP_pinna	-1.02564	4.62202	1.000	-14.7579	12.7066
		LP_sphere	.00000	4.62202	1.000	-13.7323	13.7323
		Duda_pinna	.76923	4.62202	1.000	-12.9630	14.5015
		pinna	-.25641	4.62202	1.000	-13.9887	13.4759
		Time	-8.20513	4.62202	.566	-21.9374	5.5271
		Time_filter	2.56410	4.62202	.998	-11.1682	16.2964
	Time	LP_pinna	7.17949	4.62202	.712	-6.5528	20.9118
		LP_sphere	8.20513	4.62202	.566	-5.5271	21.9374
		Duda_pinna	8.97436	4.62202	.455	-4.7579	22.7066
		pinna	7.94872	4.62202	.603	-5.7836	21.6810
		Sphere	8.20513	4.62202	.566	-5.5271	21.9374
		Time_filter	10.76923	4.62202	.234	-2.9630	24.5015
	Time_filter	LP_pinna	-3.58974	4.62202	.987	-17.3220	10.1425
		LP_sphere	-2.56410	4.62202	.998	-16.2964	11.1682
		Duda_pinna	-1.79487	4.62202	1.000	-15.5271	11.9374
		pinna	-2.82051	4.62202	.996	-16.5528	10.9118
		Sphere	-2.56410	4.62202	.998	-16.2964	11.1682
		Time	-10.76923	4.62202	.234	-24.5015	2.9630
Games-Howell	LP_pinna	LP_sphere	1.02564	5.15177	1.000	-14.6468	16.6981
		Duda_pinna	1.79487	5.15781	1.000	-13.8948	17.4846
		pinna	.76923	5.02528	1.000	-14.5445	16.0829

Multiple Comparisons

Dependent Variable: Angle

(I) Method	(J) Method	Mean Difference (I-J)	Std. Error	Sig.	95% Confidence Interval	
					Lower Bound	Upper Bound
	Sphere	1.02564	5.48174	1.000	-15.6030	17.6543
	Time	-7.17949	5.67588	.866	-24.3817	10.0227
	Time_filter	3.58974	5.22943	.993	-12.3053	19.4848
LP_sphere	LP_pinna	-1.02564	5.15177	1.000	-16.6981	14.6468
	Duda_pinna	.76923	3.98099	1.000	-11.2881	12.8266
	pinna	-.25641	3.80773	1.000	-11.7914	11.2786
	Sphere	.00000	4.39258	1.000	-13.3158	13.3158
	Time	-8.20513	4.63260	.572	-22.2624	5.8522
	Time_filter	2.56410	4.07336	.996	-9.7738	14.9020
Duda_pinna	LP_pinna	-1.79487	5.15781	1.000	-17.4846	13.8948
	LP_sphere	-.76923	3.98099	1.000	-12.8266	11.2881
	pinna	-1.02564	3.81590	1.000	-12.5856	10.5343
	Sphere	-.76923	4.39967	1.000	-14.1060	12.5675
	Time	-8.97436	4.63931	.465	-23.0513	5.1026
	Time_filter	1.79487	4.08100	.999	-10.5660	14.1557
pinna	LP_pinna	-.76923	5.02528	1.000	-16.0829	14.5445
	LP_sphere	.25641	3.80773	1.000	-11.2786	11.7914
	Duda_pinna	1.02564	3.81590	1.000	-10.5343	12.5856
	Sphere	.25641	4.24353	1.000	-12.6206	13.1335
	Time	-7.94872	4.49152	.573	-21.5960	5.6985
	Time_filter	2.82051	3.91216	.991	-9.0343	14.6753
Sphere	LP_pinna	-1.02564	5.48174	1.000	-17.6543	15.6030
	LP_sphere	.00000	4.39258	1.000	-13.3158	13.3158
	Duda_pinna	.76923	4.39967	1.000	-12.5675	14.1060
	pinna	-.25641	4.24353	1.000	-13.1335	12.6206
	Time	-8.20513	4.99697	.656	-23.3426	6.9324
	Time_filter	2.56410	4.48342	.997	-11.0215	16.1497
Time	LP_pinna	7.17949	5.67588	.866	-10.0227	24.3817
	LP_sphere	8.20513	4.63260	.572	-5.8522	22.2624
	Duda_pinna	8.97436	4.63931	.465	-5.1026	23.0513
	pinna	7.94872	4.49152	.573	-5.6985	21.5960
	Sphere	8.20513	4.99697	.656	-6.9324	23.3426
	Time_filter	10.76923	4.71881	.267	-3.5412	25.0796
Time_filter	LP_pinna	-3.58974	5.22943	.993	-19.4848	12.3053
	LP_sphere	-2.56410	4.07336	.996	-14.9020	9.7738
	Duda_pinna	-1.79487	4.08100	.999	-14.1557	10.5660
	pinna	-2.82051	3.91216	.991	-14.6753	9.0343
	Sphere	-2.56410	4.48342	.997	-16.1497	11.0215
	Time	-10.76923	4.71881	.267	-25.0796	3.5412

Homogeneous Subsets

```
 GET
  FILE='/Users/nordstoga_eide/Documents/SPSSInc/Each angle/m60.sav'.
DATASET NAME DataSet14 WINDOW=FRONT.
ONEWAY Angle BY Method
  /STATISTICS DESCRIPTIVES HOMOGENEITY WELCH
  /PLOT MEANS
  /MISSING ANALYSIS
  /POSTHOC=TUKEY GH ALPHA(0.05).
```

Oneway

Notes

Output Created		**10-JUN-2012 15:08:16**
Comments		
Input	**Data**	/Users/nordstoga_eide/Documents/SPSSInc/Each angle/m60.sav
	Active Dataset	**DataSet14**
	Filter	**<none>**
	Weight	**<none>**
	Split File	**<none>**
	N of Rows in Working Data File	**272**
Missing Value Handling	**Definition of Missing**	User-defined missing values are treated as missing.
	Cases Used	Statistics for each analysis are based on cases with no missing data for any variable in the analysis.
Syntax		ONEWAY Angle BY Method /STATISTICS DESCRIPTIVES HOMOGENEITY WELCH /PLOT MEANS /MISSING ANALYSIS /POSTHOC=TUKEY GH ALPHA(0.05).
Resources	**Processor Time**	**00:00:00,60**
	Elapsed Time	**00:00:01,00**

[DataSet14] /Users/nordstoga_eide/Documents/SPSSInc/Each angle/m60.sav

Descriptives

Angle

	N	Mean	Std. Deviation	Std. Error	95% Confidence Interval for Mean		Minimum	Maximum
					Lower Bound	Upper Bound		
LP_pinna	38	-10.7895	17.61166	2.85699	-16.5783	-5.0007	-60.00	20.00
LP_sphere	39	-6.4103	12.45776	1.99484	-10.4486	-2.3719	-30.00	20.00
Duda_pinna	39	-11.5385	22.18801	3.55292	-18.7310	-4.3459	-70.00	40.00
pinna	39	-6.1538	16.32167	2.61356	-11.4447	-.8630	-30.00	30.00
sphere	39	-12.5641	25.41425	4.06954	-20.8024	-4.3258	-80.00	30.00
Time	39	-1.2821	23.63978	3.78540	-8.9452	6.3811	-70.00	40.00
Time_filter	39	-14.8718	25.01282	4.00526	-22.9800	-6.7636	-90.00	20.00
Total	272	-9.0809	21.11908	1.28053	-11.6019	-6.5598	-90.00	40.00

Test of Homogeneity of Variances

Angle

Levene Statistic	df1	df2	Sig.
2.769	6	265	.013

ANOVA

Angle

	Sum of Squares	df	Mean Square	F	Sig.
Between Groups	5111.854	6	851.976	1.950	.073
Within Groups	115758.367	265	436.824		
Total	120870.221	271			

Robust Tests of Equality of Means

Angle

	Statistic[a]	df1	df2	Sig.
Welch	1.683	6	116.746	.131

a. Asymptotically F distributed.

Post Hoc Tests

Multiple Comparisons

Dependent Variable: Angle

	(I) Method	(J) Method	Mean Difference (I-J)	Std. Error	Sig.	95% Confidence Interval	
						Lower Bound	Upper Bound
Tukey HSD	LP_pinna	LP_sphere	-4.37922	4.76403	.969	-18.5338	9.7754
		Duda_pinna	.74899	4.76403	1.000	-13.4056	14.9036
		pinna	-4.63563	4.76403	.959	-18.7902	9.5190
		sphere	1.77463	4.76403	1.000	-12.3800	15.9292
		Time	-9.50742	4.76403	.420	-23.6620	4.6472
		Time_filter	4.08232	4.76403	.978	-10.0723	18.2369
	LP_sphere	LP_pinna	4.37922	4.76403	.969	-9.7754	18.5338
		Duda_pinna	5.12821	4.73299	.933	-8.9342	19.1906
		pinna	-.25641	4.73299	1.000	-14.3188	13.8060
		sphere	6.15385	4.73299	.851	-7.9085	20.2162
		Time	-5.12821	4.73299	.933	-19.1906	8.9342
		Time_filter	8.46154	4.73299	.558	-5.6008	22.5239
	Duda_pinna	LP_pinna	-.74899	4.76403	1.000	-14.9036	13.4056
		LP_sphere	-5.12821	4.73299	.933	-19.1906	8.9342
		pinna	-5.38462	4.73299	.916	-19.4470	8.6778
		sphere	1.02564	4.73299	1.000	-13.0367	15.0880
		Time	-10.25641	4.73299	.317	-24.3188	3.8060
		Time_filter	3.33333	4.73299	.992	-10.7291	17.3957
	pinna	LP_pinna	4.63563	4.76403	.959	-9.5190	18.7902
		LP_sphere	.25641	4.73299	1.000	-13.8060	14.3188
		Duda_pinna	5.38462	4.73299	.916	-8.6778	19.4470
		sphere	6.41026	4.73299	.825	-7.6521	20.4726
		Time	-4.87179	4.73299	.947	-18.9342	9.1906
		Time_filter	8.71795	4.73299	.521	-5.3444	22.7803
	sphere	LP_pinna	-1.77463	4.76403	1.000	-15.9292	12.3800
		LP_sphere	-6.15385	4.73299	.851	-20.2162	7.9085
		Duda_pinna	-1.02564	4.73299	1.000	-15.0880	13.0367
		pinna	-6.41026	4.73299	.825	-20.4726	7.6521
		Time	-11.28205	4.73299	.210	-25.3444	2.7803
		Time_filter	2.30769	4.73299	.999	-11.7547	16.3701
	Time	LP_pinna	9.50742	4.76403	.420	-4.6472	23.6620
		LP_sphere	5.12821	4.73299	.933	-8.9342	19.1906
		Duda_pinna	10.25641	4.73299	.317	-3.8060	24.3188
		pinna	4.87179	4.73299	.947	-9.1906	18.9342
		sphere	11.28205	4.73299	.210	-2.7803	25.3444
		Time_filter	13.58974	4.73299	.066	-.4726	27.6521
	Time_filter	LP_pinna	-4.08232	4.76403	.978	-18.2369	10.0723
		LP_sphere	-8.46154	4.73299	.558	-22.5239	5.6008
		Duda_pinna	-3.33333	4.73299	.992	-17.3957	10.7291
		pinna	-8.71795	4.73299	.521	-22.7803	5.3444
		sphere	-2.30769	4.73299	.999	-16.3701	11.7547
		Time	-13.58974	4.73299	.066	-27.6521	.4726
Games-Howell	LP_pinna	LP_sphere	-4.37922	3.48450	.869	-14.9736	6.2151
		Duda_pinna	.74899	4.55913	1.000	-13.0796	14.5776
		pinna	-4.63563	3.87209	.893	-16.3707	7.0994

Multiple Comparisons

Dependent Variable: Angle

(I) Method	(J) Method	Mean Difference (I-J)	Std. Error	Sig.	95% Confidence Interval	
					Lower Bound	Upper Bound
	sphere	1.77463	4.97227	1.000	-13.3343	16.8835
	Time	-9.50742	4.74253	.421	-23.9031	4.8883
	Time_filter	4.08232	4.91980	.981	-10.8635	19.0281
LP_sphere	LP_pinna	4.37922	3.48450	.869	-6.2151	14.9736
	Duda_pinna	5.12821	4.07464	.868	-7.3032	17.5596
	pinna	-.25641	3.28787	1.000	-10.2331	9.7203
	sphere	6.15385	4.53216	.821	-7.7123	20.0200
	Time	-5.12821	4.27885	.892	-18.1997	7.9433
	Time_filter	8.46154	4.47453	.495	-5.2238	22.1469
Duda_pinna	LP_pinna	-.74899	4.55913	1.000	-14.5776	13.0796
	LP_sphere	-5.12821	4.07464	.868	-17.5596	7.3032
	pinna	-5.38462	4.41066	.884	-18.7752	8.0060
	sphere	1.02564	5.40226	1.000	-15.3443	17.3956
	Time	-10.25641	5.19158	.439	-25.9820	5.4691
	Time_filter	3.33333	5.35400	.996	-12.8887	19.5553
pinna	LP_pinna	4.63563	3.87209	.893	-7.0994	16.3707
	LP_sphere	.25641	3.28787	1.000	-9.7203	10.2331
	Duda_pinna	5.38462	4.41066	.884	-8.0060	18.7752
	sphere	6.41026	4.83651	.838	-8.3066	21.1271
	Time	-4.87179	4.59999	.938	-18.8511	9.1075
	Time_filter	8.71795	4.78255	.538	-5.8305	23.2664
sphere	LP_pinna	-1.77463	4.97227	1.000	-16.8835	13.3343
	LP_sphere	-6.15385	4.53216	.821	-20.0200	7.7123
	Duda_pinna	-1.02564	5.40226	1.000	-17.3956	15.3443
	pinna	-6.41026	4.83651	.838	-21.1271	8.3066
	Time	-11.28205	5.55791	.405	-28.1178	5.5537
	Time_filter	2.30769	5.70992	1.000	-14.9862	19.6016
Time	LP_pinna	9.50742	4.74253	.421	-4.8883	23.9031
	LP_sphere	5.12821	4.27885	.892	-7.9433	18.1997
	Duda_pinna	10.25641	5.19158	.439	-5.4691	25.9820
	pinna	4.87179	4.59999	.938	-9.1075	18.8511
	sphere	11.28205	5.55791	.405	-5.5537	28.1178
	Time_filter	13.58974	5.51102	.187	-3.1030	30.2825
Time_filter	LP_pinna	-4.08232	4.91980	.981	-19.0281	10.8635
	LP_sphere	-8.46154	4.47453	.495	-22.1469	5.2238
	Duda_pinna	-3.33333	5.35400	.996	-19.5553	12.8887
	pinna	-8.71795	4.78255	.538	-23.2664	5.8305
	sphere	-2.30769	5.70992	1.000	-19.6016	14.9862
	Time	-13.58974	5.51102	.187	-30.2825	3.1030

Homogeneous Subsets

```
 DATASET ACTIVATE DataSet2.
SAVE OUTFILE='/Users/nordstoga_eide/Documents/SPSSInc/Each angle/m60.sav'
 /COMPRESSED.
DATASET ACTIVATE DataSet3.
DATASET CLOSE DataSet2.
ONEWAY Angle BY Method
  /STATISTICS DESCRIPTIVES HOMOGENEITY WELCH
  /PLOT MEANS
  /MISSING ANALYSIS
  /POSTHOC=TUKEY GH ALPHA(0.05).
```

Oneway

Notes

Output Created		**09-JUN-2012 21:52:13**
Comments		
Input	**Data**	/Users/nordstoga_eide/Documents/SPSSInc/Each angle/m80.sav
	Active Dataset	**DataSet3**
	Filter	**<none>**
	Weight	**<none>**
	Split File	**<none>**
	N of Rows in Working Data File	**273**
Missing Value Handling	**Definition of Missing**	User-defined missing values are treated as missing.
	Cases Used	Statistics for each analysis are based on cases with no missing data for any variable in the analysis.
Syntax		ONEWAY Angle BY Method /STATISTICS DESCRIPTIVES HOMOGENEITY WELCH /PLOT MEANS /MISSING ANALYSIS /POSTHOC=TUKEY GH ALPHA(0.05).
Resources	**Processor Time**	**00:00:00,49**
	Elapsed Time	**00:00:00,00**

[DataSet3] /Users/nordstoga_eide/Documents/SPSSInc/Each angle/m80.sav

Descriptives

Angle

	N	Mean	Std. Deviation	Std. Error	95% Confidence Interval for Mean		Minimum	Maximum
					Lower Bound	Upper Bound		
LP_pinna	39	3.0769	30.44874	4.87570	-6.7934	12.9473	-70.00	80.00
LP_sphere	39	6.6667	13.24532	2.12095	2.3730	10.9603	-10.00	40.00
Duda_pinna	39	4.3590	26.83231	4.29661	-4.3391	13.0570	-60.00	90.00
pinna	39	16.1538	20.47018	3.27785	9.5182	22.7895	-10.00	50.00
sphere	39	7.6923	19.39364	3.10547	1.4056	13.9790	-40.00	60.00
Time	39	5.6410	23.59693	3.77853	-2.0082	13.2903	-60.00	50.00
Time_filter	39	9.4872	18.20190	2.91464	3.5868	15.3876	-40.00	50.00
Total	273	7.5824	22.49219	1.36129	4.9024	10.2624	-70.00	90.00

Test of Homogeneity of Variances

Angle

Levene Statistic	df1	df2	Sig.
3.050	6	266	.007

ANOVA

Angle

	Sum of Squares	df	Mean Square	F	Sig.
Between Groups	4383.883	6	730.647	1.459	.193
Within Groups	133220.513	266	500.829		
Total	137604.396	272			

Robust Tests of Equality of Means

Angle

	Statistic[a]	df1	df2	Sig.
Welch	1.455	6	117.222	.200

a. Asymptotically F distributed.

Post Hoc Tests

Multiple Comparisons

Dependent Variable: Angle

	(I) Method	(J) Method	Mean Difference (I-J)	Std. Error	Sig.	95% Confidence Interval	
						Lower Bound	Upper Bound
Tukey HSD	LP_pinna	LP_sphere	-3.58974	5.06789	.992	-18.6467	11.4672
		Duda_pinna	-1.28205	5.06789	1.000	-16.3390	13.7749
		pinna	-13.07692	5.06789	.136	-28.1339	1.9801
		sphere	-4.61538	5.06789	.971	-19.6724	10.4416
		Time	-2.56410	5.06789	.999	-17.6211	12.4929
		Time_filter	-6.41026	5.06789	.867	-21.4672	8.6467
	LP_sphere	LP_pinna	3.58974	5.06789	.992	-11.4672	18.6467
		Duda_pinna	2.30769	5.06789	.999	-12.7493	17.3647
		pinna	-9.48718	5.06789	.501	-24.5442	5.5698
		sphere	-1.02564	5.06789	1.000	-16.0826	14.0313
		Time	1.02564	5.06789	1.000	-14.0313	16.0826
		Time_filter	-2.82051	5.06789	.998	-17.8775	12.2365
	Duda_pinna	LP_pinna	1.28205	5.06789	1.000	-13.7749	16.3390
		LP_sphere	-2.30769	5.06789	.999	-17.3647	12.7493
		pinna	-11.79487	5.06789	.235	-26.8519	3.2621
		sphere	-3.33333	5.06789	.995	-18.3903	11.7236
		Time	-1.28205	5.06789	1.000	-16.3390	13.7749
		Time_filter	-5.12821	5.06789	.951	-20.1852	9.9288
	pinna	LP_pinna	13.07692	5.06789	.136	-1.9801	28.1339
		LP_sphere	9.48718	5.06789	.501	-5.5698	24.5442
		Duda_pinna	11.79487	5.06789	.235	-3.2621	26.8519
		sphere	8.46154	5.06789	.637	-6.5954	23.5185
		Time	10.51282	5.06789	.371	-4.5442	25.5698
		Time_filter	6.66667	5.06789	.844	-8.3903	21.7236
	sphere	LP_pinna	4.61538	5.06789	.971	-10.4416	19.6724
		LP_sphere	1.02564	5.06789	1.000	-14.0313	16.0826
		Duda_pinna	3.33333	5.06789	.995	-11.7236	18.3903
		pinna	-8.46154	5.06789	.637	-23.5185	6.5954
		Time	2.05128	5.06789	1.000	-13.0057	17.1083
		Time_filter	-1.79487	5.06789	1.000	-16.8519	13.2621
	Time	LP_pinna	2.56410	5.06789	.999	-12.4929	17.6211
		LP_sphere	-1.02564	5.06789	1.000	-16.0826	14.0313
		Duda_pinna	1.28205	5.06789	1.000	-13.7749	16.3390
		pinna	-10.51282	5.06789	.371	-25.5698	4.5442
		sphere	-2.05128	5.06789	1.000	-17.1083	13.0057
		Time_filter	-3.84615	5.06789	.988	-18.9031	11.2108
	Time_filter	LP_pinna	6.41026	5.06789	.867	-8.6467	21.4672
		LP_sphere	2.82051	5.06789	.998	-12.2365	17.8775
		Duda_pinna	5.12821	5.06789	.951	-9.9288	20.1852
		pinna	-6.66667	5.06789	.844	-21.7236	8.3903
		sphere	1.79487	5.06789	1.000	-13.2621	16.8519
		Time	3.84615	5.06789	.988	-11.2108	18.9031
Games-Howell	LP_pinna	LP_sphere	-3.58974	5.31704	.993	-19.8965	12.7171
		Duda_pinna	-1.28205	6.49871	1.000	-20.9732	18.4091
		pinna	-13.07692	5.87510	.296	-30.9394	4.7855

Multiple Comparisons

Dependent Variable: Angle

(I) Method	(J) Method	Mean Difference (I-J)	Std. Error	Sig.	95% Confidence Interval	
					Lower Bound	Upper Bound
	sphere	-4.61538	5.78069	.984	-22.2080	12.9772
	Time	-2.56410	6.16845	1.000	-21.2780	16.1498
	Time_filter	-6.41026	5.68045	.917	-23.7190	10.8985
LP_sphere	LP_pinna	3.58974	5.31704	.993	-12.7171	19.8965
	Duda_pinna	2.30769	4.79158	.999	-12.3500	16.9654
	pinna	-9.48718	3.90420	.203	-21.3655	2.3911
	sphere	-1.02564	3.76063	1.000	-12.4562	10.4050
	Time	1.02564	4.33310	1.000	-12.1944	14.2457
	Time_filter	-2.82051	3.60465	.986	-13.7659	8.1248
Duda_pinna	LP_pinna	1.28205	6.49871	1.000	-18.4091	20.9732
	LP_sphere	-2.30769	4.79158	.999	-16.9654	12.3500
	pinna	-11.79487	5.40418	.318	-28.1934	4.6037
	sphere	-3.33333	5.30139	.996	-19.4324	12.7657
	Time	-1.28205	5.72173	1.000	-18.6192	16.0551
	Time_filter	-5.12821	5.19191	.955	-20.9111	10.6547
pinna	LP_pinna	13.07692	5.87510	.296	-4.7855	30.9394
	LP_sphere	9.48718	3.90420	.203	-2.3911	21.3655
	Duda_pinna	11.79487	5.40418	.318	-4.6037	28.1934
	sphere	8.46154	4.51533	.504	-5.2152	22.1383
	Time	10.51282	5.00216	.363	-4.6455	25.6711
	Time_filter	6.66667	4.38628	.732	-6.6230	19.9564
sphere	LP_pinna	4.61538	5.78069	.984	-12.9772	22.2080
	LP_sphere	1.02564	3.76063	1.000	-10.4050	12.4562
	Duda_pinna	3.33333	5.30139	.996	-12.7657	19.4324
	pinna	-8.46154	4.51533	.504	-22.1383	5.2152
	Time	2.05128	4.89093	1.000	-12.7770	16.8795
	Time_filter	-1.79487	4.25899	1.000	-14.6956	11.1058
Time	LP_pinna	2.56410	6.16845	1.000	-16.1498	21.2780
	LP_sphere	-1.02564	4.33310	1.000	-14.2457	12.1944
	Duda_pinna	1.28205	5.72173	1.000	-16.0551	18.6192
	pinna	-10.51282	5.00216	.363	-25.6711	4.6455
	sphere	-2.05128	4.89093	1.000	-16.8795	12.7770
	Time_filter	-3.84615	4.77205	.984	-18.3245	10.6322
Time_filter	LP_pinna	6.41026	5.68045	.917	-10.8985	23.7190
	LP_sphere	2.82051	3.60465	.986	-8.1248	13.7659
	Duda_pinna	5.12821	5.19191	.955	-10.6547	20.9111
	pinna	-6.66667	4.38628	.732	-19.9564	6.6230
	sphere	1.79487	4.25899	1.000	-11.1058	14.6956
	Time	3.84615	4.77205	.984	-10.6322	18.3245

Homogeneous Subsets

```
 GET
  FILE='/Users/nordstoga_eide/Documents/SPSSInc/Each angle/p10.sav'.
DATASET NAME DataSet6 WINDOW=FRONT.
DATASET ACTIVATE DataSet6.
DATASET CLOSE DataSet5.
ONEWAY Angle BY Method
  /STATISTICS DESCRIPTIVES HOMOGENEITY WELCH
  /PLOT MEANS
  /MISSING ANALYSIS
  /POSTHOC=TUKEY GH ALPHA(0.05).
```

Oneway

Notes

Output Created		**10-JUN-2012 15:48:51**
Comments		
Input	**Data**	/Users/nordstoga_eide/Documents/SPSSInc/Each angle/p10.sav
	Active Dataset	**DataSet6**
	Filter	**<none>**
	Weight	**<none>**
	Split File	**<none>**
	N of Rows in Working Data File	**273**
Missing Value Handling	**Definition of Missing**	User-defined missing values are treated as missing.
	Cases Used	Statistics for each analysis are based on cases with no missing data for any variable in the analysis.
Syntax		ONEWAY Angle BY Method /STATISTICS DESCRIPTIVES HOMOGENEITY WELCH /PLOT MEANS /MISSING ANALYSIS /POSTHOC=TUKEY GH ALPHA(0.05).
Resources	**Processor Time**	**00:00:00,53**
	Elapsed Time	**00:00:01,00**

```
[DataSet6] /Users/nordstoga_eide/Documents/SPSSInc/Each angle/p10.sav
```

Descriptives

Angle

	N	Mean	Std. Deviation	Std. Error	95% Confidence Interval for Mean		Minimum	Maximum
					Lower Bound	Upper Bound		
LP_pinna	39	-14.1026	24.46458	3.91747	-22.0331	-6.1721	-70.00	30.00
LP_sphere	39	1.2821	29.03532	4.64937	-8.1301	10.6942	-40.00	90.00
Duda_pinna	39	-19.4872	21.01988	3.36587	-26.3010	-12.6733	-70.00	10.00
pinna	39	-20.5128	24.48939	3.92144	-28.4514	-12.5743	-70.00	10.00
Sphere	39	-10.2564	35.79820	5.73230	-21.8608	1.3480	-80.00	100.00
Time	39	-13.8462	19.68373	3.15192	-20.2269	-7.4654	-60.00	20.00
Time_filter	39	-16.6667	16.75416	2.68281	-22.0977	-11.2356	-50.00	40.00
Total	273	-13.3700	25.80325	1.56168	-16.4445	-10.2954	-80.00	100.00

Test of Homogeneity of Variances

Angle

Levene Statistic	df1	df2	Sig.
2.513	6	266	.022

ANOVA

Angle

	Sum of Squares	df	Mean Square	F	Sig.
Between Groups	12653.480	6	2108.913	3.330	.004
Within Groups	168446.154	266	633.256		
Total	181099.634	272			

Robust Tests of Equality of Means

Angle

	Statistic[a]	df1	df2	Sig.
Welch	2.798	6	117.589	.014

a. Asymptotically F distributed.

Post Hoc Tests

Multiple Comparisons

Dependent Variable: Angle

	(I) Method	(J) Method	Mean Difference (I-J)	Std. Error	Sig.	95% Confidence Interval	
						Lower Bound	Upper Bound
Tukey HSD	LP_pinna	LP_sphere	-15.38462	5.69866	.102	-32.3156	1.5464
		Duda_pinna	5.38462	5.69866	.965	-11.5464	22.3156
		pinna	6.41026	5.69866	.920	-10.5208	23.3413
		Sphere	-3.84615	5.69866	.994	-20.7772	13.0849
		Time	-.25641	5.69866	1.000	-17.1874	16.6746
		Time_filter	2.56410	5.69866	.999	-14.3669	19.4951
	LP_sphere	LP_pinna	15.38462	5.69866	.102	-1.5464	32.3156
		Duda_pinna	20.76923*	5.69866	.006	3.8382	37.7002
		pinna	21.79487*	5.69866	.003	4.8639	38.7259
		Sphere	11.53846	5.69866	.402	-5.3926	28.4695
		Time	15.12821	5.69866	.114	-1.8028	32.0592
		Time_filter	17.94872*	5.69866	.030	1.0177	34.8797
	Duda_pinna	LP_pinna	-5.38462	5.69866	.965	-22.3156	11.5464
		LP_sphere	-20.76923*	5.69866	.006	-37.7002	-3.8382
		pinna	1.02564	5.69866	1.000	-15.9054	17.9567
		Sphere	-9.23077	5.69866	.670	-26.1618	7.7002
		Time	-5.64103	5.69866	.956	-22.5720	11.2900
		Time_filter	-2.82051	5.69866	.999	-19.7515	14.1105
	pinna	LP_pinna	-6.41026	5.69866	.920	-23.3413	10.5208
		LP_sphere	-21.79487*	5.69866	.003	-38.7259	-4.8639
		Duda_pinna	-1.02564	5.69866	1.000	-17.9567	15.9054
		Sphere	-10.25641	5.69866	.549	-27.1874	6.6746
		Time	-6.66667	5.69866	.905	-23.5977	10.2643
		Time_filter	-3.84615	5.69866	.994	-20.7772	13.0849
	Sphere	LP_pinna	3.84615	5.69866	.994	-13.0849	20.7772
		LP_sphere	-11.53846	5.69866	.402	-28.4695	5.3926
		Duda_pinna	9.23077	5.69866	.670	-7.7002	26.1618
		pinna	10.25641	5.69866	.549	-6.6746	27.1874
		Time	3.58974	5.69866	.996	-13.3413	20.5208
		Time_filter	6.41026	5.69866	.920	-10.5208	23.3413
	Time	LP_pinna	.25641	5.69866	1.000	-16.6746	17.1874
		LP_sphere	-15.12821	5.69866	.114	-32.0592	1.8028
		Duda_pinna	5.64103	5.69866	.956	-11.2900	22.5720
		pinna	6.66667	5.69866	.905	-10.2643	23.5977
		Sphere	-3.58974	5.69866	.996	-20.5208	13.3413
		Time_filter	2.82051	5.69866	.999	-14.1105	19.7515
	Time_filter	LP_pinna	-2.56410	5.69866	.999	-19.4951	14.3669
		LP_sphere	-17.94872*	5.69866	.030	-34.8797	-1.0177
		Duda_pinna	2.82051	5.69866	.999	-14.1105	19.7515
		pinna	3.84615	5.69866	.994	-13.0849	20.7772
		Sphere	-6.41026	5.69866	.920	-23.3413	10.5208
		Time	-2.82051	5.69866	.999	-19.7515	14.1105
Games-Howell	LP_pinna	LP_sphere	-15.38462	6.07974	.164	-33.8127	3.0435
		Duda_pinna	5.38462	5.16485	.942	-10.2678	21.0371
		pinna	6.41026	5.54295	.908	-10.3778	23.1983

Multiple Comparisons

Dependent Variable: Angle

(I) Method	(J) Method	Mean Difference (I-J)	Std. Error	Sig.	95% Confidence Interval	
					Lower Bound	Upper Bound
	Sphere	-3.84615	6.94304	.998	-24.9496	17.2573
	Time	-.25641	5.02804	1.000	-15.5037	14.9909
	Time_filter	2.56410	4.74806	.998	-11.8671	16.9953
LP_sphere	LP_pinna	15.38462	6.07974	.164	-3.0435	33.8127
	Duda_pinna	20.76923*	5.73984	.010	3.3391	38.1993
	pinna	21.79487*	6.08230	.010	3.3592	40.2306
	Sphere	11.53846	7.38078	.706	-10.8415	33.9184
	Time	15.12821	5.61705	.116	-1.9472	32.2036
	Time_filter	17.94872*	5.36788	.023	1.5808	34.3166
Duda_pinna	LP_pinna	-5.38462	5.16485	.942	-21.0371	10.2678
	LP_sphere	-20.76923*	5.73984	.010	-38.1993	-3.3391
	pinna	1.02564	5.16786	1.000	-14.6361	16.6873
	Sphere	-9.23077	6.64743	.806	-29.4932	11.0316
	Time	-5.64103	4.61126	.883	-19.6089	8.3268
	Time_filter	-2.82051	4.30425	.995	-15.8744	10.2333
pinna	LP_pinna	-6.41026	5.54295	.908	-23.1983	10.3778
	LP_sphere	-21.79487*	6.08230	.010	-40.2306	-3.3592
	Duda_pinna	-1.02564	5.16786	1.000	-16.6873	14.6361
	Sphere	-10.25641	6.94528	.757	-31.3663	10.8535
	Time	-6.66667	5.03113	.838	-21.9236	8.5902
	Time_filter	-3.84615	4.75133	.983	-18.2876	10.5953
Sphere	LP_pinna	3.84615	6.94304	.998	-17.2573	24.9496
	LP_sphere	-11.53846	7.38078	.706	-33.9184	10.8415
	Duda_pinna	9.23077	6.64743	.806	-11.0316	29.4932
	pinna	10.25641	6.94528	.757	-10.8535	31.3663
	Time	3.58974	6.54170	.998	-16.3770	23.5565
	Time_filter	6.41026	6.32904	.949	-12.9718	25.7923
Time	LP_pinna	.25641	5.02804	1.000	-14.9909	15.5037
	LP_sphere	-15.12821	5.61705	.116	-32.2036	1.9472
	Duda_pinna	5.64103	4.61126	.883	-8.3268	19.6089
	pinna	6.66667	5.03113	.838	-8.5902	21.9236
	Sphere	-3.58974	6.54170	.998	-23.5565	16.3770
	Time_filter	2.82051	4.13909	.993	-9.7243	15.3653
Time_filter	LP_pinna	-2.56410	4.74806	.998	-16.9953	11.8671
	LP_sphere	-17.94872*	5.36788	.023	-34.3166	-1.5808
	Duda_pinna	2.82051	4.30425	.995	-10.2333	15.8744
	pinna	3.84615	4.75133	.983	-10.5953	18.2876
	Sphere	-6.41026	6.32904	.949	-25.7923	12.9718
	Time	-2.82051	4.13909	.993	-15.3653	9.7243

*. The mean difference is significant at the 0.05 level.

Homogeneous Subsets

```
ONEWAY Angle BY Method
  /STATISTICS DESCRIPTIVES HOMOGENEITY WELCH
  /PLOT MEANS
  /MISSING ANALYSIS
  /POSTHOC=TUKEY GH ALPHA(0.05).
```

Oneway

Notes

Output Created		**10-JUN-2012 16:00:10**
Comments		
Input	**Data**	/Users/nordstoga_eide/Documents/SPSSInc/Each angle/p20.sav
	Active Dataset	**DataSet7**
	Filter	**<none>**
	Weight	**<none>**
	Split File	**<none>**
	N of Rows in Working Data File	**273**
Missing Value Handling	**Definition of Missing**	User-defined missing values are treated as missing.
	Cases Used	Statistics for each analysis are based on cases with no missing data for any variable in the analysis.
Syntax		ONEWAY Angle BY Method /STATISTICS DESCRIPTIVES HOMOGENEITY WELCH /PLOT MEANS /MISSING ANALYSIS /POSTHOC=TUKEY GH ALPHA(0.05).
Resources	**Processor Time**	**00:00:00,44**
	Elapsed Time	**00:00:00,00**

```
[DataSet7] /Users/nordstoga_eide/Documents/SPSSInc/Each angle/p20.sav
```

Descriptives

Angle

	N	Mean	Std. Deviation	Std. Error	95% Confidence Interval for Mean		Minimum	Maximum
					Lower Bound	Upper Bound		
LP_pinna	**39**	**-19.4872**	**24.38169**	**3.90420**	**-27.3908**	**-11.5835**	**-60.00**	**50.00**
LP_sphere	**39**	**-5.1282**	**22.34559**	**3.57816**	**-12.3718**	**2.1154**	**-60.00**	**50.00**
Duda_pinna	**39**	**-32.8205**	**25.23038**	**4.04009**	**-40.9993**	**-24.6418**	**-70.00**	**20.00**
pinna	**39**	**-29.2308**	**32.14970**	**5.14807**	**-39.6525**	**-18.8090**	**-70.00**	**80.00**
Sphere	**39**	**-8.4615**	**32.24401**	**5.16317**	**-18.9138**	**1.9908**	**-70.00**	**80.00**
Time	**39**	**-11.7949**	**23.15529**	**3.70781**	**-19.3009**	**-4.2888**	**-60.00**	**20.00**
Time_filter	**39**	**-25.8974**	**20.48336**	**3.27996**	**-32.5374**	**-19.2575**	**-70.00**	**10.00**
Total	**273**	**-18.9744**	**27.66081**	**1.67411**	**-22.2702**	**-15.6785**	**-70.00**	**80.00**

Test of Homogeneity of Variances

Angle

Levene Statistic	df1	df2	Sig.
1.158	6	266	.329

ANOVA

Angle

	Sum of Squares	df	Mean Square	F	Sig.
Between Groups	27256.410	6	4542.735	6.681	.000
Within Groups	180856.410	266	679.911		
Total	208112.821	272			

Robust Tests of Equality of Means

Angle

	Statistic[a]	df1	df2	Sig.
Welch	6.976	6	117.932	.000

a. Asymptotically F distributed.

Post Hoc Tests

Multiple Comparisons

Dependent Variable: Angle

	(I) Method	(J) Method	Mean Difference (I-J)	Std. Error	Sig.	95% Confidence Interval	
						Lower Bound	Upper Bound
Tukey HSD	LP_pinna	LP_sphere	-14.35897	5.90485	.190	-31.9026	3.1846
		Duda_pinna	13.33333	5.90485	.269	-4.2103	30.8770
		pinna	9.74359	5.90485	.650	-7.8000	27.2872
		Sphere	-11.02564	5.90485	.504	-28.5693	6.5180
		Time	-7.69231	5.90485	.850	-25.2359	9.8513
		Time_filter	6.41026	5.90485	.932	-11.1334	23.9539
	LP_sphere	LP_pinna	14.35897	5.90485	.190	-3.1846	31.9026
		Duda_pinna	27.69231*	5.90485	.000	10.1487	45.2359
		pinna	24.10256*	5.90485	.001	6.5589	41.6462
		Sphere	3.33333	5.90485	.998	-14.2103	20.8770
		Time	6.66667	5.90485	.919	-10.8770	24.2103
		Time_filter	20.76923*	5.90485	.009	3.2256	38.3129
	Duda_pinna	LP_pinna	-13.33333	5.90485	.269	-30.8770	4.2103
		LP_sphere	-27.69231*	5.90485	.000	-45.2359	-10.1487
		pinna	-3.58974	5.90485	.997	-21.1334	13.9539
		Sphere	-24.35897*	5.90485	.001	-41.9026	-6.8154
		Time	-21.02564*	5.90485	.008	-38.5693	-3.4820
		Time_filter	-6.92308	5.90485	.904	-24.4667	10.6205
	pinna	LP_pinna	-9.74359	5.90485	.650	-27.2872	7.8000
		LP_sphere	-24.10256*	5.90485	.001	-41.6462	-6.5589
		Duda_pinna	3.58974	5.90485	.997	-13.9539	21.1334
		Sphere	-20.76923*	5.90485	.009	-38.3129	-3.2256

Multiple Comparisons

Dependent Variable: Angle

	(I) Method	(J) Method	Mean Difference (I-J)	Std. Error	Sig.	95% Confidence Interval	
						Lower Bound	Upper Bound
		Time	-17.43590	5.90485	.053	-34.9795	.1077
		Time_filter	-3.33333	5.90485	.998	-20.8770	14.2103
	Sphere	LP_pinna	11.02564	5.90485	.504	-6.5180	28.5693
		LP_sphere	-3.33333	5.90485	.998	-20.8770	14.2103
		Duda_pinna	24.35897*	5.90485	.001	6.8154	41.9026
		pinna	20.76923*	5.90485	.009	3.2256	38.3129
		Time	3.33333	5.90485	.998	-14.2103	20.8770
		Time_filter	17.43590	5.90485	.053	-.1077	34.9795
	Time	LP_pinna	7.69231	5.90485	.850	-9.8513	25.2359
		LP_sphere	-6.66667	5.90485	.919	-24.2103	10.8770
		Duda_pinna	21.02564*	5.90485	.008	3.4820	38.5693
		pinna	17.43590	5.90485	.053	-.1077	34.9795
		Sphere	-3.33333	5.90485	.998	-20.8770	14.2103
		Time_filter	14.10256	5.90485	.208	-3.4411	31.6462
	Time_filter	LP_pinna	-6.41026	5.90485	.932	-23.9539	11.1334
		LP_sphere	-20.76923*	5.90485	.009	-38.3129	-3.2256
		Duda_pinna	6.92308	5.90485	.904	-10.6205	24.4667
		pinna	3.33333	5.90485	.998	-14.2103	20.8770
		Sphere	-17.43590	5.90485	.053	-34.9795	.1077
		Time	-14.10256	5.90485	.208	-31.6462	3.4411
Games-Howell	LP_pinna	LP_sphere	-14.35897	5.29584	.110	-30.4019	1.6839
		Duda_pinna	13.33333	5.61828	.224	-3.6834	30.3501
		pinna	9.74359	6.46107	.739	-9.8636	29.3507
		Sphere	-11.02564	6.47311	.616	-30.6701	8.6188
		Time	-7.69231	5.38429	.785	-24.0010	8.6164
		Time_filter	6.41026	5.09911	.869	-9.0459	21.8664
	LP_sphere	LP_pinna	14.35897	5.29584	.110	-1.6839	30.4019
		Duda_pinna	27.69231*	5.39681	.000	11.3404	44.0442
		pinna	24.10256*	6.26944	.005	5.0519	43.1532
		Sphere	3.33333	6.28184	.998	-15.7559	22.4226
		Time	6.66667	5.15278	.853	-8.9402	22.2735
		Time_filter	20.76923*	4.85401	.001	6.0648	35.4736
	Duda_pinna	LP_pinna	-13.33333	5.61828	.224	-30.3501	3.6834
		LP_sphere	-27.69231*	5.39681	.000	-44.0442	-11.3404
		pinna	-3.58974	6.54408	.998	-23.4401	16.2606
		Sphere	-24.35897*	6.55597	.007	-44.2461	-4.4718
		Time	-21.02564*	5.48363	.005	-37.6373	-4.4140
		Time_filter	-6.92308	5.20389	.835	-22.7022	8.8560
	pinna	LP_pinna	-9.74359	6.46107	.739	-29.3507	9.8636
		LP_sphere	-24.10256*	6.26944	.005	-43.1532	-5.0519
		Duda_pinna	3.58974	6.54408	.998	-16.2606	23.4401
		Sphere	-20.76923	7.29116	.079	-42.8521	1.3137
		Time	-17.43590	6.34433	.102	-36.7032	1.8314
		Time_filter	-3.33333	6.10416	.998	-21.9103	15.2436

Multiple Comparisons

Dependent Variable: Angle

(I) Method	(J) Method	Mean Difference (I-J)	Std. Error	Sig.	95% Confidence Interval	
					Lower Bound	Upper Bound
Sphere	LP_pinna	11.02564	6.47311	.616	-8.6188	30.6701
	LP_sphere	-3.33333	6.28184	.998	-22.4226	15.7559
	Duda_pinna	24.35897*	6.55597	.007	4.4718	44.2461
	pinna	20.76923	7.29116	.079	-1.3137	42.8521
	Time	3.33333	6.35659	.998	-15.9720	22.6387
	Time_filter	17.43590	6.11690	.081	-1.1808	36.0526
Time	LP_pinna	7.69231	5.38429	.785	-8.6164	24.0010
	LP_sphere	-6.66667	5.15278	.853	-22.2735	8.9402
	Duda_pinna	21.02564*	5.48363	.005	4.4140	37.6373
	pinna	17.43590	6.34433	.102	-1.8314	36.7032
	Sphere	-3.33333	6.35659	.998	-22.6387	15.9720
	Time_filter	14.10256	4.95036	.079	-.8967	29.1018
Time_filter	LP_pinna	-6.41026	5.09911	.869	-21.8664	9.0459
	LP_sphere	-20.76923*	4.85401	.001	-35.4736	-6.0648
	Duda_pinna	6.92308	5.20389	.835	-8.8560	22.7022
	pinna	3.33333	6.10416	.998	-15.2436	21.9103
	Sphere	-17.43590	6.11690	.081	-36.0526	1.1808
	Time	-14.10256	4.95036	.079	-29.1018	.8967

*. The mean difference is significant at the 0.05 level.

Homogeneous Subsets

Angle

	Method	N	Subset for alpha = 0.05			
			1	2	3	4
Tukey HSD[a]	Duda_pinna	39	-32.8205			
	pinna	39	-29.2308	-29.2308		
	Time_filter	39	-25.8974	-25.8974	-25.8974	
	LP_pinna	39	-19.4872	-19.4872	-19.4872	-19.4872
	Time	39		-11.7949	-11.7949	-11.7949
	Sphere	39			-8.4615	-8.4615
	LP_sphere	39				-5.1282
	Sig.		.269	.053	.053	.190

Means for groups in homogeneous subsets are displayed.

a. Uses Harmonic Mean Sample Size = 39,000.

Means Plots

```
ONEWAY Angle BY Method
  /STATISTICS DESCRIPTIVES HOMOGENEITY WELCH
  /PLOT MEANS
  /MISSING ANALYSIS
  /POSTHOC=TUKEY GH ALPHA(0.05).
```

Oneway

Notes

Output Created		**10-JUN-2012 16:04:01**
Comments		
Input	**Data**	/Users/nordstoga_eide/Documents/SPSSInc/Each angle/p40.sav
	Active Dataset	**DataSet8**
	Filter	**<none>**
	Weight	**<none>**
	Split File	**<none>**
	N of Rows in Working Data File	**273**
Missing Value Handling	**Definition of Missing**	User-defined missing values are treated as missing.
	Cases Used	Statistics for each analysis are based on cases with no missing data for any variable in the analysis.
Syntax		ONEWAY Angle BY Method /STATISTICS DESCRIPTIVES HOMOGENEITY WELCH /PLOT MEANS /MISSING ANALYSIS /POSTHOC=TUKEY GH ALPHA(0.05).
Resources	**Processor Time**	**00:00:00,44**
	Elapsed Time	**00:00:01,00**

```
[DataSet8] /Users/nordstoga_eide/Documents/SPSSInc/Each angle/p40.sav
```

Descriptives

Angle

	N	Mean	Std. Deviation	Std. Error	95% Confidence Interval for Mean		Minimum	Maximum
					Lower Bound	Upper Bound		
LP_pinna	**39**	**-21.5385**	**28.42705**	**4.55197**	**-30.7534**	**-12.3235**	**-50.00**	**90.00**
LP_sphere	**39**	**-24.6154**	**20.11103**	**3.22034**	**-31.1346**	**-18.0961**	**-50.00**	**40.00**
Duda_pinna	**39**	**-19.7436**	**18.84664**	**3.01788**	**-25.8530**	**-13.6342**	**-50.00**	**20.00**
pinna	**39**	**-23.3333**	**19.91209**	**3.18849**	**-29.7881**	**-16.8786**	**-50.00**	**20.00**
Sphere	**39**	**-24.3590**	**21.86019**	**3.50043**	**-31.4452**	**-17.2727**	**-50.00**	**20.00**
Time	**39**	**-14.1026**	**23.69965**	**3.79498**	**-21.7851**	**-6.4200**	**-50.00**	**40.00**
Time_filter	**39**	**-21.7949**	**21.86944**	**3.50191**	**-28.8841**	**-14.7056**	**-50.00**	**40.00**
Total	**273**	**-21.3553**	**22.31118**	**1.35033**	**-24.0137**	**-18.6969**	**-50.00**	**90.00**

Test of Homogeneity of Variances

Angle

Levene Statistic	df1	df2	Sig.
.888	6	266	.504

ANOVA

Angle

	Sum of Squares	df	Mean Square	F	Sig.
Between Groups	3080.586	6	513.431	1.032	.405
Within Groups	132317.949	266	497.436		
Total	135398.535	272			

Robust Tests of Equality of Means

Angle

	Statistic[a]	df1	df2	Sig.
Welch	.985	6	118.053	.439

a. Asymptotically F distributed.

Post Hoc Tests

Multiple Comparisons

Dependent Variable: Angle

	(I) Method	(J) Method	Mean Difference (I-J)	Std. Error	Sig.	95% Confidence Interval	
						Lower Bound	Upper Bound
Tukey HSD	LP_pinna	LP_sphere	3.07692	5.05070	.996	-11.9290	18.0828
		Duda_pinna	-1.79487	5.05070	1.000	-16.8008	13.2110
		pinna	1.79487	5.05070	1.000	-13.2110	16.8008
		Sphere	2.82051	5.05070	.998	-12.1854	17.8264
		Time	-7.43590	5.05070	.761	-22.4418	7.5700
		Time_filter	.25641	5.05070	1.000	-14.7495	15.2623
	LP_sphere	LP_pinna	-3.07692	5.05070	.996	-18.0828	11.9290
		Duda_pinna	-4.87179	5.05070	.961	-19.8777	10.1341
		pinna	-1.28205	5.05070	1.000	-16.2879	13.7238
		Sphere	-.25641	5.05070	1.000	-15.2623	14.7495
		Time	-10.51282	5.05070	.367	-25.5187	4.4931
		Time_filter	-2.82051	5.05070	.998	-17.8264	12.1854
	Duda_pinna	LP_pinna	1.79487	5.05070	1.000	-13.2110	16.8008
		LP_sphere	4.87179	5.05070	.961	-10.1341	19.8777
		pinna	3.58974	5.05070	.992	-11.4161	18.5956
		Sphere	4.61538	5.05070	.970	-10.3905	19.6213
		Time	-5.64103	5.05070	.923	-20.6469	9.3649
		Time_filter	2.05128	5.05070	1.000	-12.9546	17.0572
	pinna	LP_pinna	-1.79487	5.05070	1.000	-16.8008	13.2110
		LP_sphere	1.28205	5.05070	1.000	-13.7238	16.2879
		Duda_pinna	-3.58974	5.05070	.992	-18.5956	11.4161
		Sphere	1.02564	5.05070	1.000	-13.9802	16.0315

Multiple Comparisons

Dependent Variable: Angle

	(I) Method	(J) Method	Mean Difference (I-J)	Std. Error	Sig.	95% Confidence Interval	
						Lower Bound	Upper Bound
		Time	-9.23077	5.05070	.531	-24.2367	5.7751
		Time_filter	-1.53846	5.05070	1.000	-16.5444	13.4674
	Sphere	LP_pinna	-2.82051	5.05070	.998	-17.8264	12.1854
		LP_sphere	.25641	5.05070	1.000	-14.7495	15.2623
		Duda_pinna	-4.61538	5.05070	.970	-19.6213	10.3905
		pinna	-1.02564	5.05070	1.000	-16.0315	13.9802
		Time	-10.25641	5.05070	.398	-25.2623	4.7495
		Time_filter	-2.56410	5.05070	.999	-17.5700	12.4418
	Time	LP_pinna	7.43590	5.05070	.761	-7.5700	22.4418
		LP_sphere	10.51282	5.05070	.367	-4.4931	25.5187
		Duda_pinna	5.64103	5.05070	.923	-9.3649	20.6469
		pinna	9.23077	5.05070	.531	-5.7751	24.2367
		Sphere	10.25641	5.05070	.398	-4.7495	25.2623
		Time_filter	7.69231	5.05070	.731	-7.3136	22.6982
	Time_filter	LP_pinna	-.25641	5.05070	1.000	-15.2623	14.7495
		LP_sphere	2.82051	5.05070	.998	-12.1854	17.8264
		Duda_pinna	-2.05128	5.05070	1.000	-17.0572	12.9546
		pinna	1.53846	5.05070	1.000	-13.4674	16.5444
		Sphere	2.56410	5.05070	.999	-12.4418	17.5700
		Time	-7.69231	5.05070	.731	-22.6982	7.3136
Games-Howell	LP_pinna	LP_sphere	3.07692	5.57593	.998	-13.8615	20.0154
		Duda_pinna	-1.79487	5.46150	1.000	-18.4039	14.8142
		pinna	1.79487	5.55760	1.000	-15.0906	18.6803
		Sphere	2.82051	5.74225	.999	-14.6021	20.2431
		Time	-7.43590	5.92641	.870	-25.4010	10.5292
		Time_filter	.25641	5.74316	1.000	-17.1688	17.6817
	LP_sphere	LP_pinna	-3.07692	5.57593	.998	-20.0154	13.8615
		Duda_pinna	-4.87179	4.41341	.925	-18.2403	8.4967
		pinna	-1.28205	4.53178	1.000	-15.0076	12.4435
		Sphere	-.25641	4.75643	1.000	-14.6650	14.1522
		Time	-10.51282	4.97720	.357	-25.5981	4.5725
		Time_filter	-2.82051	4.75752	.997	-17.2324	11.5914
	Duda_pinna	LP_pinna	1.79487	5.46150	1.000	-14.8142	18.4039
		LP_sphere	4.87179	4.41341	.925	-8.4967	18.2403
		pinna	3.58974	4.39022	.982	-9.7081	16.8876
		Sphere	4.61538	4.62175	.953	-9.3908	18.6216
		Time	-5.64103	4.84866	.905	-20.3463	9.0643
		Time_filter	2.05128	4.62288	.999	-11.9583	16.0609
	pinna	LP_pinna	-1.79487	5.55760	1.000	-18.6803	15.0906
		LP_sphere	1.28205	4.53178	1.000	-12.4435	15.0076
		Duda_pinna	-3.58974	4.39022	.982	-16.8876	9.7081
		Sphere	1.02564	4.73492	1.000	-13.3185	15.3697
		Time	-9.23077	4.95664	.511	-24.2551	5.7935
		Time_filter	-1.53846	4.73602	1.000	-15.8859	12.8090

Multiple Comparisons

Dependent Variable: Angle

(I) Method	(J) Method	Mean Difference (I-J)	Std. Error	Sig.	95% Confidence Interval	
					Lower Bound	Upper Bound
Sphere	LP_pinna	-2.82051	5.74225	.999	-20.2431	14.6021
	LP_sphere	.25641	4.75643	1.000	-14.1522	14.6650
	Duda_pinna	-4.61538	4.62175	.953	-18.6216	9.3908
	pinna	-1.02564	4.73492	1.000	-15.3697	13.3185
	Time	-10.25641	5.16284	.432	-25.8959	5.3831
	Time_filter	-2.56410	4.95141	.999	-17.5605	12.4323
Time	LP_pinna	7.43590	5.92641	.870	-10.5292	25.4010
	LP_sphere	10.51282	4.97720	.357	-4.5725	25.5981
	Duda_pinna	5.64103	4.84866	.905	-9.0643	20.3463
	pinna	9.23077	4.95664	.511	-5.7935	24.2551
	Sphere	10.25641	5.16284	.432	-5.3831	25.8959
	Time_filter	7.69231	5.16384	.750	-7.9502	23.3349
Time_filter	LP_pinna	-.25641	5.74316	1.000	-17.6817	17.1688
	LP_sphere	2.82051	4.75752	.997	-11.5914	17.2324
	Duda_pinna	-2.05128	4.62288	.999	-16.0609	11.9583
	pinna	1.53846	4.73602	1.000	-12.8090	15.8859
	Sphere	2.56410	4.95141	.999	-12.4323	17.5605
	Time	-7.69231	5.16384	.750	-23.3349	7.9502

Homogeneous Subsets

Angle

	Method	N	Subset for alpha = 0.05
			1
Tukey HSD[a]	LP_sphere	39	-24.6154
	Sphere	39	-24.3590
	pinna	39	-23.3333
	Time_filter	39	-21.7949
	LP_pinna	39	-21.5385
	Duda_pinna	39	-19.7436
	Time	39	-14.1026
	Sig.		.367

Means for groups in homogeneous subsets are displayed.

a. Uses Harmonic Mean Sample Size = 39,000.

Means Plots

```
ONEWAY Angle BY Method
  /STATISTICS DESCRIPTIVES HOMOGENEITY WELCH
  /PLOT MEANS
  /MISSING ANALYSIS
  /POSTHOC=TUKEY GH ALPHA(0.05).
```

Oneway

Notes

Output Created		**10-JUN-2012 16:07:25**
Comments		
Input	**Data**	/Users/nordstoga_eide/Documents/SPSSInc/Each angle/p60.sav
	Active Dataset	**DataSet9**
	Filter	**<none>**
	Weight	**<none>**
	Split File	**<none>**
	N of Rows in Working Data File	**271**
Missing Value Handling	**Definition of Missing**	User-defined missing values are treated as missing.
	Cases Used	Statistics for each analysis are based on cases with no missing data for any variable in the analysis.
Syntax		ONEWAY Angle BY Method /STATISTICS DESCRIPTIVES HOMOGENEITY WELCH /PLOT MEANS /MISSING ANALYSIS /POSTHOC=TUKEY GH ALPHA(0.05).
Resources	**Processor Time**	**00:00:00,49**
	Elapsed Time	**00:00:00,00**

```
[DataSet9] /Users/nordstoga_eide/Documents/SPSSInc/Each angle/p60.sav
```

Descriptives

Angle

	N	Mean	Std. Deviation	Std. Error	95% Confidence Interval for Mean		Minimum	Maximum
					Lower Bound	Upper Bound		
LP_pinna	**38**	**-17.6316**	**33.48531**	**5.43203**	**-28.6379**	**-6.6252**	**-100.00**	**100.00**
LP_sphere	**38**	**-8.6842**	**28.49097**	**4.62185**	**-18.0490**	**.6805**	**-30.00**	**100.00**
Duda_pinna	**39**	**-6.6667**	**16.59634**	**2.65754**	**-12.0466**	**-1.2868**	**-30.00**	**30.00**
pinna	**39**	**-4.3590**	**21.98024**	**3.51966**	**-11.4841**	**2.7662**	**-30.00**	**100.00**
sphere	**39**	**-18.2051**	**23.26866**	**3.72597**	**-25.7480**	**-10.6623**	**-80.00**	**30.00**
Time	**39**	**-8.9744**	**25.93462**	**4.15286**	**-17.3814**	**-.5673**	**-90.00**	**50.00**
Time_filter	**39**	**-13.0769**	**17.79323**	**2.84920**	**-18.8448**	**-7.3090**	**-50.00**	**30.00**
Total	**271**	**-11.0701**	**24.73487**	**1.50254**	**-14.0283**	**-8.1119**	**-100.00**	**100.00**

Test of Homogeneity of Variances

Angle

Levene Statistic	df1	df2	Sig.
1.399	6	264	.215

ANOVA

Angle

	Sum of Squares	df	Mean Square	F	Sig.
Between Groups	6678.872	6	1113.145	1.854	.089
Within Groups	158510.796	264	600.420		
Total	165189.668	270			

Robust Tests of Equality of Means

Angle

	Statistic[a]	df1	df2	Sig.
Welch	1.979	6	116.478	.074

a. Asymptotically F distributed.

Post Hoc Tests

Multiple Comparisons

Dependent Variable: Angle

	(I) Method	(J) Method	Mean Difference (I-J)	Std. Error	Sig.	95% Confidence Interval	
						Lower Bound	Upper Bound
Tukey HSD	LP_pinna	LP_sphere	-8.94737	5.62148	.688	-25.6501	7.7553
		Duda_pinna	-10.96491	5.58533	.441	-27.5602	5.6304
		pinna	-13.27260	5.58533	.213	-29.8679	3.3227
		sphere	.57355	5.58533	1.000	-16.0217	17.1688
		Time	-8.65722	5.58533	.714	-25.2525	7.9381
		Time_filter	-4.55466	5.58533	.983	-21.1499	12.0406
	LP_sphere	LP_pinna	8.94737	5.62148	.688	-7.7553	25.6501
		Duda_pinna	-2.01754	5.58533	1.000	-18.6128	14.5777
		pinna	-4.32524	5.58533	.987	-20.9205	12.2700
		sphere	9.52092	5.58533	.614	-7.0744	26.1162
		Time	.29015	5.58533	1.000	-16.3051	16.8854
		Time_filter	4.39271	5.58533	.986	-12.2026	20.9880
	Duda_pinna	LP_pinna	10.96491	5.58533	.441	-5.6304	27.5602
		LP_sphere	2.01754	5.58533	1.000	-14.5777	18.6128
		pinna	-2.30769	5.54894	1.000	-18.7949	14.1795
		sphere	11.53846	5.54894	.368	-4.9487	28.0256
		Time	2.30769	5.54894	1.000	-14.1795	18.7949
		Time_filter	6.41026	5.54894	.910	-10.0769	22.8974
	pinna	LP_pinna	13.27260	5.58533	.213	-3.3227	29.8679
		LP_sphere	4.32524	5.58533	.987	-12.2700	20.9205
		Duda_pinna	2.30769	5.54894	1.000	-14.1795	18.7949
		sphere	13.84615	5.54894	.165	-2.6410	30.3333

Multiple Comparisons

Dependent Variable: Angle

	(I) Method	(J) Method	Mean Difference (I-J)	Std. Error	Sig.	95% Confidence Interval	
						Lower Bound	Upper Bound
		Time	4.61538	5.54894	.981	-11.8718	21.1025
		Time_filter	8.71795	5.54894	.701	-7.7692	25.2051
	sphere	LP_pinna	-.57355	5.58533	1.000	-17.1688	16.0217
		LP_sphere	-9.52092	5.58533	.614	-26.1162	7.0744
		Duda_pinna	-11.53846	5.54894	.368	-28.0256	4.9487
		pinna	-13.84615	5.54894	.165	-30.3333	2.6410
		Time	-9.23077	5.54894	.641	-25.7179	7.2564
		Time_filter	-5.12821	5.54894	.968	-21.6154	11.3590
	Time	LP_pinna	8.65722	5.58533	.714	-7.9381	25.2525
		LP_sphere	-.29015	5.58533	1.000	-16.8854	16.3051
		Duda_pinna	-2.30769	5.54894	1.000	-18.7949	14.1795
		pinna	-4.61538	5.54894	.981	-21.1025	11.8718
		sphere	9.23077	5.54894	.641	-7.2564	25.7179
		Time_filter	4.10256	5.54894	.990	-12.3846	20.5897
	Time_filter	LP_pinna	4.55466	5.58533	.983	-12.0406	21.1499
		LP_sphere	-4.39271	5.58533	.986	-20.9880	12.2026
		Duda_pinna	-6.41026	5.54894	.910	-22.8974	10.0769
		pinna	-8.71795	5.54894	.701	-25.2051	7.7692
		sphere	5.12821	5.54894	.968	-11.3590	21.6154
		Time	-4.10256	5.54894	.990	-20.5897	12.3846
Games-Howell	LP_pinna	LP_sphere	-8.94737	7.13221	.870	-30.5799	12.6852
		Duda_pinna	-10.96491	6.04727	.545	-29.4848	7.5550
		pinna	-13.27260	6.47263	.394	-32.9790	6.4338
		sphere	.57355	6.58710	1.000	-19.4602	20.6073
		Time	-8.65722	6.83764	.865	-29.4169	12.1025
		Time_filter	-4.55466	6.13392	.989	-23.3119	14.2025
	LP_sphere	LP_pinna	8.94737	7.13221	.870	-12.6852	30.5799
		Duda_pinna	-2.01754	5.33142	1.000	-18.2888	14.2537
		pinna	-4.32524	5.80943	.989	-21.9642	13.3137
		sphere	9.52092	5.93669	.680	-8.4911	27.5329
		Time	.29015	6.21351	1.000	-18.5430	19.1233
		Time_filter	4.39271	5.42949	.983	-12.1540	20.9394
	Duda_pinna	LP_pinna	10.96491	6.04727	.545	-7.5550	29.4848
		LP_sphere	2.01754	5.33142	1.000	-14.2537	18.2888
		pinna	-2.30769	4.41027	.998	-15.6922	11.0768
		sphere	11.53846	4.57661	.168	-2.3625	25.4394
		Time	2.30769	4.93040	.999	-12.6959	17.3113
		Time_filter	6.41026	3.89621	.654	-5.3918	18.2123
	pinna	LP_pinna	13.27260	6.47263	.394	-6.4338	32.9790
		LP_sphere	4.32524	5.80943	.989	-13.3137	21.9642
		Duda_pinna	2.30769	4.41027	.998	-11.0768	15.6922
		sphere	13.84615	5.12551	.112	-1.6789	29.3712
		Time	4.61538	5.44373	.979	-11.8841	21.1149
		Time_filter	8.71795	4.52834	.471	-5.0132	22.4491

Multiple Comparisons

Dependent Variable: Angle

(I) Method	(J) Method	Mean Difference (I-J)	Std. Error	Sig.	95% Confidence Interval	
					Lower Bound	Upper Bound
sphere	LP_pinna	-.57355	6.58710	1.000	-20.6073	19.4602
	LP_sphere	-9.52092	5.93669	.680	-27.5329	8.4911
	Duda_pinna	-11.53846	4.57661	.168	-25.4394	2.3625
	pinna	-13.84615	5.12551	.112	-29.3712	1.6789
	Time	-9.23077	5.57935	.648	-26.1344	7.6728
	Time_filter	-5.12821	4.69050	.928	-19.3607	9.1043
Time	LP_pinna	8.65722	6.83764	.865	-12.1025	29.4169
	LP_sphere	-.29015	6.21351	1.000	-19.1233	18.5430
	Duda_pinna	-2.30769	4.93040	.999	-17.3113	12.6959
	pinna	-4.61538	5.44373	.979	-21.1149	11.8841
	sphere	9.23077	5.57935	.648	-7.6728	26.1344
	Time_filter	4.10256	5.03629	.983	-11.2043	19.4094
Time_filter	LP_pinna	4.55466	6.13392	.989	-14.2025	23.3119
	LP_sphere	-4.39271	5.42949	.983	-20.9394	12.1540
	Duda_pinna	-6.41026	3.89621	.654	-18.2123	5.3918
	pinna	-8.71795	4.52834	.471	-22.4491	5.0132
	sphere	5.12821	4.69050	.928	-9.1043	19.3607
	Time	-4.10256	5.03629	.983	-19.4094	11.2043

Homogeneous Subsets

Angle

	Method	N	Subset for alpha = 0.05
			1
Tukey HSD[a,b]	sphere	39	-18.2051
	LP_pinna	38	-17.6316
	Time_filter	39	-13.0769
	Time	39	-8.9744
	LP_sphere	38	-8.6842
	Duda_pinna	39	-6.6667
	pinna	39	-4.3590
	Sig.		.169

Means for groups in homogeneous subsets are displayed.

a. Uses Harmonic Mean Sample Size = 38,709.

b. The group sizes are unequal. The harmonic mean of the group sizes is used. Type I error levels are not guaranteed.

Means Plots

```
ONEWAY Angle BY Method
  /STATISTICS DESCRIPTIVES HOMOGENEITY WELCH
  /PLOT MEANS
  /MISSING ANALYSIS
  /POSTHOC=TUKEY GH ALPHA(0.05).
```

Oneway

Notes

Output Created		**10-JUN-2012 16:10:58**
Comments		
Input	**Data**	/Users/nordstoga_eide/Documents/SPSSInc/Each angle/p80.sav
	Active Dataset	**DataSet10**
	Filter	**<none>**
	Weight	**<none>**
	Split File	**<none>**
	N of Rows in Working Data File	**273**
Missing Value Handling	**Definition of Missing**	User-defined missing values are treated as missing.
	Cases Used	Statistics for each analysis are based on cases with no missing data for any variable in the analysis.
Syntax		ONEWAY Angle BY Method /STATISTICS DESCRIPTIVES HOMOGENEITY WELCH /PLOT MEANS /MISSING ANALYSIS /POSTHOC=TUKEY GH ALPHA(0.05).
Resources	**Processor Time**	**00:00:00,46**
	Elapsed Time	**00:00:00,00**

```
[DataSet10] /Users/nordstoga_eide/Documents/SPSSInc/Each angle/p80.sav
```

Descriptives

Angle

	N	Mean	Std. Deviation	Std. Error	95% Confidence Interval for Mean		Minimum	Maximum
					Lower Bound	Upper Bound		
LP_pinna	**39**	**9.2308**	**24.10335**	**3.85963**	**1.4174**	**17.0442**	**-60.00**	**70.00**
LP_sphere	**39**	**13.8462**	**19.41451**	**3.10881**	**7.5527**	**20.1396**	**-10.00**	**70.00**
Duda_pinna	**39**	**5.6410**	**19.97299**	**3.19824**	**-.8335**	**12.1155**	**-40.00**	**50.00**
pinna	**39**	**17.9487**	**29.12581**	**4.66386**	**8.5072**	**27.3902**	**-10.00**	**150.00**
sphere	**39**	**6.6667**	**19.64599**	**3.14588**	**.2982**	**13.0352**	**-40.00**	**50.00**
Time	**39**	**9.4872**	**22.70506**	**3.63572**	**2.1271**	**16.8473**	**-20.00**	**60.00**
Time_filter	**39**	**.7692**	**27.27874**	**4.36809**	**-8.0735**	**9.6120**	**-80.00**	**90.00**
Total	**273**	**9.0842**	**23.76904**	**1.43857**	**6.2521**	**11.9164**	**-80.00**	**150.00**

Test of Homogeneity of Variances

Angle

Levene Statistic	df1	df2	Sig.
.279	6	266	.946

ANOVA

Angle

	Sum of Squares	df	Mean Square	F	Sig.
Between Groups	7342.857	6	1223.810	2.225	.041
Within Groups	146328.205	266	550.106		
Total	153671.062	272			

Robust Tests of Equality of Means

Angle

	Statistic[a]	df1	df2	Sig.
Welch	1.837	6	117.960	.098

a. Asymptotically F distributed.

Post Hoc Tests

Multiple Comparisons

Dependent Variable: Angle

	(I) Method	(J) Method	Mean Difference (I-J)	Std. Error	Sig.	95% Confidence Interval	
						Lower Bound	Upper Bound
Tukey HSD	LP_pinna	LP_sphere	-4.61538	5.31136	.977	-20.3957	11.1650
		Duda_pinna	3.58974	5.31136	.994	-12.1906	19.3701
		pinna	-8.71795	5.31136	.656	-24.4983	7.0624
		sphere	2.56410	5.31136	.999	-13.2162	18.3444
		Time	-.25641	5.31136	1.000	-16.0368	15.5239
		Time_filter	8.46154	5.31136	.687	-7.3188	24.2419
	LP_sphere	LP_pinna	4.61538	5.31136	.977	-11.1650	20.3957
		Duda_pinna	8.20513	5.31136	.717	-7.5752	23.9855
		pinna	-4.10256	5.31136	.987	-19.8829	11.6778
		sphere	7.17949	5.31136	.827	-8.6009	22.9598
		Time	4.35897	5.31136	.983	-11.4214	20.1393
		Time_filter	13.07692	5.31136	.178	-2.7034	28.8573
	Duda_pinna	LP_pinna	-3.58974	5.31136	.994	-19.3701	12.1906
		LP_sphere	-8.20513	5.31136	.717	-23.9855	7.5752
		pinna	-12.30769	5.31136	.240	-28.0880	3.4726
		sphere	-1.02564	5.31136	1.000	-16.8060	14.7547
		Time	-3.84615	5.31136	.991	-19.6265	11.9342
		Time_filter	4.87179	5.31136	.970	-10.9085	20.6521
	pinna	LP_pinna	8.71795	5.31136	.656	-7.0624	24.4983
		LP_sphere	4.10256	5.31136	.987	-11.6778	19.8829
		Duda_pinna	12.30769	5.31136	.240	-3.4726	28.0880
		sphere	11.28205	5.31136	.342	-4.4983	27.0624

Multiple Comparisons

Dependent Variable: Angle

	(I) Method	(J) Method	Mean Difference (I-J)	Std. Error	Sig.	95% Confidence Interval	
						Lower Bound	Upper Bound
		Time	8.46154	5.31136	.687	-7.3188	24.2419
		Time_filter	17.17949*	5.31136	.023	1.3991	32.9598
	sphere	LP_pinna	-2.56410	5.31136	.999	-18.3444	13.2162
		LP_sphere	-7.17949	5.31136	.827	-22.9598	8.6009
		Duda_pinna	1.02564	5.31136	1.000	-14.7547	16.8060
		pinna	-11.28205	5.31136	.342	-27.0624	4.4983
		Time	-2.82051	5.31136	.998	-18.6009	12.9598
		Time_filter	5.89744	5.31136	.925	-9.8829	21.6778
	Time	LP_pinna	.25641	5.31136	1.000	-15.5239	16.0368
		LP_sphere	-4.35897	5.31136	.983	-20.1393	11.4214
		Duda_pinna	3.84615	5.31136	.991	-11.9342	19.6265
		pinna	-8.46154	5.31136	.687	-24.2419	7.3188
		sphere	2.82051	5.31136	.998	-12.9598	18.6009
		Time_filter	8.71795	5.31136	.656	-7.0624	24.4983
	Time_filter	LP_pinna	-8.46154	5.31136	.687	-24.2419	7.3188
		LP_sphere	-13.07692	5.31136	.178	-28.8573	2.7034
		Duda_pinna	-4.87179	5.31136	.970	-20.6521	10.9085
		pinna	-17.17949*	5.31136	.023	-32.9598	-1.3991
		sphere	-5.89744	5.31136	.925	-21.6778	9.8829
		Time	-8.71795	5.31136	.656	-24.4983	7.0624
Games-Howell	LP_pinna	LP_sphere	-4.61538	4.95595	.966	-19.6439	10.4132
		Duda_pinna	3.58974	5.01253	.991	-11.6059	18.7854
		pinna	-8.71795	6.05379	.778	-27.0705	9.6346
		sphere	2.56410	4.97928	.999	-12.5333	17.6615
		Time	-.25641	5.30237	1.000	-16.3174	15.8045
		Time_filter	8.46154	5.82898	.772	-9.2000	26.1231
	LP_sphere	LP_pinna	4.61538	4.95595	.966	-10.4132	19.6439
		Duda_pinna	8.20513	4.46020	.526	-5.3039	21.7141
		pinna	-4.10256	5.60503	.990	-21.1465	12.9413
		sphere	7.17949	4.42281	.668	-6.2160	20.5750
		Time	4.35897	4.78363	.970	-10.1387	18.8567
		Time_filter	13.07692	5.36143	.199	-3.2084	29.3622
	Duda_pinna	LP_pinna	-3.58974	5.01253	.991	-18.7854	11.6059
		LP_sphere	-8.20513	4.46020	.526	-21.7141	5.3039
		pinna	-12.30769	5.65512	.322	-29.4955	4.8801
		sphere	-1.02564	4.48612	1.000	-14.6129	12.5617
		Time	-3.84615	4.84223	.985	-18.5183	10.8260
		Time_filter	4.87179	5.41378	.971	-11.5654	21.3089
	pinna	LP_pinna	8.71795	6.05379	.778	-9.6346	27.0705
		LP_sphere	4.10256	5.60503	.990	-12.9413	21.1465
		Duda_pinna	12.30769	5.65512	.322	-4.8801	29.4955
		sphere	11.28205	5.62567	.421	-5.8211	28.3852
		Time	8.46154	5.91355	.783	-9.4777	26.4008
		Time_filter	17.17949	6.38998	.115	-2.1762	36.5352

Multiple Comparisons

Dependent Variable: Angle

(I) Method	(J) Method	Mean Difference (I-J)	Std. Error	Sig.	95% Confidence Interval	
					Lower Bound	Upper Bound
sphere	LP_pinna	-2.56410	4.97928	.999	-17.6615	12.5333
	LP_sphere	-7.17949	4.42281	.668	-20.5750	6.2160
	Duda_pinna	1.02564	4.48612	1.000	-12.5617	14.6129
	pinna	-11.28205	5.62567	.421	-28.3852	5.8211
	Time	-2.82051	4.80780	.997	-17.3901	11.7491
	Time_filter	5.89744	5.38301	.927	-10.4504	22.2452
Time	LP_pinna	.25641	5.30237	1.000	-15.8045	16.3174
	LP_sphere	-4.35897	4.78363	.970	-18.8567	10.1387
	Duda_pinna	3.84615	4.84223	.985	-10.8260	18.5183
	pinna	-8.46154	5.91355	.783	-26.4008	9.4777
	sphere	2.82051	4.80780	.997	-11.7491	17.3901
	Time_filter	8.71795	5.68319	.724	-8.5101	25.9460
Time_filter	LP_pinna	-8.46154	5.82898	.772	-26.1231	9.2000
	LP_sphere	-13.07692	5.36143	.199	-29.3622	3.2084
	Duda_pinna	-4.87179	5.41378	.971	-21.3089	11.5654
	pinna	-17.17949	6.38998	.115	-36.5352	2.1762
	sphere	-5.89744	5.38301	.927	-22.2452	10.4504
	Time	-8.71795	5.68319	.724	-25.9460	8.5101

*. The mean difference is significant at the 0.05 level.

Homogeneous Subsets

Angle

	Method	N	Subset for alpha = 0.05	
			1	2
Tukey HSD[a]	Time_filter	39	.7692	
	Duda_pinna	39	5.6410	5.6410
	sphere	39	6.6667	6.6667
	LP_pinna	39	9.2308	9.2308
	Time	39	9.4872	9.4872
	LP_sphere	39	13.8462	13.8462
	pinna	39		17.9487
	Sig.		.178	.240

Means for groups in homogeneous subsets are displayed.

a. Uses Harmonic Mean Sample Size = 39,000.

Means Plots

References

[1] Shaw, E. A. G. (2007) Acoustical Characteristics of the Outer Ear, in Encyclopedia of Acoustics, Volume Three (ed M. J. Crocker), John Wiley and Sons, Inc., Hoboken, NJ, USA. doi: 10.1002/9780470172537.ch105

[2] Shaw, E. A. G. and Teranishi, "Sound pressure generated in an external-ear replica and real human ears by a nearby point source," *J. Acoust. Soc. Am.,* Vol. 44, No. 1 pp. 240-249, 1968

[3] Shaw, E. A. G. "Transformation of sound pressure level from the free field to the eardrum in the horizontal plane", *J. Acoust. Soc. Am.*, Vol 56,pp 1848-1861,1974

[4] Shaw, E. A. G. "The external ear: New knowledge" *Ears molds and associated Problems*, Proc. Seventh Danavox Symposium, Dalsgaard, S.C Ed., Scand. Audiol. (suppl. 5=, pp. 24-50, 1975

[5] Shaw, E. A. G. "The acoustics of the external ear," *Acoustical Factors affecting Hearing Aid performance*, Studebaker, G. A. And Hochberg, I. Eds., pp 109-124, Baltimore, MD: University Park press, 1980

[6] Shaw, E. A. G. "Acoustical features of the human external ear", *Binaural and spatial hearing in real and virtual environments* Gilkey, R. H and Anderson, T. R, Eds., pp 25-47, Mahwah, HL: Lawrence Earlbaum Associates, 1997

[7] Teranishi, R. and Shaw, E. A. G. "External-ear acoustic models with simple geometry", *J. Acoust. Soc. Am.*, Vol. 44, No. 1, pp 257-263, 1968.

[8] L. Rayleigh "On our perception of sound direction", *Phil. Mag.*, vol. 13, pp. 214-232, 1907.

[9] Brown, C.P and Duda, R.O (1998). "A structural model for binaural sound synthesis," IEEE Trans. Speech audio Process. **6**, 476-488

[10] Anthony, F., Jahn, M.D and Santos-Sacchi, J. "Physiology of the ear" 2.nd ed. Singular thomson learning, 2001ISBN 1-56593-994-8

[11] Gardner, W.G and Martin, K.D., "HRTF Measurements of a KEMAR," J. Acoust. Soc. Amer., Vol. 97, 3907-3908, 1995. See also http:// www.sound.media.mit.edu/KEMAR.html.

[12] Kuhn, G.F. "Acoustics and measurements pertaining to directional hearing," in *Directional hearing*, Yost, W.A. and Gourevitch, G. Eds. Berlin, Germany: Springer-Verlag, 1987, pp. 3-25.

[13] Algazi,V. R. Duda,R. O. Thompson,D. M. and Avendano,C. "The CIPIC HRTF Database," Proc. 2001 IEEE Workshop on Applications of Signal Processing to Audio and Electroacoustics, pp. 99-102, Mohonk Mountain House, New Paltz, NY, Oct. 21-24, 2001.

[14] Yegnanarayana, B, Raykar, C. R and Duraiswami, R "Extracting the frequencies of the pinna spectral notches in measured head related impulse responses" J. Acoust. Soc Am. **118** (1), July 2005, pp 364-374

[15] Rodriguez, S. G and Ramirez, M.A "Extracting and modeling approximated pinna-related transfer functions from hrtf data" Proceedings of ICAD 05-Eleventh Meeting of the International Conference on Auditory Display, Limerick, Ireland, July 6-9, 2005

[16] Langendujk, E.H. A and Bronkhorst, A.W. **2002**. "Contribution of spectral cues to human sound localization," J. Acoust. Soc. Am **112**, 1583-1596

[17] Moore, B. C. J., Oldfield, S.R, and Dooley, G. (**1989**). "Detection and discrimination of spectral peaks and notches at 1 and 8 kHz," J. Acoust. Soc. Am **85**, 820-836

[18] Hebrank, J. H and Wright, D. "Spectral cues used in the localization of sound sources in the median plane," *J. Acoust. Soc. Am.*, Vol. 56, No.6, pp 1829-1834,1974

[19] B. G. Shinn-Cunningham, N. I. Durlach, and R. M. Held, "Adapting to Supernormal Auditory Localization Cues," *J. Acoust. Soc. Am.*, vol. 103, pp. 3656- 3666,1998.

[20] Han, H.L "Measuring a dummy head in search of pinna cues," *J.Aud. Eng. Soc.,* Vol.42, No. 1/2, pp 15-37, Jan. and Fe., 1994

[21] Satarzadeh, P., Algazi, R.V. and Duda, R.O. "Physical and filter pinna Models Based on Anthropometry" . In *Proc. 122nd Convention of the Audio Engineering Society*, Vienna, Austria, May 5-8 2007

[22] Algazi, R.V, Duda, R.O, Thompson, D. M and Morrison, R. P, "Structural composition and decomposition of HRTFs" 2001 IEEE ASSP Workshop on Applications of Signal Proessing to Audio and Acoustics, pp. 103-106, New Paltz, NY, Oct. 2001

[23] Spagnol, S., Geronazzo, M. and Avanzini, F. "Structural Modeling Of Pinna Related Transfer Functions" *Proc. Int. Conf. on Sound and Music Computing (SMC 2010)*

[24] Geronazzo, M. and Spagnol, S. and Avanzini, F. "A Head-Related Transfer Function Model for Real-Time Customized 3-D Sound Rendering" *IEEE Signal-Image Technology and Internet-Based Systems (SITIS), 2011 Seventh International Conference*, pp.174-179

[25] Gray, H. "Anatomy of the human body". Philadelphia: Lea and Febiger, 1918; Bartleby.com, 2000. www.bartleby.com/107/. 2012

[26] Sand, O, Sjaastad,O, Haug, E and Bjalie, J.G, "Menneskekroppen" 2.nd ed,Oslo,Gyldendal norsk forlag 2006

[27] Algazi, V.R. and Duda, R.O. and Thompson, D.M. "The use of head-and-torso models for improved spatial sound synthesis" Preprint 5712, 113th Convention of the Audio Engineering Society, Los Angeles, CA, Oct. 2002

[28] Tønsberg, Ø. "Localization of Sounds in the Horizontal Plane using the QuietPro System", Masters thesis, NTNU 2009

[29] U.S Centers for Disease Control and Prevention. *Audiometry Procedures Manual*,2005. Found at http://www.cdc.gov/nchs/data/nhanes/nhanes_05_06/AU.pdf

[30] Budowick, M. Bjalle, J. G., Rolstad, B., Toverud, K. C "Anatomisk atlas", 10.th ed. Oslo, Gyldendal forlag AS 2001

[31] Kuhn, G.F, "Model for the interaural time differences in the azimuthal plane", *J. Acoust.Soc. Amer.*, vol. 62, pp. 157-167, July 1977

[32] Blauert, J.P, "Spatial hearing", rev. ed. Cambridge, MA:MIT Press,1997

[33] Moore, B. C. J. "An introduction to the psychology of hearing". London: Academic press, 5. ed., 2003

[34] Huang, J. and Ohnishi, N. and Sugie, N., "Spatial localization of sound sources: azimuth and elevation estimation", *Instrumentation and Measurement Technology Conference, 1998. IMTC/98. Conference Proceedings. IEEE* vol. 1, pp. 330-333

[35] Strutt, J. W (Lord Rayleigh),"On the acoustic shadow of a sphere" *Phil. Trans.R. Soc. London* , vol. 203A, pp. 87-97 1904; *The theory of sound*, 2nd ed. New York: Dower, 1945

[36] Cheng, C.I. and Wakefield, G.H., "Introduction to head-related transfer functions (HRTFs): Representations of HRTFs in time, frequency, and space", *J. Aud.Eng.Soc.*, Vol 49, No. 4, pp. 231-249, 2001

[37] Hammershøi, D and Møller, H "Binaural technique - Basic Methods for Recording, Synthesis, and Reproduction" *Communication Acoustics, J. Blauert (ed.), Springer Verlag*, (2005).

[38] Algazi, V.R. Avendano, C. and Duda, R.O., "Estimation of a spherical-head model from anthropometry" *J. Aud. Eng. Soc* Vol. 49, No.6 pp. 427-479, 2001

[39] Levene, H, "Robust tests for equality of variances". Inkgram Olkin, Harold Hotelling *Stanford University Press* 1960, pp. 278-292

[40] Genuit, K. "Ein Modell zur Beschreibung von Außenohrübertragungseigenschaften", doctoral dissertation, Rheinisch-Westfalichen Technichen Hochschule Aachen, Germany, 1984.

[41] Wenzel, E.M. and Arruda, M. and Kistler, D.J. and Wightman, F.L. "Localization using nonindividualized head-related transfer functions" *J. acoust. Soc. Am* Vol. 94, No. 1, pp. 111-123, 1993

[42] Møller, H. and Sørensen, M.F. and Jensen, C.B. and Hammershøi, D."Binaural technique: Do we need individual recordings?" *J. Aud. Eng. Soc.*, Vol. 44, No. 6, pp. 451-469, 1996

[43] Gupta, N. and Barreto, A. and Choudhury, M., "Modeling head-related transfer functions based on pinna anthropometry" Second International Latin American and Carribian Conferebce for Engineering and Technology, Miami, FL, 2004

[44] Spagnol, S. and Geronazzo, M. and Avanzini, F. "Fitting pinna-related transfer functions to anthropometry for binaural sound rendering" *Multimedia Signal Processing (MMSP), 2010 IEEE International Workshop*, pp 194-199, 2012

[45] Spagnol, S. and Hiipakka, M. and Pulkki, V., "A single-azimuth pinna-related transfer function database" *Proc. of the 14.th Int. Conference on Digital Audio Effects (DAFx-11)* Paris, France, September 19-23, 2011

[46] Batteu, D. W, "The role of the pinna in human localization" *Proc. R. Soc. London. series B, Biological Sciences,* 168(1011):158-180, August 1967

[47] Katz, B. F. G and Parseihian, G, "Perceptually based head-related transfer function database optimization" *J. Acoust. Soc. Am* 131, february 2012

[48] Keyrouz, F. and Diepold, K. "A new HRTF interpolation approach for fast synthesis of dynamic environmental interaction" *Journal-Audio Engineering Society* vol.56, no. 1, 2008 Audio engineering Society inc

[49] Vetterli, M "Sound field analysis along a circle and its applications to HRTF interpolation" *J. Audio Eng. Soc* vol.56 no. 3, 2008, Citeseer

[50] Best, V., Charlie, C., Jin, C and van Schaik, A, "The role of high frequencies in speech localization", *The journal of the Acoustical Society f America*, vol. 103, no.5, pp. 2634-2648, 1998

[51] Fiala, P. and Huijssen, J. and Pluymers, B. and Hallez, R. and Desmet, W., "Fast Multipole BEM modeling of head related transfer functions of a dummy head and torso" ISMA 2010 Conference, Leuven, Belgium

[52] SPSS Inc. (2011). IBM SPSS statistics . Rel 20.0.0. SPSS Inc., Chicago IL.